NON-ENZYMATIC UREA DETECTION BASED ON MOLECULARLY IMPRINTED ELECTROCHEMICAL BIOSENSOR

YOSSAWAT RAYANASUKHA

A THESIS SUBMITTED IN PARTIAL FULFILLMENT OF

THE REQUIREMENT FOR THE DEGREE OF

DOCTOR OF PHILOSOPHY PROGRAM IN NANOSCIENCE AND NANOTECHNOLOGY

COLLEGE OF NANOTECHNOLOGY

KING MONGKUT'S INSTITUTE OF TECHNOLOGY LADKRABANG

2016

KMITL-2016-NT-D-001-007

Thesis Title	Non-Enzymatic Urea Detection based on Molecularly Imprinted Electrochemical Biosensor
Student	Mr. Yossawat Rayanasukha
Student ID	52670254
Degree	Doctor of Philosophy
Program	Nanoscience and Nanotechnology
Year	2016
Thesis Advisor	Professer Dr. Jiti Nukeaw
Thesis Co advisor	Dr. Supanit Porntheeraphat

ABSTRACT

Blood tests are one of the physician's basic tools to see a detailed analysis of any disease marker, dysfunction of the various organs and waste products in the body. Blood Urea Nitrogen (BUN) is nitrogen concentration in blood human serum. The BUN measurement is one of the chemistry panels to concern about the malfunction of liver and kidneys. Consequently, BUN detection is very challenge to fabricate as a detection kit. The detection of urea molecules via biosensors is an alternative method. Normally, the enzyme urease is used as a catalyst in the hydrolysis reaction. Since the enzyme stability is a major problem of biosensor development, a non-enzymatic system is a very challenge approach to improve the efficiency of biosensor devices.

In this thesis, we demonstrate the detection of urea based on the molecularly imprinted polymers (MIPs) biosensors. To fabricate the MIPs urea sensors, PMMA is used as the matrix polymer while urea molecules are used as molecular templates. The MIPs sensors are prepared by solvent-assisted drop casting method on gold-coated electrodes and ion-sensitive field effect transistors (ISFET). The surface morphology of polymeric films was characterized by scanning electron

microscope (SEM). Then, Fourier transform infrared spectroscopy (FTIR) and UV-Vis spectroscopy were employed to confirm the urea templates removal. To evaluate the MIP sensors, cyclic voltammetry (CV), amperometry, and potentiometry methods were employed. Our results exhibit that the MIPs sensors on gold-coated electrodes show two linear ranges between 2 - 100 μM and 0.1 - 100 mM while the MIPs on ISFET sensors provide the linearity in the range of 01 - 100 mM. The MIPs sensors not only evidently present the selectivity to urea molecules at low concentrations but also be able to determine the amount of urea in human blood serum between 95.3% - 105.6%. In addition, the MIPs sensors also exhibit high reproducibility, repeatability and storage stability.

We successfully detect the urea molecules by using the MIPs urea sensors, which fabricate by solvent-assisted drop casting technique. The MIPs urea sensors show the limit of detection (LOD) in the scale of millimolar, which is suitable for the measurement of urea in the human blood serum. The MIPs urea sensors can be integrated with microfluidic platforms to become handheld device for chemical sensing and clinical diagnostic in the near future.

Keywords: molecularly imprinted polymer; non-enzymatic sensor; urea detection; electrochemical sensor; ion-sensitive field effect transistor.

หัวข้อวิทยานิพนธ์	ไบโอเซนเซอร์ไฟฟ้าเคมีสำหรับการตรวจวัดยูเรียโดยไม่ใช้เอนไซม์ด้วยเทคนิคการสร้างแม่แบบโมเลกุล
นักศึกษา	นายยศวัต รายณะสุข
รหัสประจำตัว	52670254
ปริญญา	ปรัชญาดุษฎีบัณฑิต
สาขาวิชา	นาโนวิทยาและนาโนเทคโนโลยี
พ.ศ.	2559
อาจารย์ที่ปรึกษาวิทยานิพนธ์	ศาสตราจารย์ ดร.จิติ หนูแก้ว
อาจารย์ที่ปรึกษาวิทยานิพนธ์ร่วม	ดร.ศุภนิจ พรธีระภัทร

บทคัดย่อ

วิทยานิพนธ์ฉบับนี้เป็นการสร้างไบโอเซนเซอร์ไฟฟ้าเคมีสำหรับการตรวจวัดยูเรียด้วยเทคนิคการสร้างพอลิเมอร์แม่แบบโมเลกุล (molecularly imprinted polymers, MIPs) พอลิเมอร์แม่แบบโมเลกุลถูกเตรียมด้วยกระบวนการหยดและระเหยตัวทำละลาย (solvent-assisted drop casting) ซึ่งเป็นกระบวนการที่ไม่ซับซ้อน บนขั้วไฟฟ้าทอง (Au electrode) และทรานซิสเตอร์สนามไฟฟ้าชนิดไวต่อไอออน (Ion-selective field effect transistor, ISFET) เซนเซอร์ไฟฟ้าเคมีแม่แบบโมเลกุลใช้พอลิเมทิลเมทาคริเลต (PMMA) เป็นพอลิเมอร์และยูเรียเป็นโมเลกุลแม่แบบ โดยทำการศึกษาสัณฐานวิทยาชั้นฟิล์มพอลิเมอร์ด้วยกล้องจุลทรรศน์อิเล็กตรอนแบบส่องกราด (SEM) จากนั้นทำการศึกษาการล้างโมเลกุลแม่แบบออกจากชั้นฟิล์มพอลิเมอร์ โดยใช้เทคนิคฟูเรียร์ทรานสฟอร์มอินฟราเรดสเปกโทรสโกปี (FTIR) และยูวี-วิสสเปกโทรสโคปี (UV-Vis) จากนั้นศึกษาสมบัติทางไฟฟ้าเคมีด้วยเทคนิคไซคลิกโวลแทมเมทรี (Cyclic voltammetry, CV) แอมเปอโรเมทรี (Amperometry) และโพเทนทิโอเมทรี (Potentiometry) สำหรับการสร้างไบโอเซนเซอร์ไฟฟ้าเคมีแม่แบบโมเลกุล ซึ่งพบว่าอัตราส่วนที่เหมาะสมของพอลิเมทิลเมทาคริเลตและยูเรีย อยู่ที่ 2.5 และ 0.4 เปอร์เซนต์โดยน้ำหนักต่อปริมาตรตามลำดับ จากผลการศึกษาแสดงให้เห็นว่า พอลิเมอร์แม่แบบโมเลกุลบนขั้วไฟฟ้าทอง มีช่วงการตอบสนองที่เป็นเชิงเส้นอยู่สองช่วงคือ 2 - 100 ไมโครโมลาร์ (μM) และ 0.1 – 100 มิลลิโมลาร์ (mM) และมีขีดจำกัดของการตรวจสอบคือ 0.8 ไมโครโมลาร์ อัตราส่วนสัญญาณการตอบสนองต่อสัญญาณรบกวนเท่ากับ 3 (S/N = 3) ขณะที่พอลิเมอร์แม่แบบโมเลกุลบน

ISFET มีช่วงการตอบสนองที่เป็นเชิงเส้นคือ 0.1 – 100 มิลลิโมลาร์ และมีขีดจำกัดของการตรวจสอบคือ 0.1 มิลลิโมลาร์ อัตราส่วนสัญญาณการตอบสนองต่อสัญญาณรบกวนเท่ากับ 3 นอกจากนี้เซนเซอร์พอลิเมอร์แม่แบบโมเลกุลแสดงให้เห็นถึงความสามารถในการทำซ้ำ การวัดซ้ำ ความเสถียรในการเก็บรักษาที่ยอดเยี่ยม รวมทั้งยังสามารถตรวจสอบยูเรียในตัวอย่างซีรั่มเลือดของมนุษย์ได้ โดยมีค่าการตรวจสอบอยู่ที่ 95.3 – 105.6 เปอร์เซนต์ ดังนั้นไบโอเซนเซอร์ไฟฟ้าเคมีที่สร้างด้วยเทคนิคพอลิเมอร์แม่แบบโมเลกุลมีศักยภาพสำหรับการพัฒนาอุปกรณ์การวินิจฉัยทางการแพทย์

คำสำคัญ: พอลิเมอร์แม่แบบโมเลกุล; เซนเซอร์แบบไม่ใช้เอนไซม์; การตรวจวัดยูเรีย; เซนเซอร์ไฟฟ้าเคมี; ทรานซิสเตอร์สนามไฟฟ้าที่ไวต่อไอออน

ACKNOWLEDGMENT

First of all, I would like to express my sincere gratitude to my advisor Professor Dr. Jiti Nukeaw and my co-advisor Dr. Supanit Porntheeraphat for the continuous support of my Ph.D. study and related research, for their patience and invaluable suggestions, motivation, immense knowledge, and supports throughout my educational life. I could not have imagined having a better advisor and mentor for my Ph.D. study.

Besides my advisor, I would like to thank the rest of my thesis committee: Dr. Navaphun Kayunkid, Assistant Professor Dr. Thutiyaporn Thiwawong, Assistant Professor Dr. Darinee Phromyothin, and Dr. Annop Klamchuen, for their insightful comments and encouragement, but also for the hard question which incented me to widen my research from various perspectives.

My sincere thanks also goes to Associate Professor Dr. Seeroong Prichanont, Dr. Chanchana Thanachayanont, Dr. Nongluck Houngkamhang, Dr. Pornpimol Sritongkam, and Dr. Win Bunjongpru, who provided me an opportunity to join their team and who gave access to the laboratory and research facilities. Without thier precious support it would not be possible to conduct this research. I would also like to thank Dr. Sakon Rahong, his guidance helped me in writing of this thesis.

A special thanks to Dr. Sirapat Pratontep. His guidance helped me in all the time of research. I would like to thank you for encouraging my research and for allowing me to grow as a research scientist.

I wish to acknowledge the Thailand Excellent Physics Center (ThEP Center), and the National Nanotechnology Center (NANOTEC), NSTDA, Ministry of Science and Technology, through its program of Center of Excellence Network for all its financial support.

Last but not the least, I would like to thank my family. My parents Mr. Wuttichai Rayanasukha and Mrs. Ravaing Rayanasukha, and my brother Mr. Nuttiwut

Rayanasukha and Ms. Sirajit Vuttivong for support and encouragement throughout writing this thesis, my life in general, and incented me to strive towards my goal. This accomplishment would not have been possible without them. Thank you.

YOSSAWAT RAYANASUKHA

TABLE OF CONTENTS

LIST OF TABLES

LIST OF FIGURES

ABBREVIATIONS AND SYMBOLS

AA	Ascorbic Acid
Ag/AgCl	Silver/Silver chloride
ATR	Attenuated Total Reflectance
Au	Gold
BUN	Blood Urea Nitrogen
CdS	Cadmium Sulfide
CE	Counter Electrode
Cr	Creatinine
ChemFET	Chemical-Sensitive Field Effect Transistor
CS	Chitosan
CV	Cyclic Voltametry
DA	Dopamine
DI water	De-ionized water
DMF	Dimethylformamide
EIS	Electrochemical Impedance Spectroscopy
ENFET	Enzyme Field Effect Transistor
EVAL	Poly(Ethylene-co-Vinyl Alcohol)
FTIR	Fourier Transform Infrared Spectrometer
FE-SEM	Filed-Emission Scanning Electron Microscope
IHP	Inner Helmholtz Plane
ISFET	Ion-Sensitive Field Effect Transistor
MCP	Mercaptopyridine
MIPs	Molecularly Imprinted Polymers
MOSFET	Metal Oxide Semiconductor Field Effect Transistor
NIPs	Non-Molecularly Imprinted Polymers
OHP	Outer Helmholtz Plane

PMMA	Poly(methyl methacrylate)
PPy	Polypyrrole
Pt	Platinum
RE	Reference Electrode
REFET	Reference ISFET
RSD	Relative Standard Deviation
SEM	Scanning Electron Microscope
SPE	Solid Phase Extraction
UA	Uric Acid
Ur	Urease
UV-vis	Ultraviolet-Visible
WE	Working Electrode
I_{DS}	Drain-Source Current
V_{DS}	Drain-Source Voltage
V_{GS}	Gate-Source voltage

CHAPTER 1

INTRODUCTION

1.1 Overview

Biosensor research has a growing number over the last two decades. Biosensors can be applied to a variety of samples including body fluids, food samples, cell cultures, and can be used to analyze environmental samples [1]. The available biosensor should be low cost, small size, portable and capable of being used by non-specialist operators. Many biosensor devices were developed, whereas the electrochemical technique is one approach to fabricate biosensors because their output can be detect in electrical signals. The electrical signal can be easy to translate and read out by conventional electronic circuits, which can be developed to be a portable device. Other advantages of electrochemical biosensors are robustness, simple-to-use, and ability to be used in turbid samples [2–4].

The blood test is a significant application for biosensor development. Blood Urea Nitrogen or BUN is one of many substances can be measured by blood testing, which can impart about the kidney failure or liver malfunction. For healthy people, the normal range of BUN is 5 – 20 mg/dl (1.8 - 7.1 mmol/L). The causes of an increase in BUN are kidney failure, renal failure (acute or chronic), urinary tract obstruction, gastrointestinal bleeding and dehydration, while causes of a decrease in BUN are a hepatic failure, nephrotic syndrome, cachexia (low-protein and high-carbohydrate diets) [5–7].

In present, An instrument referred to as biosensors being used as clinical diagnostic tools in point-of-care testing and can be generally found as one well-known is the glucose sensor [8]. In contrast, a portable device for measuring and detecting the urea concentration in the blood is unavailable. After that, the urease based urea biosensor has been interesting and developing for clinical diagnostic

devices [9-10]. However, urease enzyme was reported about limitations such as enzyme activity, enzyme stability, and unspecific to urea [11–14].

To improve limitations of biosensor based enzyme, a non-enzymatic urea sensor was developed [15,16]. However, non-enzymatic urea sensors have disadvantage in the poor selectivity and narrow range of the linearity response, which not suitable for applied to measure urea in blood human serum. Apart from that, molecularly imprinted polymers (MIPs) technique has been developing for selective membranes as an artificial receptor. Chen et al. [17] synthesized the chitosan for MIPs electrochemical urea detection with high selectivity, stability, repeatability, and reproducibility. This chitosan-based MIPs was later improved by incorporating CdS quantum dots, and the detection limit of the resulting sensor was extended to as low as a picomolar level [18]. Although these published works show splendid sensor performances, the obtained sensors are fabricated with complicated methods and the detection ranges are not suitable for urea measurement application.

To achieve this goal, we have to overcome above issues. The first issue is the MIPs fabrication method. This work demonstrates a simply fabrication method for MIPs urea sensor, which prepared by solvent-assisted drop casting techniques. The other major issue is the detection ranges of the fabricated sensor. We present the MIPs sensor for urea determination in detection range covered millimolar level, which has a potential to determine the concentration of urea in blood human serum.

Here we report molecularly imprinted electrode using the solvent evaporation technique for urea detection. Poly(methyl methacrylate) (PMMA) and urea were used as the functional polymer and the molecule template, respectively, and were drop-cast on to a gold-coated electrode on printed circuit board. The MIPs membrane was also exposed to UV irradiation to strengthen the coated membrane. The prepared MIPs on the gold-coated electrode was studied electrochemical characteristics and evaluated their properties such as the sensitivity, linearity range,

detection limit, reproducibility, repeatability, and stability. The last topic, the urea measurement in the blood human serum of the MIPs sensor was investigated.

Finally, after studied electrochemical characteristics between the MIPs sensing membrane and urea target molecules. We reported a novel molecularly imprinted sensor based on the ion-sensitive field effect transistor (ISFET) device for urea detection. The sensitivity, selectivity, repeatability and reproducibility of the fabricated MIPs-ISFET sensor have been evaluated.

1.2 Scope of this research

This research aims to fabricate Molecularly Imprinted Polymers (MIPs) film as sensing membrane for urea detection. MIPs have been prepared on Au electrodes and on ISFET sensors for first time. The polymeric selective membranes were fabricated by using PMMA and urea as the functional polymer and molecular templates, respectively. The surface morphology of MIPs was observed by scanning electron microscope (SEM). Then, the characteristic removal templates were investigated by Fourier transform infrared spectroscopy (FTIR) and UV-VIS spectroscopy. The fabricated MIPs sensors were used to detect urea molecules. After that, MIPs sensors have been evaluated their properties such as the sensitivity, linearity range, limit of detection, reproducibility, repeatability, and stability. Furthermore, a similarity structural of urea molecules and coexisting molecules were employed as the interfere molecule for selectivity studies. Finally, the fabricated MIPs sensors were applied to measure the urea in the blood human serum for clinical diagnostics.

Currently, a portable device for measuring and detecting the urea concentration in the blood is unavailable, due to the stability and storage of the enzyme method. In this work, I demonstrated the MIPs-urea sensor, which has a high stability and also can be storaged in ambient. Consequently, MIPs-urea sensor is promising to apply as a portable urea sensor device.

1.3 Objectives of this research

This research focuses on the fabrication the MIPs layer by solvent-assisted drop casting method for urea detection in order to fulfill the following objectives:

1.3.1 Fabrication the MIPs selective membrane on the gold-coated electrode and ISFET sensor for urea determination with a simple fabrication method, which prepared by solvent-assisted drop casting techniques.

1.3.2 Evaluation the MIPs sensors in sensitivity, selectivity, and stability, which can be improved limitations of urease enzyme.

1.3.3 Development the MIPs sensors for urea detection in the real sample (blood human serum) which is promising to apply as a portable urea sensor device for clinical diagnostic.

1.4 Benefit from this research

1.4.1 I success to fabricate the MIPs selective membrane for urea detection on the gold-coated electrode and ISFET sensor, which never reported about fabricated MIPs films on ISFET sensor.

1.4.2 I obtained the electrochemical characteristic of the MIPs sensors which has a high sensitivity and selectivity for urea and has a high stability.

1.4.3 MIPs sensors can be used to detect the urea molecules in the human blood serum, which has a potential to develop for clinical diagnostic devices.

1.5 Details of this research

The works of this thesis were divided into five chapters have a detail as follows:

Chapter 1 is the introduction mention the significant of the urea detection and the advantages of a molecularly imprinted technique for application to biosensors. After that, the scope of this research, the objective, and the benefits expected to be derived from this research.

Chapter 2 is general background about the MIPs biosensor which includes principles of biosensors, electroanalytical chemistry, the ion-sensitive field effect transistor (ISFET), molecularly imprinted technique and fabrication process. The last topic is the literature review about electrochemical biosensor for urea detection in recent years.

Chapter 3 and 4 are fabrication the MIPs selective membrane on the gold-coated electrode and the ISFET sensor, respectively. The results consist of the surface morphology, validation of template removal, and electrochemical behaviors of the MIPs sensors were investigated. Finally, the fabricated MIPs sensors were used measuring the urea in the blood human serum samples.

Chapter 5 is conclusions and outlook of this work.

CHAPTER 2

GENERAL BACKGROUND

2.1 Chemical and biological sensor

The International Union of Pure and Applied Chemistry (IUPAC) provides a definition of "chemical sensor is a device that transforms chemical information, ranging from the concentration of a specific sample component to total composition analysis, into an analytically useful signal" [19]. The best known of chemical sensor is the glass electrode for pH measurement, which indicates the amount of hydrogen ion in a solution. Biosensors are chemical sensors in which the recognition system utilizes a biochemical and biological mechanism [20]. Figure 2.1 shows a typical two basic components of chemical sensors and biosensors contain: recognition and conversion.

1. Recognition system or receptor is a biological substance and not biologically substances, performing to detect and convert data volumes from molecular biochemistry to physico-chemical changes such as enzymes, cells, tissue, microbes, antibodies, selective membrane, nucleic acids, and molecularly imprinted polymers. The most important of recognition systems are specific to an analyte.
2. Conversion system or transducer is a device to converts a physico-chemical signal output from the recognition system such as chemical substance, ions, lights, weight, and heat into measurable electrical signals. These cause biosensors will be transducer various types. The transducer may be called detector, sensor, or electrode.

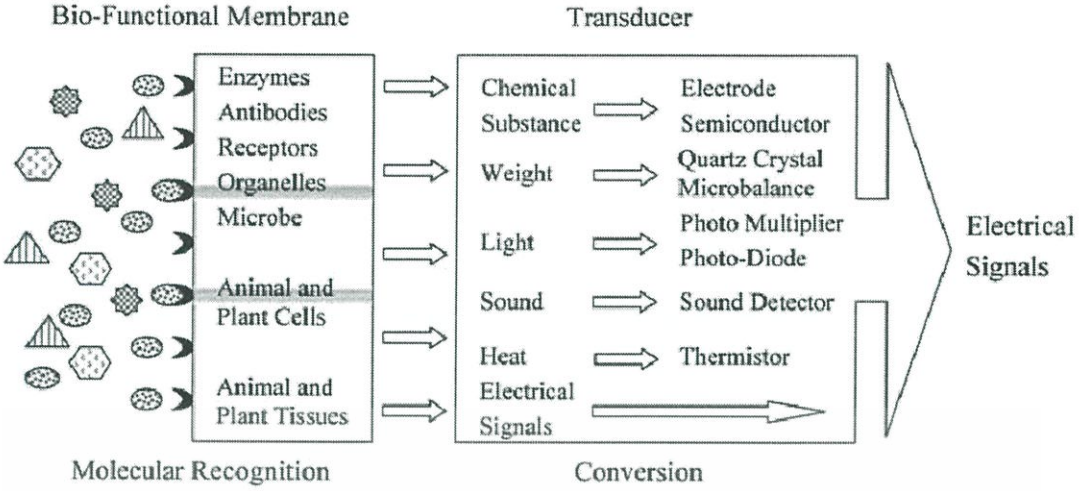

Figure 2.1 Components of biosensors [21].

An electrochemical biosensor is a combination of electroanalytical technique and specificity of the biological recognition element (bio-chemical receptor). The biological receptors were immobilized or entrapped on the electrode as a conductor material or semiconductor or ion conductor material. The aim of this technique is changing the samples quantity by receptors and using electrodes detect output from the receptor with amperometric, potentiometric, and other methods. The electrochemical biosensor first pioneered by Leland C. Clark and Champ Lyons in 1962 [22]. They invented biosensor for measuring the glucose by using enzyme glucose oxidase immobilized onto Clark oxygen electrode.

Table 2.1 shows measurement types and electrochemical transducers for electrochemical biosensors. The measurable electrical signal will be related to the concentration of an analyte. The combination of the biological recognition and electrochemical electrode will occured new devices that an effective to analytical sample, where advantages are easy to use, compact size and affordable.

Table 2.1 Types of measurement, Types of electrochemical transducer, with corresponding analytes to be measured [20].

Measurement type	Transducer	Transducer analyte
1. Potentiometric	ion-selective electrode (ISE) glass electrode gas electrode metal electrode	K^+, Cl^-, Ca^{2+}, F^- H^+, Na^+... CO_2, NH_3 redox species
2. Amperometric	metal or carbon electrode chemically modified electrodes (CME)	O_2, sugars, alcohols... sugars, alcohols, phenols oligonucleotides..
3. Conductometric, impedimetric	interdigitated electrodes, metal electrode	urea, charged species, oligonucleotides..
4. Ion charge or field effect	ion-sensitive field effect transistor (ISFET), enzyme FET (ENFET)	H^+, K^+

2.2 Molecularly imprinted polymers

Molecularly imprinted polymers (MIPs) is a synthetic receptor (artificial receptor) that produced recognition sites for a specific target molecule in a synthetic polymer matrix. A molecular imprinting technique using synthetic polymer matrix was first published in the year 1972-1973 by Gunter Wulff and A. Sarhan [23,24]. A vinyl was applied as the functional polymer for preparing polymer membrane while a racemate was used as molecular templates. After that, in the year 1989, Daniel J. O'Shannessy, et al. [25] reported about the molecular imprinted polymer employing L-phenylalanine anilide as molecular templates and methacrylic acid as the functional monomer. The synthesized polymer film can distinguish L-phenylalanine (printing molecule) and amide derivatives of amino acids. The preparation of MIPs, target molecules was used as a template for imprinting in the polymer structure.

Then molecular templates was removed from polymer matrix, so that the molecular cavities has complementary to the template in size, shape, and functional groups [26,27]. The advantages of the MIPs include, high binding affinity and selectivity towards the analyze molecule (template molecule), high resistance to physical strength, stability against various chemicals and environment of using (temperature, organic solvents, acid and alkaline, and heavy metal ions), lifetimes can be as long as several years at room temperature, furthermore the polymeric membrane easily to synthesis and polymer is cheap price [28–30]. Figure 2.2 illustrates the fabrication procedure of MIPs sensing membrane has 3 steps [31] as follows:

1. Complexation of a template: Mixing the molecular template and the functional monomer in solutions to form a complex (the solvent for this step can be dissolved the molecular template and the functional monomer). For some cases may be added a cross-linker to assist bonding between the polymer and the substrate or the polymer and the template to be attached as well.
2. Polymerization of the complex: After complexation of functional monomer and the molecular template successfully. This template-polymer complex is deposited and polymerized on the substrate. Many techniques can be employed for the co-deposition of the polymer and the molecular template, such as polymerization [32–34], sol-gel synthesis [35–37], electrodeposition [38,39] and solvent evaporation [40,41]. Each technique has its own pros and cons to suit a particular chemical system.
3. Removal of the molecular template: After washing the template from the polymer matrix (the solvent for this step can be dissolved the molecular template, but not dissolved the functional polymer), cavities or recognitions sites are morphologically (size and shape) and chemical groups similar to target molecules hence the prepared polymer film have a specific to the analyte and highly selective.

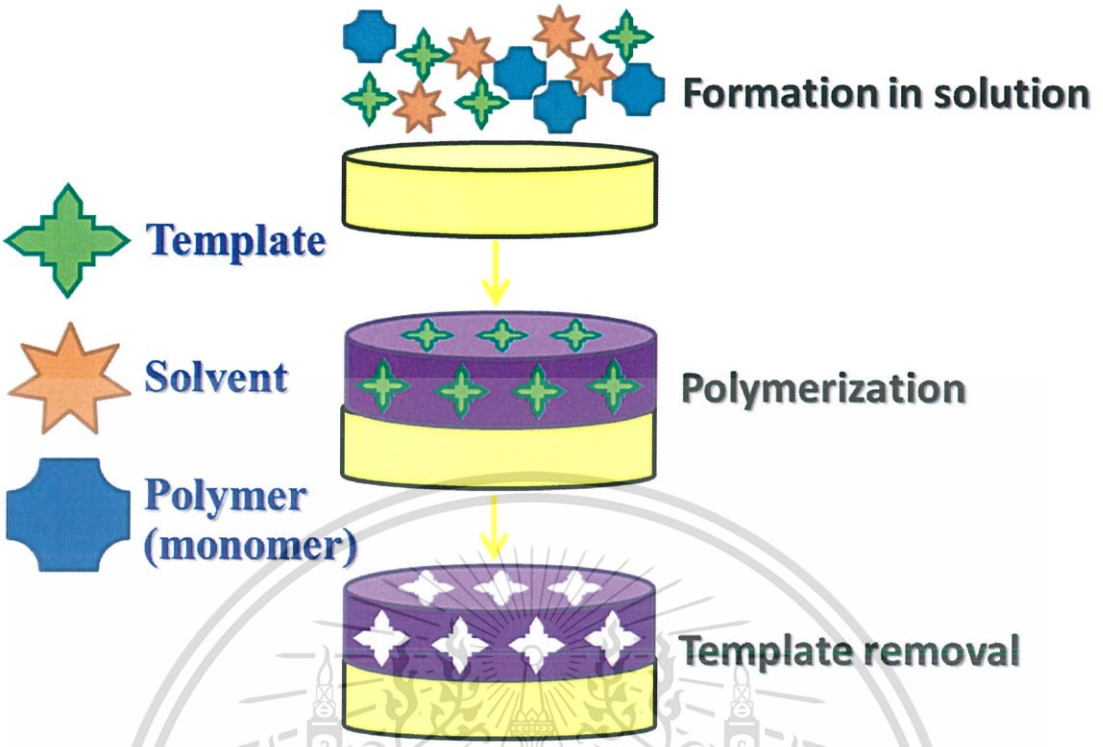

Figure 2.2 Fabrication procedure of MIPs sensing membrane.

Molecular detection is a reverse step of removal the template. The analyte molecule and binding sites will reassemble in the polymer film to form a complex again. The MIPs can applicable to a variety fields and target molecules. An example the application of molecular imprinting technique such as separation and extraction [42–44], drug delivery [45–47], using an artificial receptor for antibodies. [48–51], And applied for the sensor [52–55]. The MIPs usefulness in sensor applications since 1993 by Eva Hedborg, et al [56]. They prepared polymer membranes containing molecular imprints against l-phenylalanine anilide and applied as sensing layer in field-effect capacitors. The C-V measurement results showed that the imprinted polymer membrane can be measured l-phenylalanine anilide and tyrosinanilide in ethanol solution. In addition, The molecularly imprinted techniques are widely applied in sensor development for determinations of molecules [57,58], viruses [59], entire cells [60], and heavy metal [61–63]. The MIPs sensor can be used to various measurement

techniques, especially the amperometry and voltammetry techniques were interested for imprinting polymer films based electrochemical sensors [64,65]. In addition, the MIPs membranes can also be developed as chemical sensors and biosensors with other measurement techniques were shown in Table 2.2

The response of electrochemical MIPs electrodes to target molecules is similarity with enzymatic mechanism, which can be classified into two strategies for molecular detection.

1. Increment signal: After template combined with polymer film, the chemical reaction between polymeric membrane and template molecule may produce charge or electron or ions, leading to higher response signals [66–68]. This process is similar to enzyme catalyzes, which reactions break down the analyte and increasing the response is occurred from the products of their reactions [69,70].
2. Decrement signal: The template molecules that are bound into the cavities the template obstruced charge transfer to the surface of the electrode which results in the reduction of response signals [71–73]. The measuring process of MIPs sensor is similar to the biochemical detection methods via the inhibition of enzymatic activities, in which particular enzymes are exposed to certain target molecules and the response is obtained from the reduction of their activities [74,75].

Table 2.2 Measurement techniques employed in MIPs based sensors [76].

Transducer	Analyte (example)	Useful rang (μM)
General Formates		
ellipsometry	vitamin K_1	qualitative
surface plasmon resonance	theophylline	5000 - 33000
capacitance	phenylalanine anilide	qualitative
	phenylalanine	6000
conductometry	atrazine	0.005 - 0.05
surface acoustic wave	solvent vapors	0.1 μL/L
quartz crystal microbalance	solvent vapors	4 μL/L
	glucose	1000 - 20000
	S-propranolol	50 - 1300
love-wave	2-methoxy 3-methylpyrazine	n.c.
infrared evanescent wave	2,4-D	4.5 - 1000
Analyte Generates Signal		
fluorescence	dansyl phenylalanine	25 - 250
	PAH (pyrene)	0.00015 - 0.2
amperometry	morphine	3.5 - 35
Competitive Binding Formats		
colorimetry	chloramphenicol	10 - 3000
voltammetry	2,4-D	0.01 - 100
Polymer Generates Signal		
pH	glucose	1000 - 25000
fluorescence	cAMP	0.1 - 100

2.3 Electroanalytical chemistry

Electroanalytical chemistry is an analytical technique concerned with the relationship between the electrical signals and chemical reactions. Electrical quantities (current, potential, resistance, and conductance) depend on the parameters or the rate of chemical reactions. This can be used to wide range applications of chemical analytical such as environmental monitoring, food freshness and bioprocess monitoring, and biomedical analysis [19]. Electrochemical processes are analyzed at the electrode-solution interface unlike other chemical measurement techniques are related homogeneous bulk solutions. The difference of electroanalytical techniques (amperometry, potentiometry, and impedance spectroscopy) effects to the kinds of the electrical signal using for the quantitation.

The electroanalytical techniques have two principal types are potentiometric and potentiostatic. Potentiometric is a process that no electric current flows in electrochemical cell (zero-current), the sample composition is obtained by measuring the potential across the electrode–solution interface. Potentiostatic (controlled-potential) is a technique to studies the charge transfer at the electrode-solution interface that is based on the electricity flow (non-zero-current). The electrode was applied voltage from an external source which causes electron transfer across the electrode–solution interface. Both types of the electroanalytical technique include least two electrodes and sample solution (electrolyte) is called the electrochemical cell. One of two electrodes is an electrode that response to the target analyte and this termed the indicator electrode or working electrode. The second electrode is an electrode with constant potential in various solutions and is termed the reference electrode.

Electrochemical cells can be classified into two categories including galvanic and electrolytic cells. Galvanic cells are used to produce electrical energy from a chemical reaction within the electrochemical cell. Electrolytic cells are required

electricity from an external source to cause a chemical reaction between electrode and electrolyte.

2.3.1 Faradaic processes

The aim of electrochemical analysis is to study an electrical current response, which is related to the concentration of an analyte. This can be done by monitoring the electron transfer during the redox processes (oxidation-reduction) of the substance to analyze.

$$O + ne^- \leftrightarrow R \qquad 2.1$$

where O is oxidized form of redox couple.

R is reduced form of redox couple.

For the electrochemical systems that are based on the laws of thermodynamics, the potential of the electrode can be used to determine the concentration of electroactive species at the surface, according to the Nernst equation.

$$E = E^0 + \frac{2.3RT}{nF} log \frac{C_O}{C_R} \qquad 2.2$$

where E is cell potential.

E^0 is standard potential of redox reaction.

R is universal gas constant (8.314 $JK^{-1}mol^{-1}$)

T is the Kelvin temperature.

n is number of electrons transferred in reaction.

F is the Faraday constant (96,487 coulombs).

C_O,C_R are ion concentration of oxidation and reduction reaction.

Redox reactions at the surface of the electrodes cause the electricity current from the movement of charges or electrons across the electrode–solution interface. The resulting current of the change in redox reactions according to the Faraday's law was called the faradaic current. However, the changing of electric current caused the movement of charge on the surface, the accumulation of electrical charge or electrons are not transferred between the electrode–solution interfaces, the current it is termed nonfaradaic current.

2.3.2 Mass transport

Mass transport formed by three distinct categories. These categories of mass transport were shown in Figure 2.3.

1. Diffusion: Movement occurs under the influence of different concentrations, will diffuse from regions of high concentrations to regions of lower concentrations. This process reduces the difference of concentration.
2. Migration: The movement of charged particles in accordance with an electric field. The positive charge move toward the cathode and negative charge move adversative.
3. Convection: Moving to the electrode by physical movement, the external mechanical energy that causes driving forces such as stirring or flow of solution or rotating or vibrating electrode.

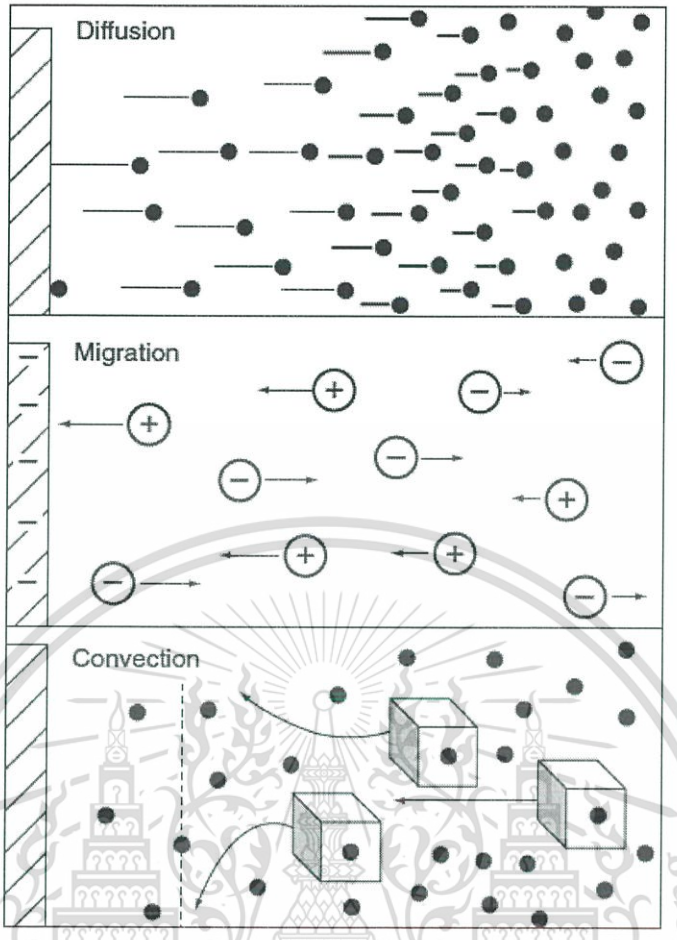

Figure 2.3 The categories of mass transport [77].

2.3.3 Electrochemical cell

The electrochemical cell for controlled-potential experiments usually contains a closed beaker volume of 5 - 50 ml and the three electrodes (e.g., working, reference, and counter) where all are immersed in the sample solution (Figure 2.4). The working electrode is the electrodes for observation the chemical reactions of interest. The reference electrode procures a stable potential (independent on the sample composition) and using compared the potential of the working electrode. The counter electrode is often used the inert metal such as platinum wire or graphite rod for an increase as the current-carrying.

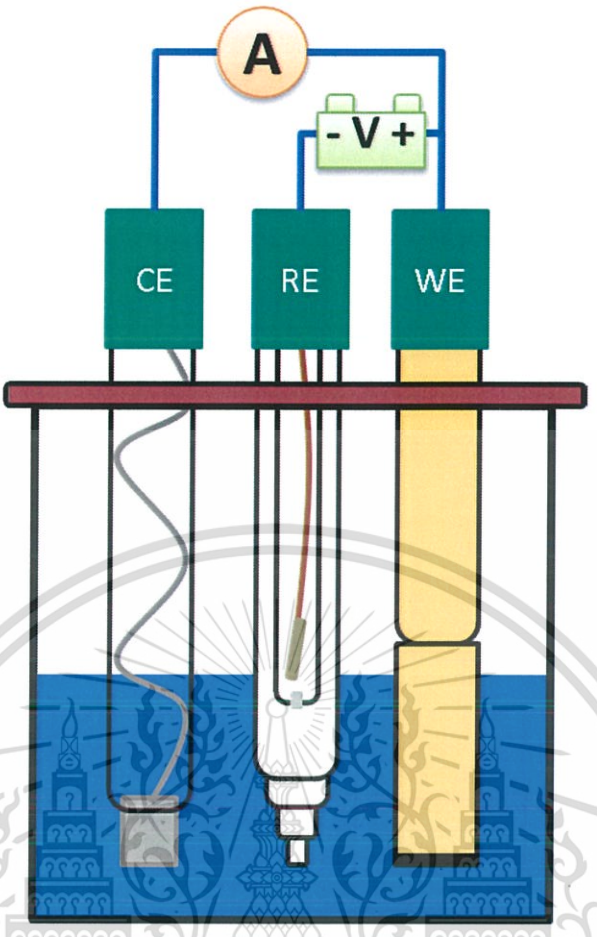

Figure 2.4 Schematic diagram of an electrochemical cell: working electrode (WE), reference electrode (RE), counter electrode (CE).

2.3.4 Electrochemical electrode

Electrodes are major components that performing connects between the electrolyte and an instrument. For the electrochemical cell, require least two electrodes are a working and a reference electrode. In some electroanalytical technique (i.e. voltammetry and amperometry) can be used a three-electrode system, which a third electrode is helpful for electron transfer and that is termed auxiliary or counter electrode.

2.3.4.1 Working electrode

The performance of the electrochemical process is based on the working electrode materials. The working electrode should be a high signal-to-noise, as well as a high repeated response. Therefore, the working electrode selection depends on two factors, the redox behavior of the sample and the background response. Other considerations include the potential window, electrical conductivity, surface reproducibility, mechanical properties, cost, availability, and toxicity. The popular working electrodes used in the electrochemical analysis including.

1. Mercury electrodes are a very interesting electrode for an electrochemical procedure because it has a high hydrogen overvoltage when compared to the solid electrode material, which extends the cathodic potential. Moreover, mercury electrodes have a highly reproducible, readily renewable, and smooth surface. Disadvantages of using mercury are narrow an anodic potential due to oxidation of mercury and the toxicity.
2. Solid electrodes are suitable electrodes for analyzing samples in anodic potential. Popular materials for the working electrodes are inert metals and carbon materials, such as platinum, gold and glassy carbon. Additionally, specific applications can also use silver, nickel, and copper.
3. Chemically modified electrodes (CMEs) refer to a system of electrodes that changes the surface with chemicals or receptors. The modified surface electrodes are an enhanced performance for different samples analysis.
4. Ion-selective electrode (ISE) is an electrochemical electrode specific to ions by employing a selective membrane coated or immobilized on electrodes. For example, the pH measurement at which determine the hydrogen ion of a solution.

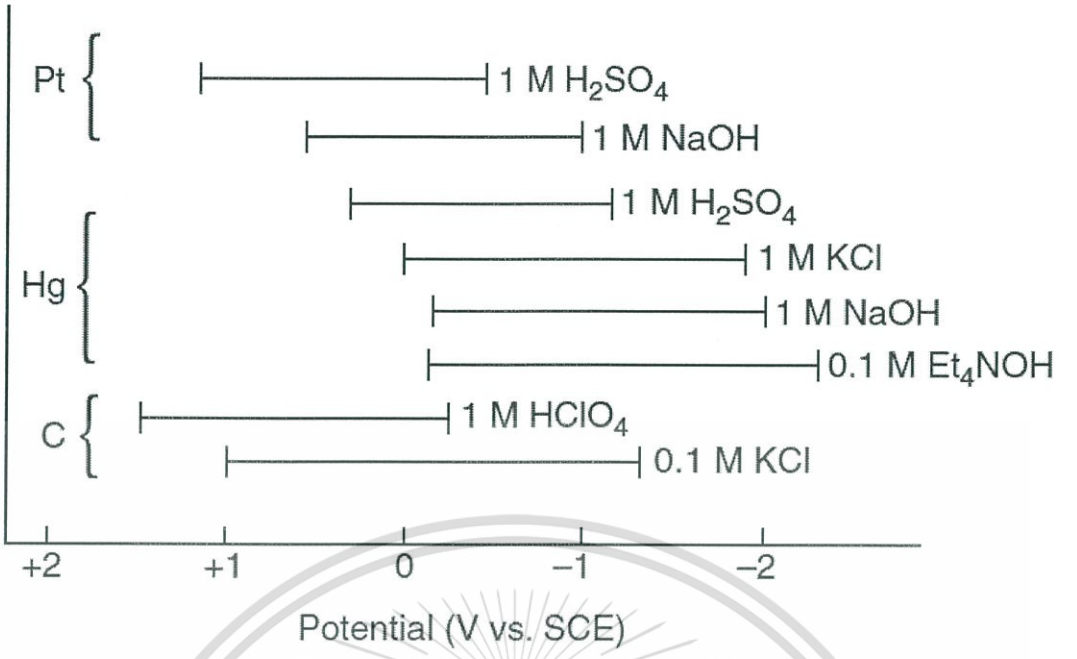

Figure 2.5 The accessible potential of platinum, mercury, and carbon electrodes, in various solvents.

2.3.4.2 Reference electrode

The reference electrode is an exact potential electrode, independent of ions concentration in the sample solution. In addition, the reference electrode requires good stability properties, does not change with temperature, and easily storage. Normally, the applied potential or output voltage of electrochemical cell using differential potential between the working electrodes versus the reference electrode. Reference electrodes for the electroanalytical chemistry can be classified three types.

1. Hydrogen reference electrode consists of the cleaned sheet platinum was coated with platinum powder (platinized platinum). This is inserted into a glass tube containing hydrogen gas where can be pressure control. The standard hydrogen electrode (SHE) will be saturated with hydrogen gas all the time, under the pressure of one atmosphere (atm). The standard hydrogen electrode has the potential of 0.00 volts.

2. Saturated calomel electrode (SCE) consists of two layers of glass tubes, the inner glass tube has a wire lead (Pt wire) immersing in a mixture of mercury and mercury (I) chloride (Hg_2Cl_2 or Calomel). The outer glass tube is a solution of saturated potassium chloride (KCl). The electrode has a porous tip for a contact with the external solution. This porous tip is a salt bridge.
3. Silver/Silver chloride reference electrode (Ag/AgCl) is a glass tube electrode with a wire lead (Ag wire) that is coated with silver salts (AgCl). It is immersed in a saturated potassium chloride solution. The end of the glass tube is a porous material for a contact between potassium chloride and sample solution.

2.3.5 Supporting electrolyte

Electrochemical measurements are generally performing in a solvent that containing a supporting electrolyte. The solvent selection will consider by the solubility of the analyte and redox activity. In addition, properties of a solvent such as electrical conductivity, electrochemical activity, chemical reactivity, and the solvent should not react with the analyte were inspected. Water is used as a solvent more than other intermediaries. Besides, there are other non-aqueous solvents also been used e.g., acetonitrile, propylene carbonate, dimethylformamide (DMF), methanol, and dimethylsulfoxide (DMSO).

Electrochemical experiments are required supporting electrolytes to reducing the resistance of the solution, eliminating electromigration effects, and maintain the strength of ionic strength. [78] The supporting electrolyte may be an inorganic salt, mineral acid, or buffer which it depends on solvents. When the solvent is water, the supporting electrolytes are commonly used potassium chloride or nitrate, ammonium chloride, sodium hydroxide, or hydrochloric acid. While tetraalkylammonium salts are often employed in organic solvents. For systems are require pH control, buffers (acetate, phosphate, or citrate) are useful for maintaining the pH

value. The supporting electrolyte should be the preparation from high purity chemicals and should not be oxidized or reduced easily. The electrolyte concentration range is 0.1 - 1.0 M, which the concentration greater than the concentration of all electroactive species.

2.4 Electrical double layer

The electrical double layer is the array of charged particles and/or dipole existing at all material interface. In electrochemistry, this layer considers to the ionic regions formed in solution to offset the excess of the charge on the electrode (q_e). The electrode has a positive charged will attract a layer of negative ions and electrode that is negatively charged, it will attract a layer of positive ions. Thus, the interface must be a neutral charged, $q_e + q_s = 0$ (when q_s is the charge of the ions in nearby solution). The electrical double layer as shown in Figure 2.6 consisting of two ions layers.

The inner layer (closest to the electrode) was called compact layer, this layer includes the inner Helmholtz plane (IHP) and the outer Helmholtz plane (OHP). The inner Helmholtz plane contains molecules of solvent and specifically adsorbed ions. The outer Helmholtz plane is an imaginary plane by dragging through the center of the solvated ions at closest to the surface. These ions are nonspecifically absorbed and are attracted to the surface by the coulomb forces.

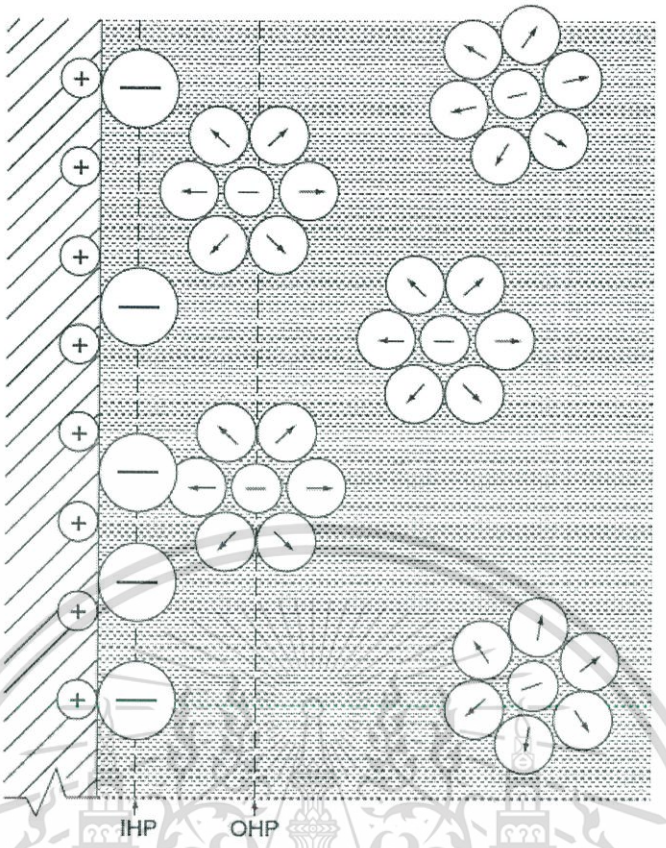

Figure 2.6 The electrical double layer represented the electrode–solution interface.

The outer layer (beyond the compact layer) was called diffusion layer, this area has distributed of ions in three dimensions, which extend from the OHP to the bulk solution. The ionic distribution demonstrates the counterbalance between other forces of the electrical field and disorders caused by the random thermal motion. The equilibrium between these two opposing effects indicates that the concentration of ionic species in accordance with the Boltzmann equation.

$$C(x) = C(0)exp^{(-zF\emptyset/RT)} \qquad 2.3$$

where $C(x)$ is ion concentration in distance from the surface.

$zF\emptyset$ is electrostatic energy.

RT is thermal energy.

The total charge of the compact and diffuse layer equals to the net charge on the electrode. The potential across the double-layer area related two parts, a linear from surface electrode until the OHP and an exponential function up to the diffuse layer. The potential drops across two-part of the double-layer shown in Figure 2.7 which depending on the ionic strength. The thickness of the double layer may extend to more than 10 nm.

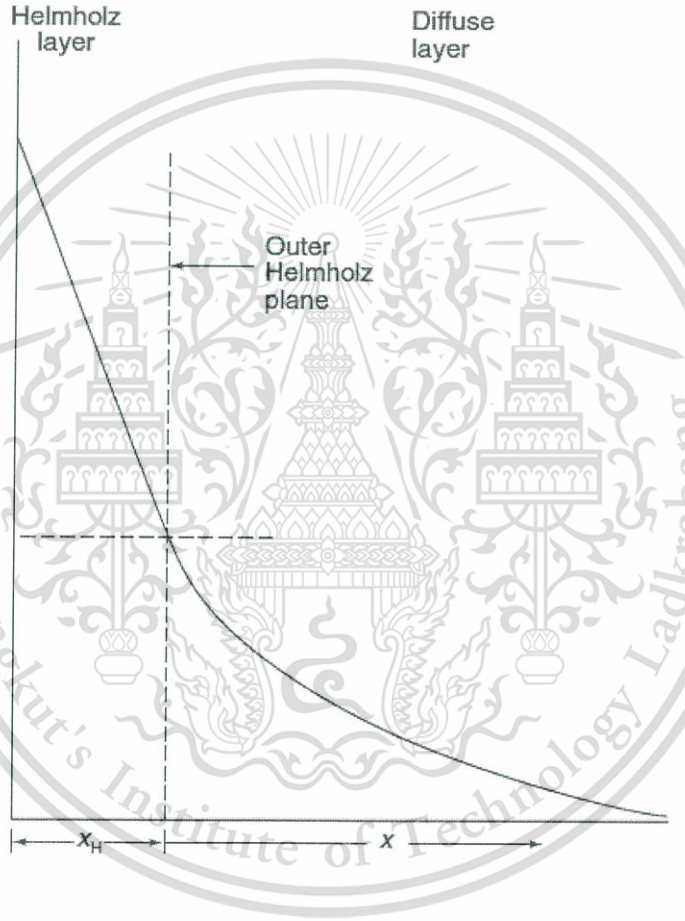

Figure 2.7 The potential across the electrical double layer.

2.5 Cyclic voltammetry

Cyclic voltammetry is most commonly used technique for the acquisition of qualitative information about the electrochemical reaction and is often the first choice in the electroanalytical study. The cyclic voltammetry is capable of providing the thermodynamics of redox reaction and kinetics of heterogeneous electron transfer and coupled chemical reactions. The operation process consists of applying potential of a stationary working electrode and an unstirring solution, in the waveform of a triangle as shown in Figure 2.8. The number of scan cycles depends on the desired information. During scans, the electricity current was measured from the applied potential. The resulting current–potential plot, known as the cyclic voltammogram, is a display of current signal (vertical axis) versus the excitation potential (horizontal axis).

The expected of a reversible redox couple was illustrated in Figure 2.9. It is supposed the initial state that only the oxidized form *"O"*. A potential scan the first half cycle is a negative going (forward scan), from a potential when no reduction reaction. The applied potential is increased, a cathodic current increasing until a peak reached. The maximum current is called cathodic peak current (i_{pc}) and the potential where the peak current called cathodic peak potential (E_{pc}). After that, the direction of potential scan is reversed (reverse scan), the reduced form *"R"* (generated in the forward half-cycle) are reoxidized back to *"O"*. The resulting current in anodic current is termed anodic peak current (i_{pa}) and the potential where the peak current as known, anodic peak potential (E_{pa}).

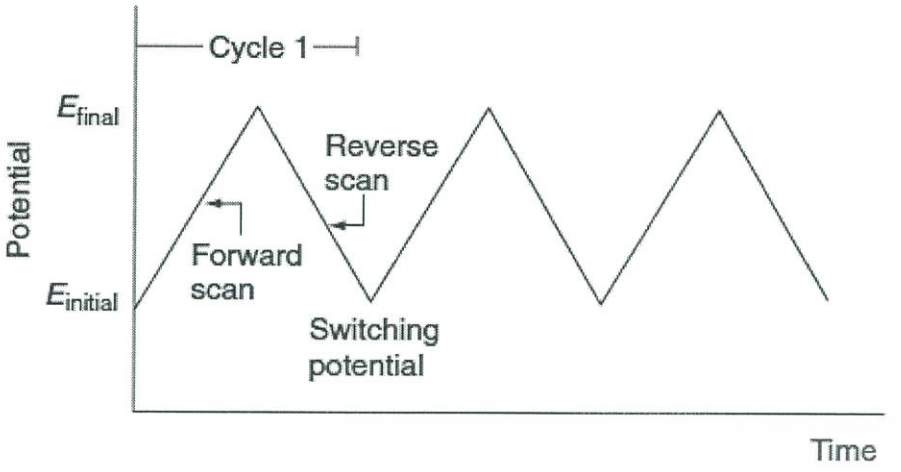

Figure 2.8 Pattern of potential–time in a cyclic voltammetric experiment.

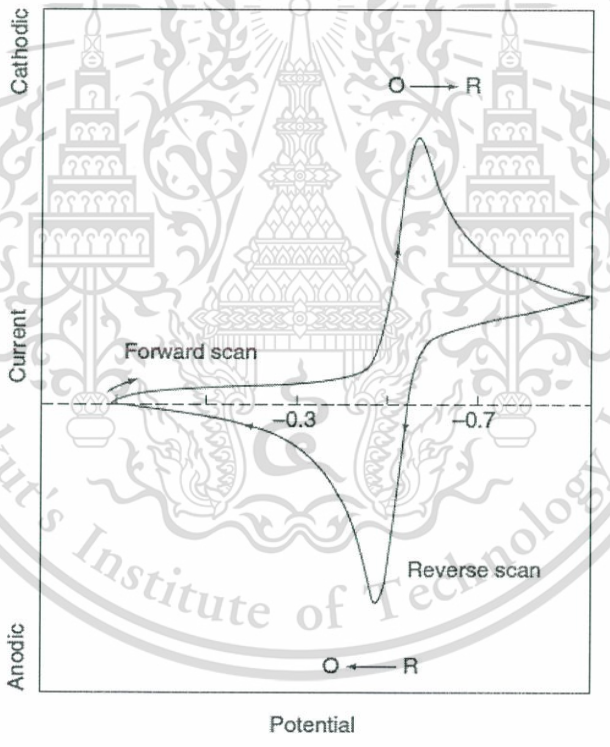

Figure 2.9 Typical cyclic voltammogram for a reversible redox process.

Data interpretation of cyclic voltammogram is characterized by four significant parameters, two peak currents and two peak voltages. The basic principles for analyzing the cyclic voltammetric response was developed by Nicholson and Shain

[79]. For reversible couple cyclic voltammetric, the peak current (i_p) (at of 25°C) can be determined from the Randles-Sercik equation.

$$i_p = (2.69 \times 10^5) AC \sqrt[3]{n} \sqrt{Dv} \quad 2.4$$

where n is the number of electrons.

A is the electrode area (in cm^2).

C is the concentration (in mol/cm^3).

D is the diffusion coefficient (in cm^2/s).

v is the potential scan rate (in V/s).

The electric current is directly proportional to the concentration and the square root of the scan rate. Thus, the scan rate is an indicator of the reaction at a surface electrode that controlled by mass transport. The ratio of peak current reverse-to-forward i_{pr}/i_{pf} is indicative of reversible redox reactions. Typically, the current peaks are measured by extending the preceding baseline current (background current) and find out the difference between the current peak and the baseline.

The position of the potential peak (E_p) relate to the formal potential (E^0) of redox process. The formal potential for a reversible reaction is center between E_{pa} and E_{pc} which can be calculating by equation 2.5, and calculate the number of electron transfer (n) from the equation 2.6.

$$E^o = \frac{E_{pa}+E_{pc}}{2} \quad 2.5$$

$$\Delta E_p = E_{pa} - E_{pc} \cong \frac{0.059}{n} \quad 2.6$$

2.6 Chronoamperometry

Chronoamperometry is a controlled-potential technique which measured the current response from applied stepping potentials of the working electrode. The applied potential starting at non-faradaic reaction occurs (E_1) to a potential that change the electroactive species on the surface of the electrode (E_2) as displayed in Figure 2.10 (a). In this experiment used a stationary working electrode and unstirred solution, the reaction is based on the mass transfer by diffusion only. The current–time curve reflects to changing the concentration gradient in the vicinity of the surface. Accordingly, Figure 2.10 (b) displays the current response decreasingly in time, as given by the Cottrell equation.

$$i(t) = nAFC\sqrt{\frac{D}{\pi t}} \qquad 2.7$$

where n is the number of electrons.

A is the electrode area (in cm^2).

F is Faraday's constant (96,487 coulombs).

C is the concentration (in mol/cm^3).

D is the diffusion coefficient (in cm^2/s).

t is time.

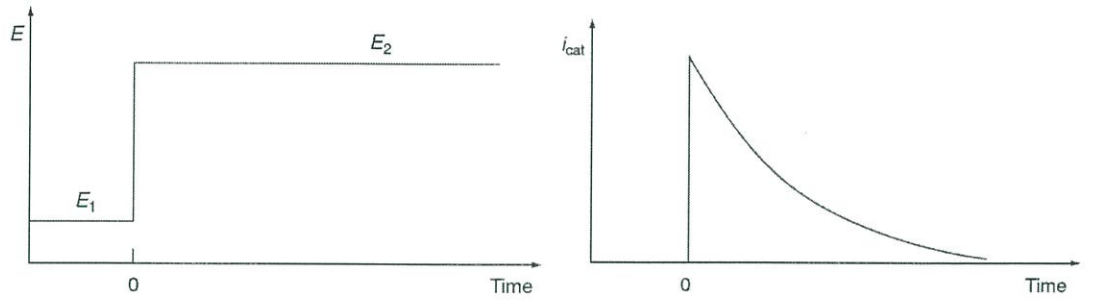

Figure 2.10 The potential–time waveform (a) and the resulting current–time response (b) for Chronoamperometry experiment.

2.7 Potentiometry

Potentiometry is a technique that exploits the potential of a galvanic cell, depends on the activity of ions in the solution. Thereby, information on the composition of a sample is obtained through the appearing potential between two electrodes. One of two electrode is the indicator electrode or working electrode, this electrode was coated with the ion-sensing membrane (ISM) when integrated with working electrode was so call ion-selective electrode (ISE). The potentiometric electrodes have been widely used for direct monitoring of ionic species e.g., protons, calcium, fluoride, and potassium ions in complex samples. The other electrode is the reference electrode which does not depend on the concentration of ions in the solution and has a constant voltage. Figure 2.11 illustrates the electrochemical cell for potentiometric technique. The potential of the cell is proportional to the difference potential of the working electrode versus reference electrode and the concentration of ions in solution.

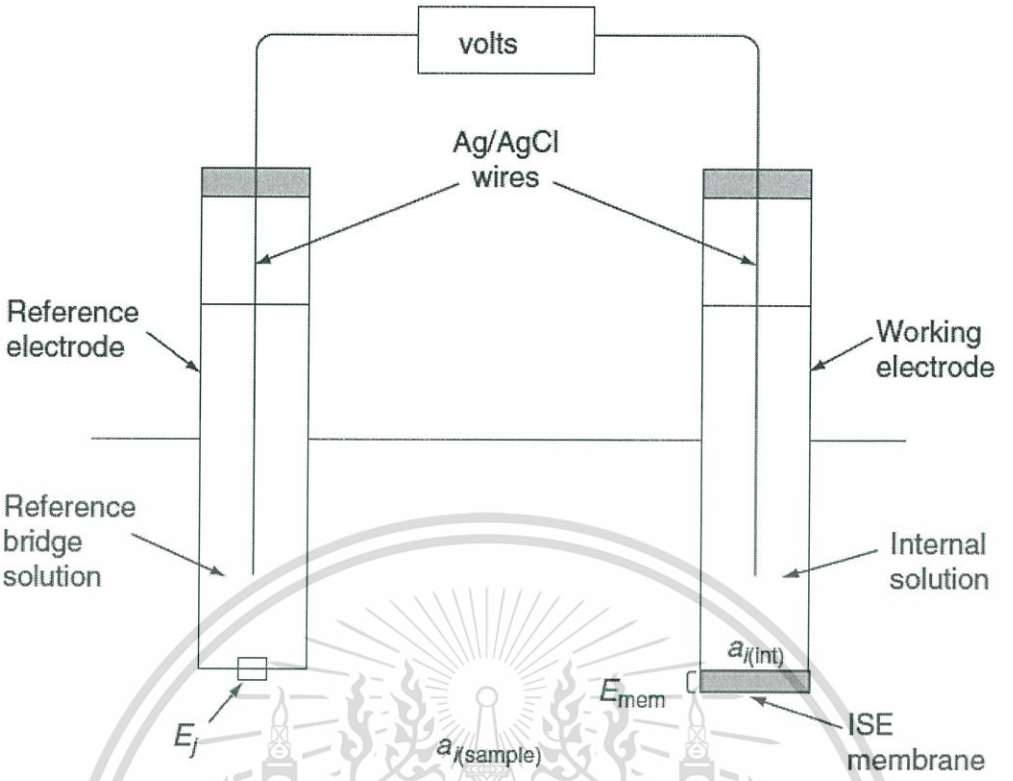

Figure 2.11 Schematic of electrochemical cell for potemtiometry experiment.

2.8 Ion-sensitive field effect transistor

Ion-Sensitive Field Effect Transistor (ISFET) was invented by Piet Bergveld in 1970 [80]. He presented the experimental about removal the metal gate electrode of MOSFET (Metal Oxide Semiconductor Field Effect Transistor) device and measuring the electrical characteristic of this device in varying hydrogen ion (H^+) solution. The result displays the voltage at the interface between the insulating layer and solution dependent on the hydrogen ion concentration or the pH value. After that, the metal gate electrode was replaced by the metal chloride reference electrode for the stability of electrical signal measurements. [81]. The structural difference between MOSFET and ISFET was illustrated in Figure 2.12. The ISFET is a solid-state electronic device that manufactures by same technology with microchips has significant

advantages. The sensing area is very small, a single miniature chip would be contained multiple gates and used to sense several ions simultaneously. Other advantages include the in situ impedance transformation and the ability for temperature and noise compensation [82,83].

The ion-sensing membrane was added on a gate surface of ISFET which is the response to the hydrogen ions. Properties of the materials used for the ion-sensing membrane must be an insulator and able to resist the corrosive in acidity and alkalinity as well. Popular materials were employed ion sensing membrane of ISFET e.g., amorphous-Si [84,85], Ta_2O_5 [84], WO_3 [84], Al_2O_3 [86], Si_3N_4 [87], SnO_2 [88], and TiO_2 [89].

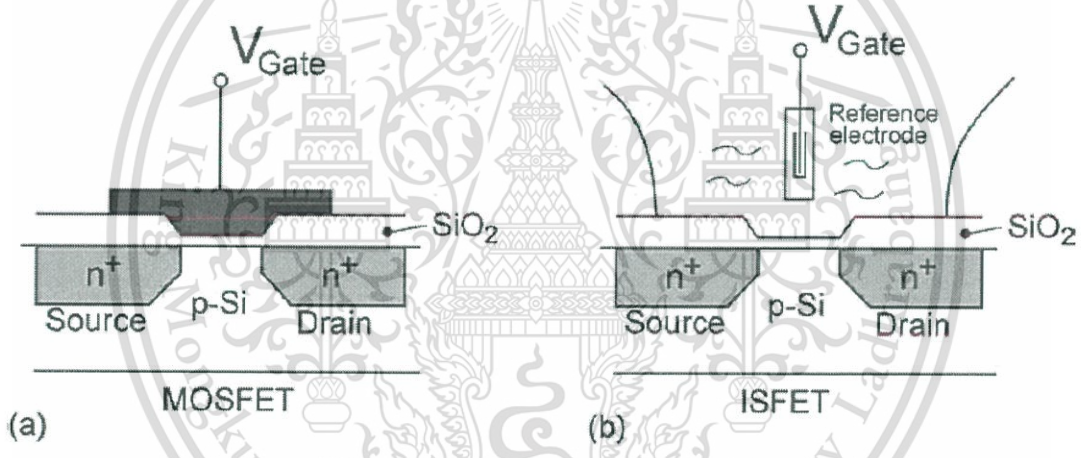

Figure 2.12 Schematic structure of MOSFET (a) and ISFET (b) [90].

The response to ions of ISFET sensor can be explained by the relationship between the insulator–solution interfaces. The schematic of the insulator–solution interfaces was shown in Figure 2.13. Normally, the surface of the insulator consists of a hydroxyl group (-OH) in the case of silicon dioxide the hydroxyl groups are SiOH. The hydroxyl groups on the surface of silicon dioxide commonly are neutral and act as proton donor or proton acceptor which can change the total charge at the surface to a positive or negative [91]. Thus, changing a pH value of the solution would cause

changing of the voltage at the insulator–solution interfaces, the drain current can transfer from drain to source electrode of the transistor.

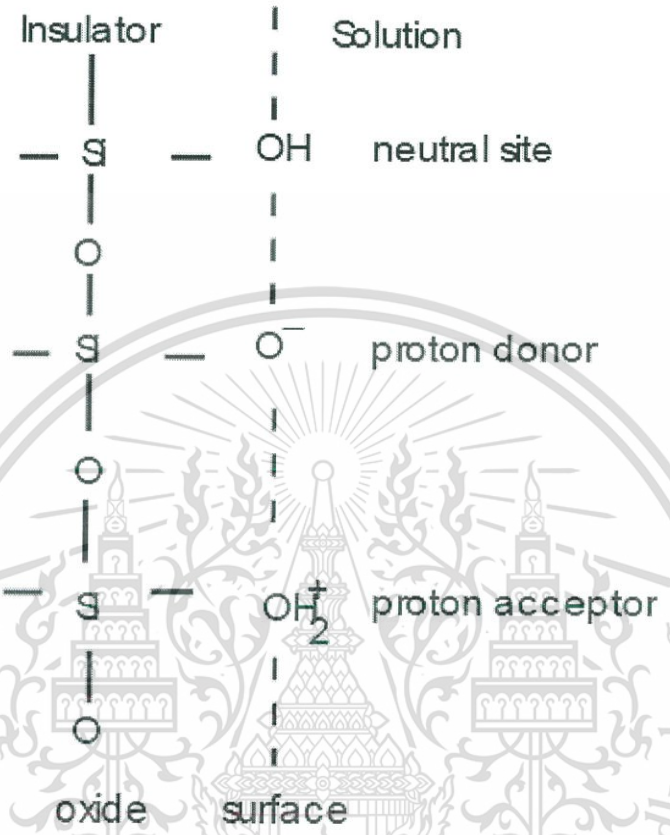

Figure 2.13 The insulator–solution interfaces of silicon dioxide.

The applications of ISFET technology has expanded and a wide-ranging field. Particularly, the applications in biomedical science and environmental monitoring are remarkable. The key development is the coating on the gate electrode surface or the fabrication of ion sensing membrane to analytical biochemistry that the ISFET can perform. The ISFET biosensor was introduced in 1980 by Caras and Janata [92]. They presented integration between the enzyme and ISFET sensor that was called enzyme field effect transistor (ENFET). The penicillinase enzyme was immobilized on the surface ISFET sensor for penicillin detection. This sensor can be measured penicillin

in the concentration range between 0.1 - 25 mM. Moreover, the ISFET platform has been applied as biosensors for the detection of biomolecules such as glucose [93], triglycerides [94], creatinine [95] galactose and polyphenol [96]. Since ISFET sensors have a small size, thus the ISFET was developed to sensor arrays for sensing several ions. Sibbald et al. [97] reported about a ChemFET (chemical-sensitive field effect transistor), this sensor can measure 4 type ions simultaneously e.g., potassium, sodium, calcium, and pH in whole blood samples. Presently, a variety of ISFET-type biosensors has been developed and exploited including ImmunoFET (Immunologically modified FET) [98], DNA-FET (DNA modified FET) [99,100], and CPFET (Cell-potential FET) [101].

2.9 Literature review

The biosensors for urea detection using the electrochemical method was invented first time by Guibault and Montalvo in 1969 - 1970 [102,103]. The urease enzyme was immobilized on the glass electrode with an ammonium ion (NH_4^+) sensing membrane (Figure 2.14). The urease catalyzes the hydrolysis of urea to produce ammonium and bicarbonate ions as shown in Figure 2.15. This ammonium ion electrode will measure the concentration of ammonium ions which is the product of urea hydrolyzed. The invented urea biosensor can measured urea concentration in the range of 0.6 - 200 mg/100 ml.

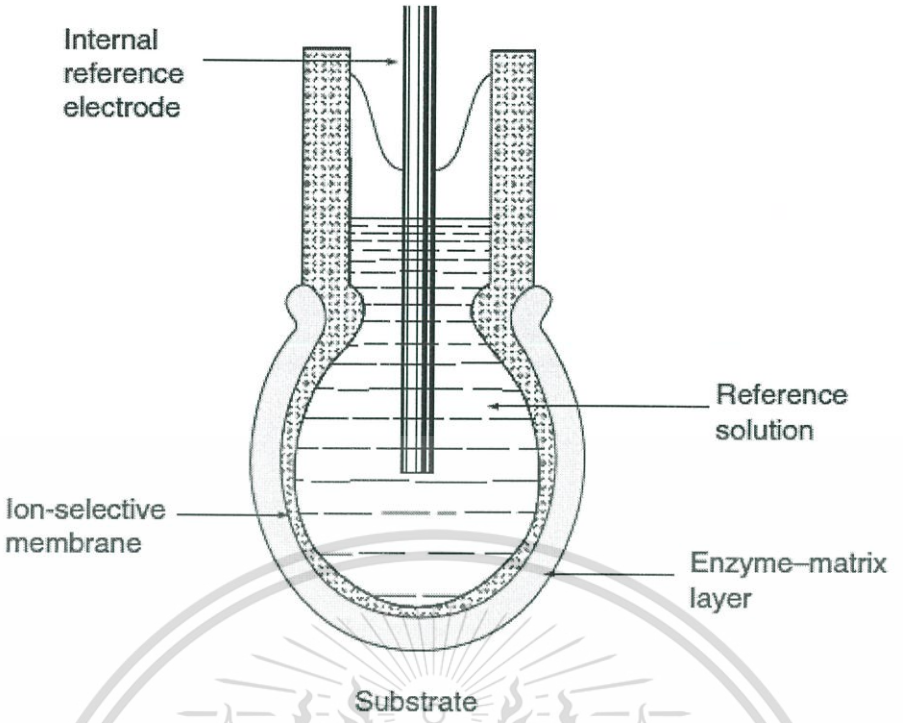

Figure 2.14 Urea biosensor using immobilized the urease enzyme on the ammonium ion electrode [102,103].

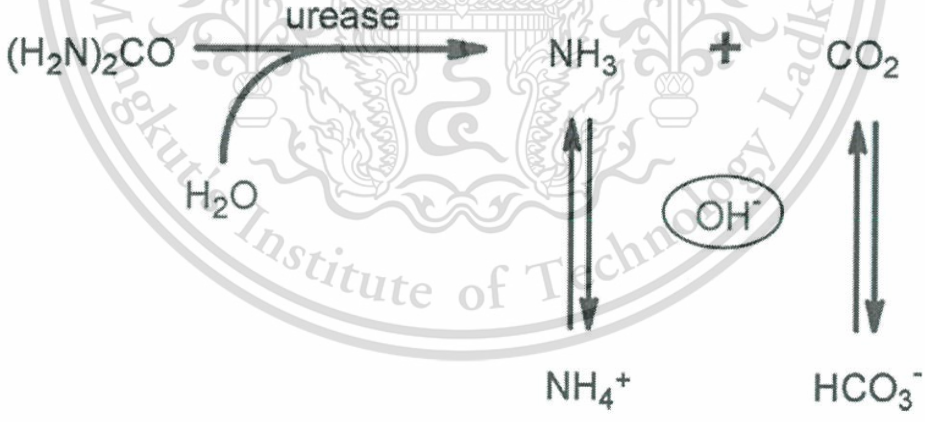

Figure 2.15 The urease catalyzes the hydrolysis of urea [104].

After that, in 1972 Guibault and Shu [105] has developed a urea biosensor using urease enzyme and the carbon dioxide sensor as a transducer, which the hydrolysis of urea produces a carbon dioxide (Figure 2.15). The fabricated urease

based biosensor with carbon dioxide sensor can be measured urea in the concentration range between 1.0×10^{-4} - 1.0×10^{-1} M. In addition, urea can determine by measuring ammonia (NH_3) [106] and pH changes [107].

The development of urea biosensor using urease enzyme combines with ISFET sensor, the schematic was shown in Figure 2.16. For urea biosensor microdevice, urease enzyme was immobilized on the ISFET surface and detect pH change, which is product from enzymatic hydrolysis [108–110]. Many methods were used immobilized urease on the surface of ISFET sensors such as entrapment in a polymer structure, covalent bond, and using crosslinker [111–115]. The advantages of ISFET sensor for applied to urea biosensors consisting of rapid response, small size, and integrated multi-sensor in a single chip. However, the difficulties of ISFET biosensor for urea detection are the drift (shift of the response signal) and change the pH of the sample solutions. This problem was solved by using the two types of ISFET sensors in a single microchip. One type of ISFET sensor was immobilized by urease for sensing to urea, other type is bare ISFET sensor for reference ISFET (REFET). The output signal was calculated from difference voltage of two types ISFET sensors. In order to compensate the signal causing the drift of the ISFET and change the pH of the sample solutions [116]. Applications of electrochemical urea biosensors in field of clinical diagnostics, food science, and environment by measuring urea in many samples such as saliva [117], blood serum [118], hemodialysis [119], urine [120], milk [121], heavy metal [122].

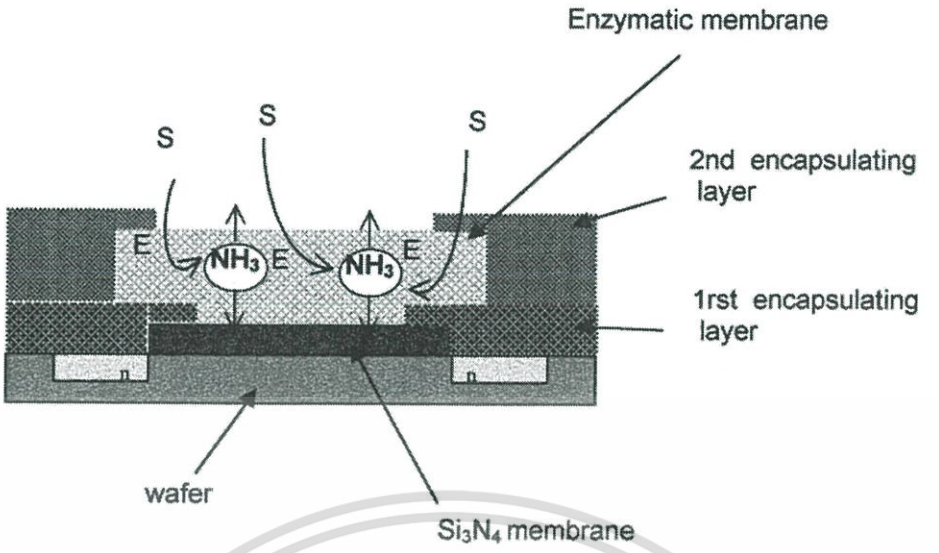

Figure 2.16 Schematic representation of the ENFET layout and the response mechanism [123].

Since using of urease enzyme as urea biosensor has limited in enzyme activity, enzyme stability, and the environment of using. A non-enzymatic biosensor has been developed for solving the limitations of urease. In 2013, Mondal and Sangaranarayanan [15] published non-enzymatic urea sensor, which has the advantages of (i) More economical; (ii) having a fast response time; (iii) easy to prepare; (iv) non-enzyme; (v) insensitive to minor variations in temperature and pH of the medium. Figure 2.17 illustrates the preparation process and detection mechanism of urea sensor non-enzymatic type. The conducting polymer namely polypyrrole (PPy) was coated on the platinum (Pt) electrode by the electrochemical polymerization technique. The measurement process is measured urea in hydrochloric acid (HCl), in the acid condition, urea was hydrolyzed to producing ammonium ion and then ammonium ion was reducing by polypyrrole coated on the platinum electrode. Determination of urea for this sensor is available for two electrical signal types are current and impedance (Figure 2.18). The response of the polypyrrole coated platinum to urea was found to be linearity in the range of 80 -

1440 μM, with the limit of detection for urea is 40 μM. The disadvantage of polypyrrole coated platinum easily interferes from other molecules. Figure 2.19 displays the current response of this sensor has decreased when addition other molecules into the urea sample solution, indicate that the polypyrrole coated platinum electrode low selectivity to urea.

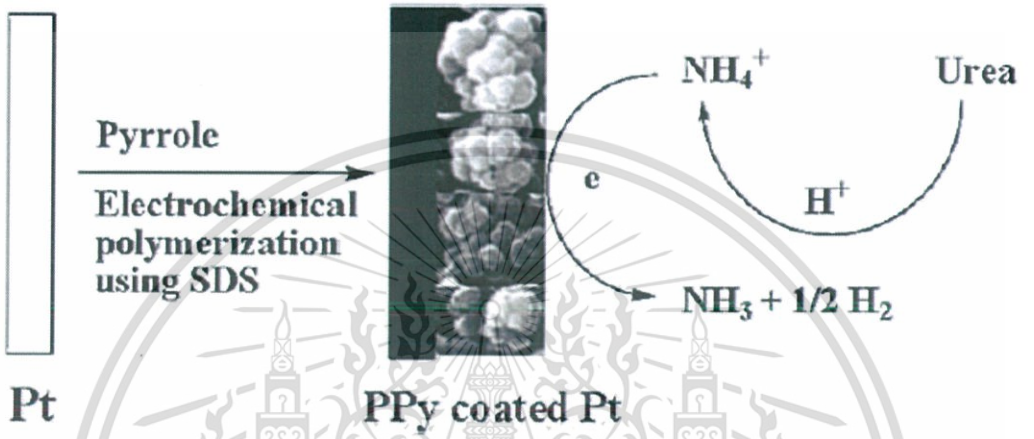

Figure 2.17 Preparation process and detection mechanism of polypyrrole coated platinum electrode for urea sensor [15].

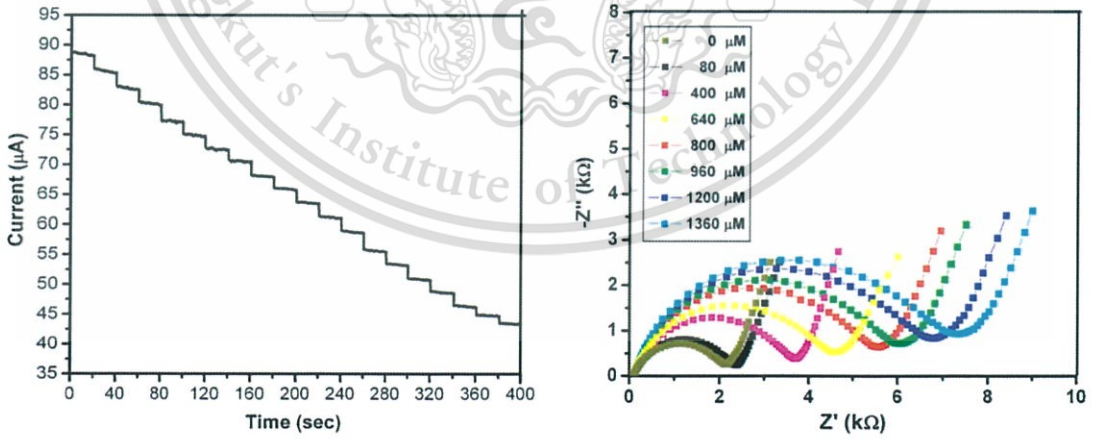

Figure 2.18 Determination of urea by polypyrrole coated platinum electrode using current detection (left) and impedance detection (right) [15].

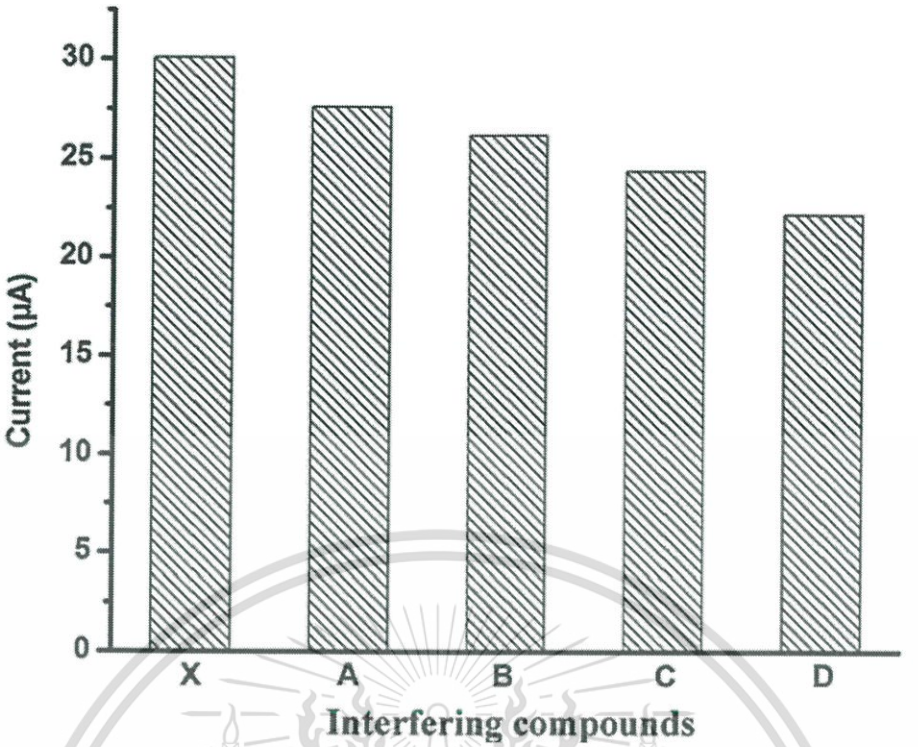

Figure 2.19 The current response of polypyrrole coated the platinum electrode to urea concentration 160 μM (X), and addition 25 μM of ascorbic acid (A), 50 μM of uric acid (B), 30 μM of NaCl (C), 15 μM of CaCl (D) [15].

The other type of non-enzymatic urea biosensor was invented by R. C. Bianchi, et al [16]. The gold electrode was modified by 4-mercaptopyridine (MCP) and L,L-diphenylalanine, respectively. L,L-diphenylalanine is the peptide which catalyzed urea similar to urea hydrolysis by urease. After that, the gold oxyhydroxide (AuOH) clusters on the surface of the gold electrode occurred redox reaction to producing ammonia (NH_3) and gas carbon dioxide (CO_2). Figure 2.20 shows the measurement mechanism of peptide-modified gold electrode urea sensor, which the linearity response in the range of 0.1 - 1.1 mM, with the limit of detection is 0.06 mM.

Both types of non-enzymatic urea biosensors show the disadvantages in the narrow range of the linearity response as between 0.8 - 1.5 mM, which not suitable for applied to measure urea in blood human serum.

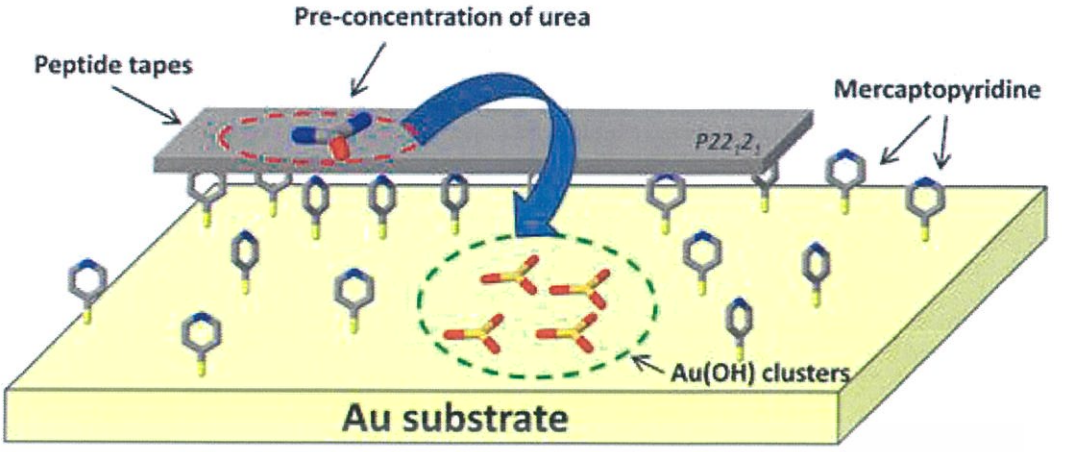

Figure 2.20 Mechanism of peptide-modified gold electrode for urea detection [16].

Molecularly imprinted polymers (MIPs) was applied for the urea molecule by Taher Alizadeh in 2010 [32]. Alizadeh presented the MIPs using as an adsorber for solid phase extraction (SPE). The MIPs was synthesized by using methacrylic acid (MAA) as functional monomer, ethylene glycol dimethacrylate (EGDMA) as cross-linker and urea as the template molecule. Polymerization process takes in a water bath at 60°C for 12 h. And then, urea template was washed by hot ethanol, ethanol/water, and 0.1 M of sulfuric acid solution.

The developed MIPs was evaluated the selectivity and adsorption capacity to urea and molecular structurally similar to urea including four species e.g., thiourea, hydroxyurea, ethylenediamine, and thiocyanate. Figure 2.21 illustrates the MIPs highly selectivity to urea when compared with other molecules. Particularly, comparison with thiourea is very structural similarity due to the sulfur atom (S) has the larger size than oxygen atom (O) in urea. In addition, the higher electronegativity of oxygen than sulfur makes the polarity of –C=O group in urea higher than –C=S group in thiourea resulting in the stronger interaction taken place in the cavity sites of MIPs. Figure 2.22 shows calibration curve of MIPs has linear range between 0.6 – 8.3 μM, with the limit of detection was obtained to be 0.14 μM.

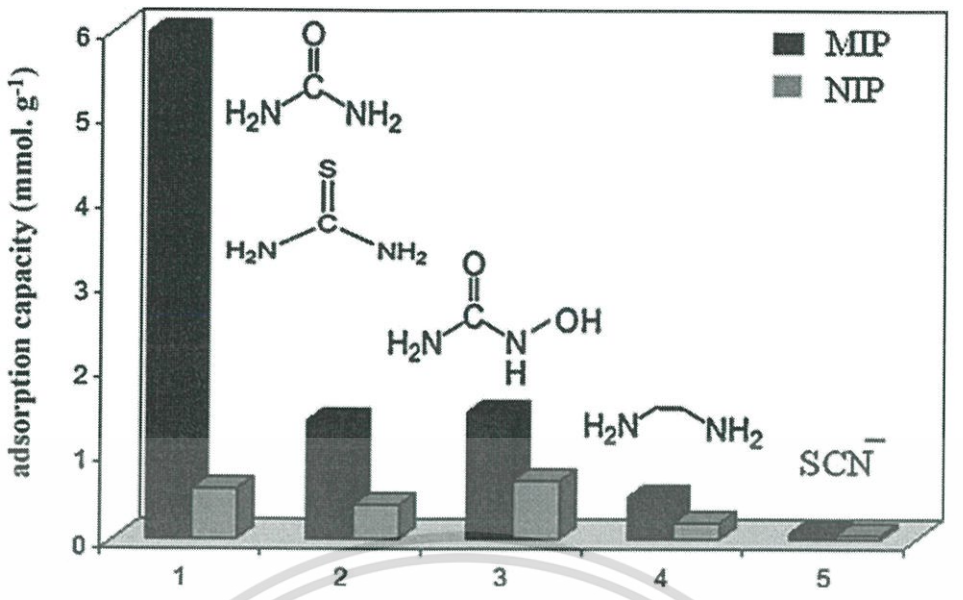

Figure 2.21 Selectivity of developed MIPs to different molecules which are structurally similar to urea [32].

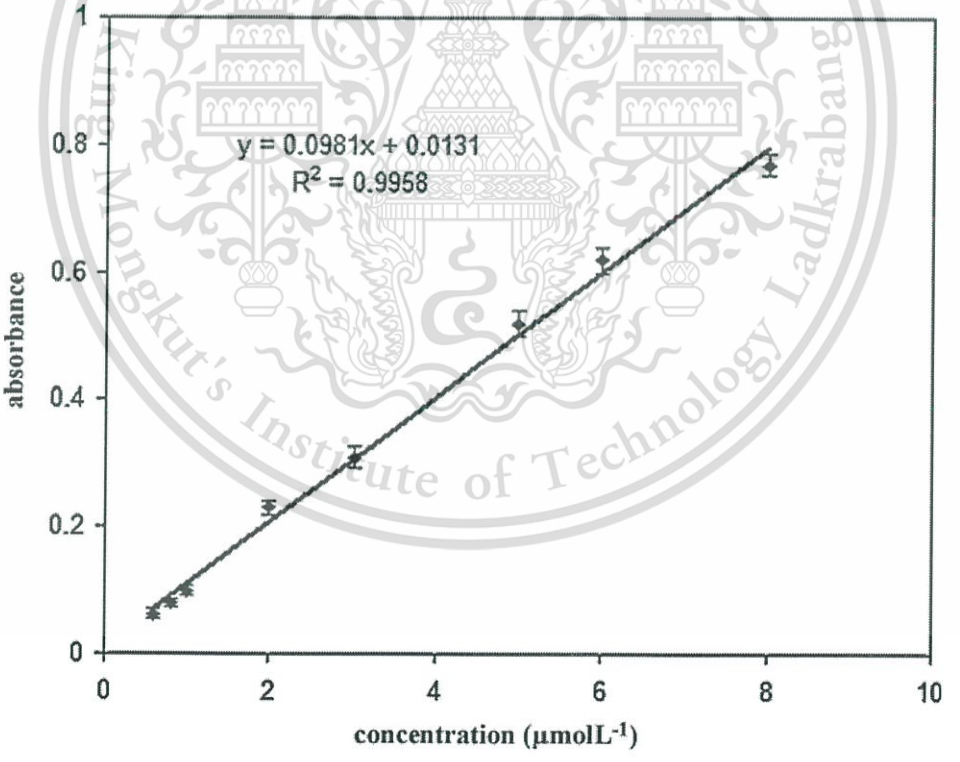

Figure 2.22 Calibration curve for urea determination by using MIPs based SPE [32].

In the same year, Basma Khadro et al. [41] presented the MIPs films on gold substrates for urea detection by an electrochemical technique. The preparation of urea-imprinted thin film includes four steps: (I) mixing polymer using poly(ethylene-co-vinyl alcohol), (EVAL) and urea template in DMSO, and casting on a gold electrode. (II) Removal DMSO by solvent evaporation at ambient temperature. (III) Washing template urea by rinsing 20 mL of methanol and deionized water for 10 min, repeated three times. (IV) Immersion the polymer films overnight in phosphate buffered saline (PBS) before use. The urea detection was determined by electrochemical impedance spectroscopy (EIS) technique using a three-electrode system. The EVAL modified electrode was used as the working electrode, the platinum strip and Ag/AgCl (saturated KCl) were used as counter and reference electrode. Figure 2.23 displays the responseof the urea-imprinted electrode. This sensor represents a detection limit as 10 ng/ml, and a linear range of 0.02 - 3 µg/ml. In addition, The EVAL MIPs thin film exhibits a good stability during prolonged storage.

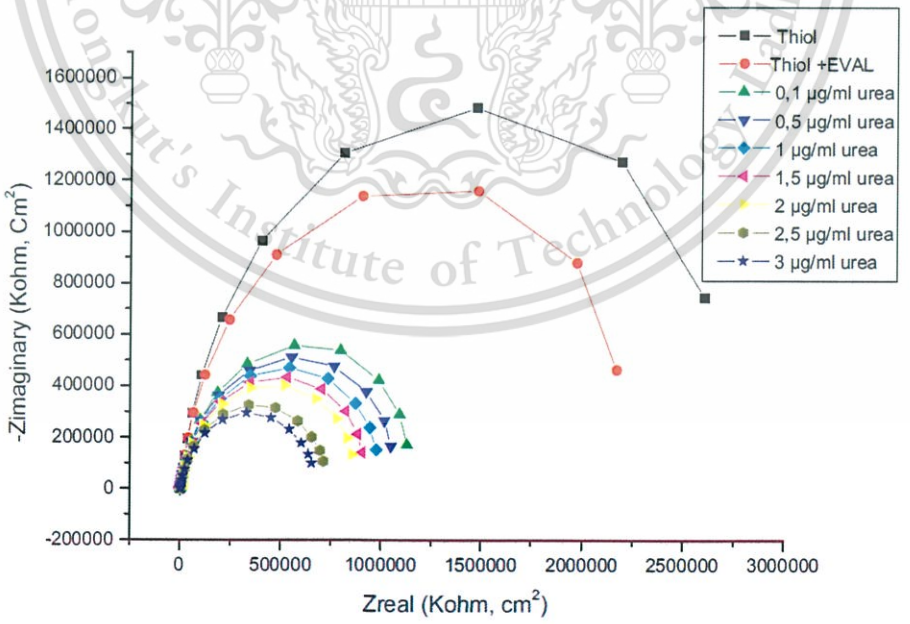

Figure 2.23 Nyquist plots of impedance spectra for urea-imprinted at various urea concentrations [41].

Molecularly imprinted polymers for urea electrochemical sensor to be developed by Yan-Ping Chen et al. in 2011 [17]. The urea MIPs electrochemical sensors were prepared by coating the chitosan-urea solution on the gold electrode by potentiostatic electrodeposition. Au disk electrodes were cleaned by mechanical polishing with Al_2O_3 and electrochemical cycling in 1.0 M of H_2So_4 solution. After that, the chitosan-urea solution was deposited on the gold electrode. The urea template was removed from the polymer film with stirring in 0.1 M of KCl solution for 20 min. The fabrication process of urea MIPs electrochemical sensor based on chitosan (CS) was shown in Figure 2.24.

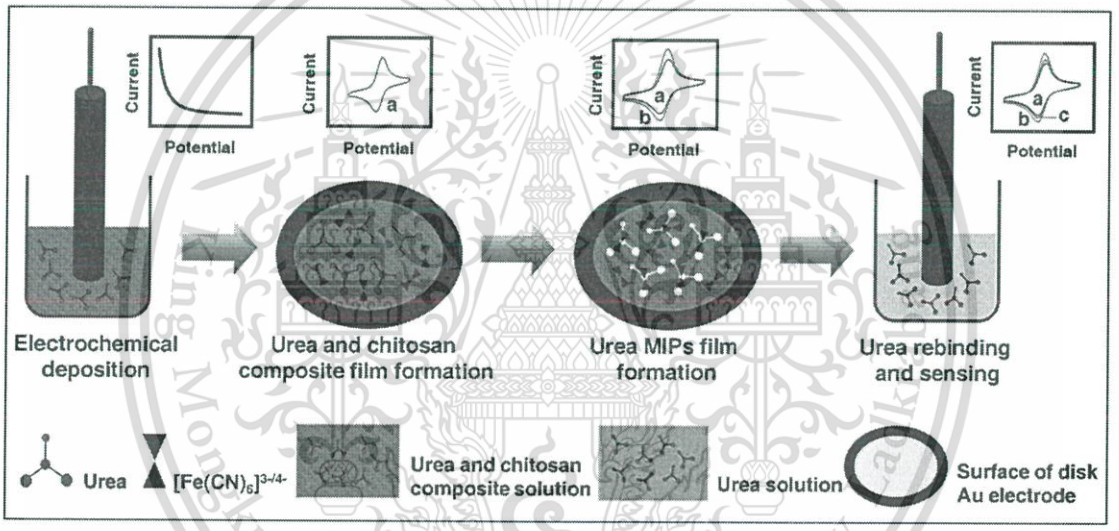

Figure 2.24 Schematic diagram of the fabrication urea MIPs electrochemical sensor based chitosan [17].

Figure 2.25 displays the EIS characteristics of the electrodes at different fabrication stages for studies the electron transfer between electrode surface and solution. The result exhibits the Au bare electrode lowest impedance. When Au electrode was coated by urea-CS solution impedance increased, because the polymer film obstructed electron transfer to surface electrode. And then, the urea templates was removed from polymer layer, the polymer film became porosity the

impedance was reduced. The urea MIPs electrochemical sensor based chitosan was used to detection urea samples by cyclic voltammogram. Figure 2.26 shows the response of the fabricated MIPs sensor to different concentrations of urea in aqueous solutions. The response of the chitosan coated Au electrode illustrate the linearity between 1.0×10^{-8} - 4.0×10^{-5} M, and the limit of detection for urea is 8.0×10^{-9} M.

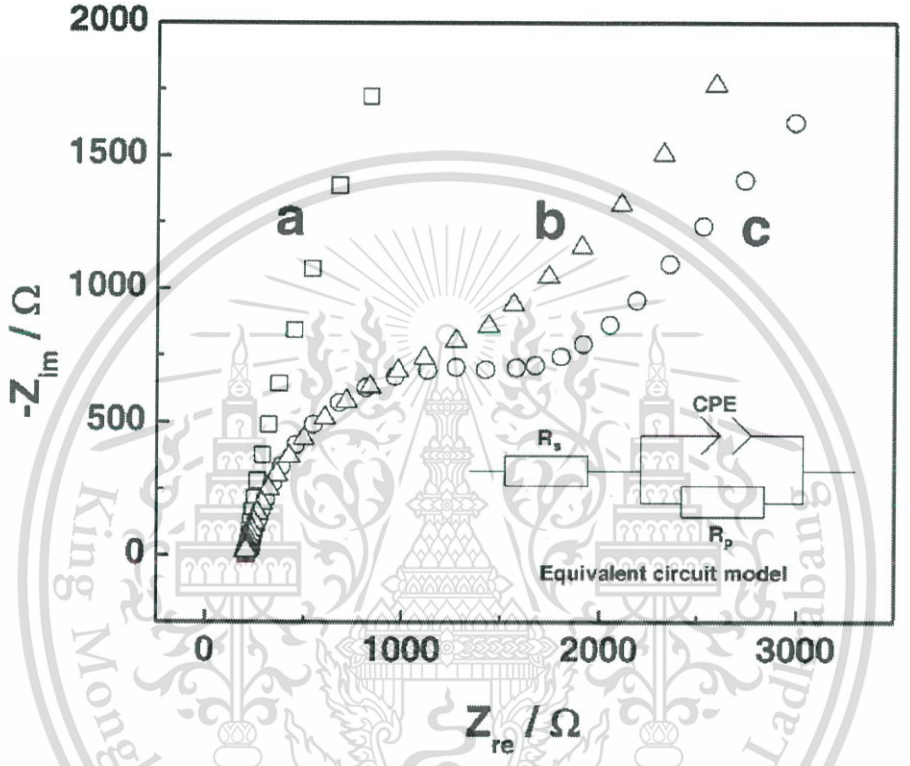

Figure 2.25 EIS of bare Au electrode (a), MIPs-Au electrode (b), and urea-CS/Au electrode (c) [17].

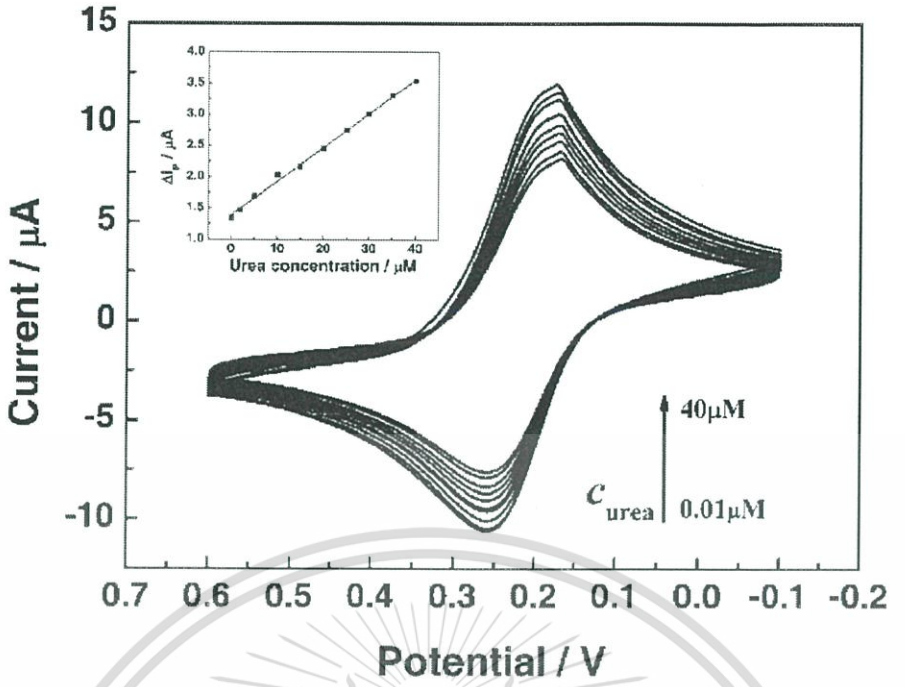

Figure 2.26 Cyclic votametry response of the MIPs sensor for urea detection [17].

The selectivity of the chitosan MIPs sensor, structural similarities molecule to urea such as thiourea, acetamide, DMF, ammonia, methyl carbamate, and hydroxyurea was chosen for the experiment. In addition, the potential application of the sensor is detected urea in serum samples, some co-existences molecule (uric acid (UA), ascorbic acid (AA), dopamine (DA), and creatinine (Cr)) was used for testing the MIPs sensor also. Figure 2.27 represents the selectivity of MIPs sensors. The result exhibits the urea MIPs electrochemical sensor based chitosan highly selective to urea. After that, this sensor demonstrates a detection urea in serum samples, the sensor show recoveries test in the range 96.3 – 103.3 %, which has a potential to apply the sensor for clinical diagnostic.

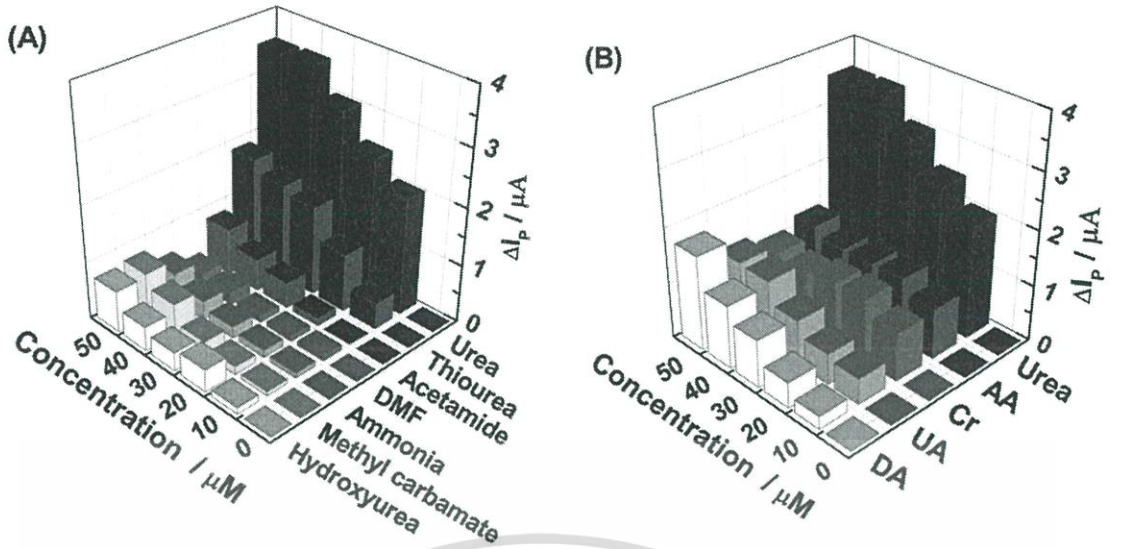

Figure 2.27 The current response of the MIPs electrochemical sensor for structural similarities (A), and co-existences (B) [17].

The next year, the same research group was led by Yan-Ping Chen [18]. This work presented doping CdS quantum dots in the molecularly imprinted film based chitosan. The urea electrochemical sensor was fabricated by electrodeposition technique. Addition CdS quantum dots in the polymer film affect the limit of detection as low as to 1.0×10^{-12} M and the response of the MIPs sensor shows two linearity ranges of urea detection between 5.0×10^{-12} - 4.0×10^{-10} M and 5.0×10^{-10} - 7.0×10^{-8} M (Figure 2.28). Furthermore, the urea MIPs electrochemical sensor based chitosan exhibits good reproducibility, repeatability, and stability.

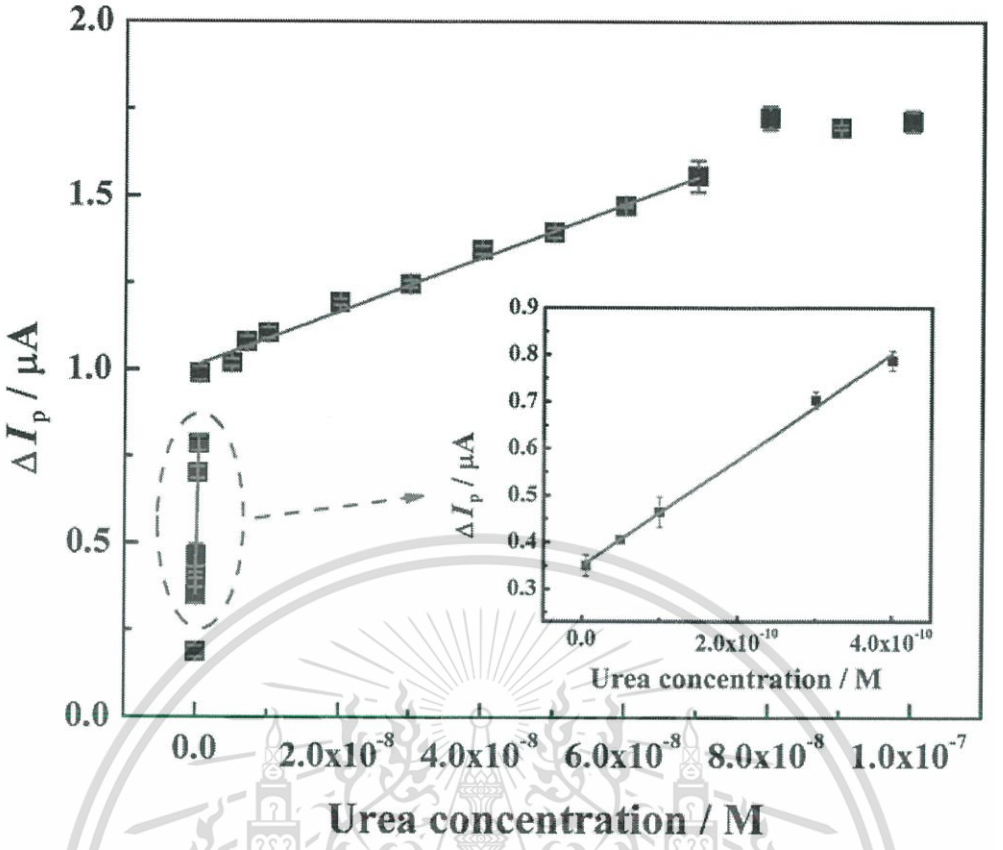

Figure 2.28 Calibration cruve of the urea MIPs electrochemical sensor based chitosan doping with CdS quantum dots [18].

Taher Alizadeh and Aezam Akbari (2013) [73] reported the nano-sized molecularly imprinted polymers (nano-MIPs) for a capacitive urea-sensor. The nano-sized urea-MIPs was prepared by suspension polymerization in silicone oil and using acrylic acid as the monomer. The synthesized urea-MIPs nanoparticles have average dimensional size about of 50 nm. After that, the nano-sized MIPs was mixed with PVC in solution. The mixture solution was dropped on a graphite disk electrode. Figure 2.29 displays response of different electrodes and different urea concentration. It found that the MIPs electrode has impedance increasing when urea concentration increased. The capacitance value can be calculated from impedance, this indicates that the capacitance depends on urea concentration.

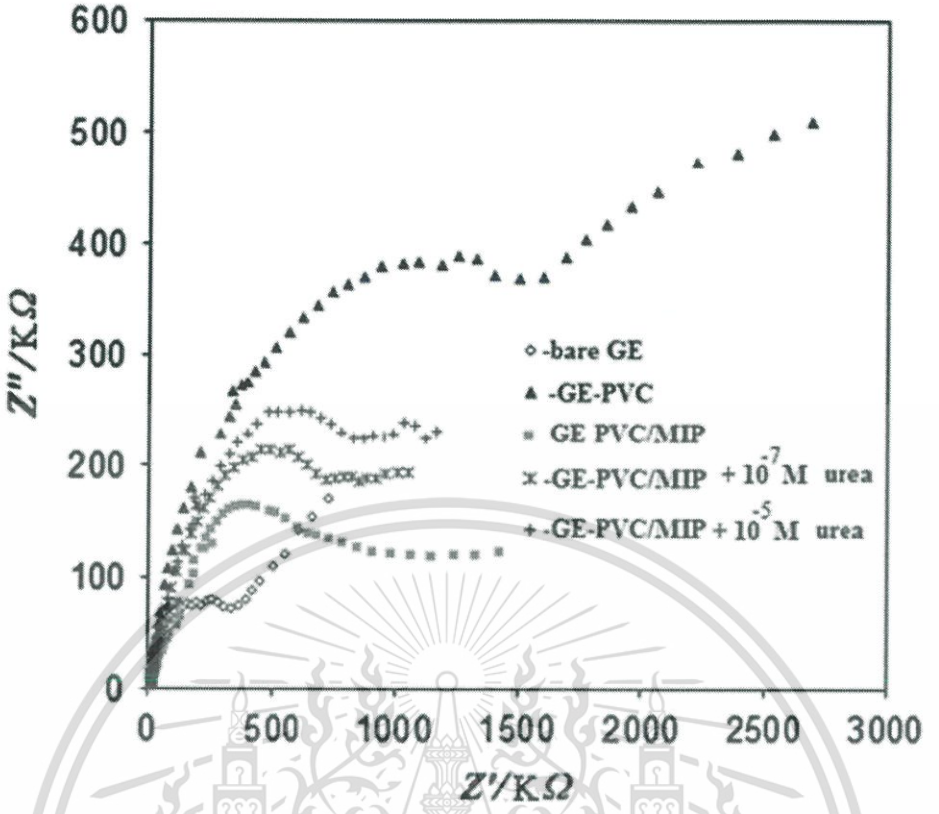

Figure 2.29 Nyquist plots recorded for different electrodes and different urea concentration [73].

The selectivity of the nano-MIPs sensor was observed by other compounds including thiourea, glucose, arginine, cysteine, and tryptophan. Figure 2.30 (I) shows the response of the nano-MIPs sensor to urea higher than other compounds. These indicate that the prepared nano-MIPs capacitive sensor is highly selective to urea. Figure 2.30 (II) represents calibration curve of the sensor for urea detection. This sensor demonstrates a detection limit as low as 5 picomolar and a very wide linear range of 1×10^{-11} - 1×10^{-4} M

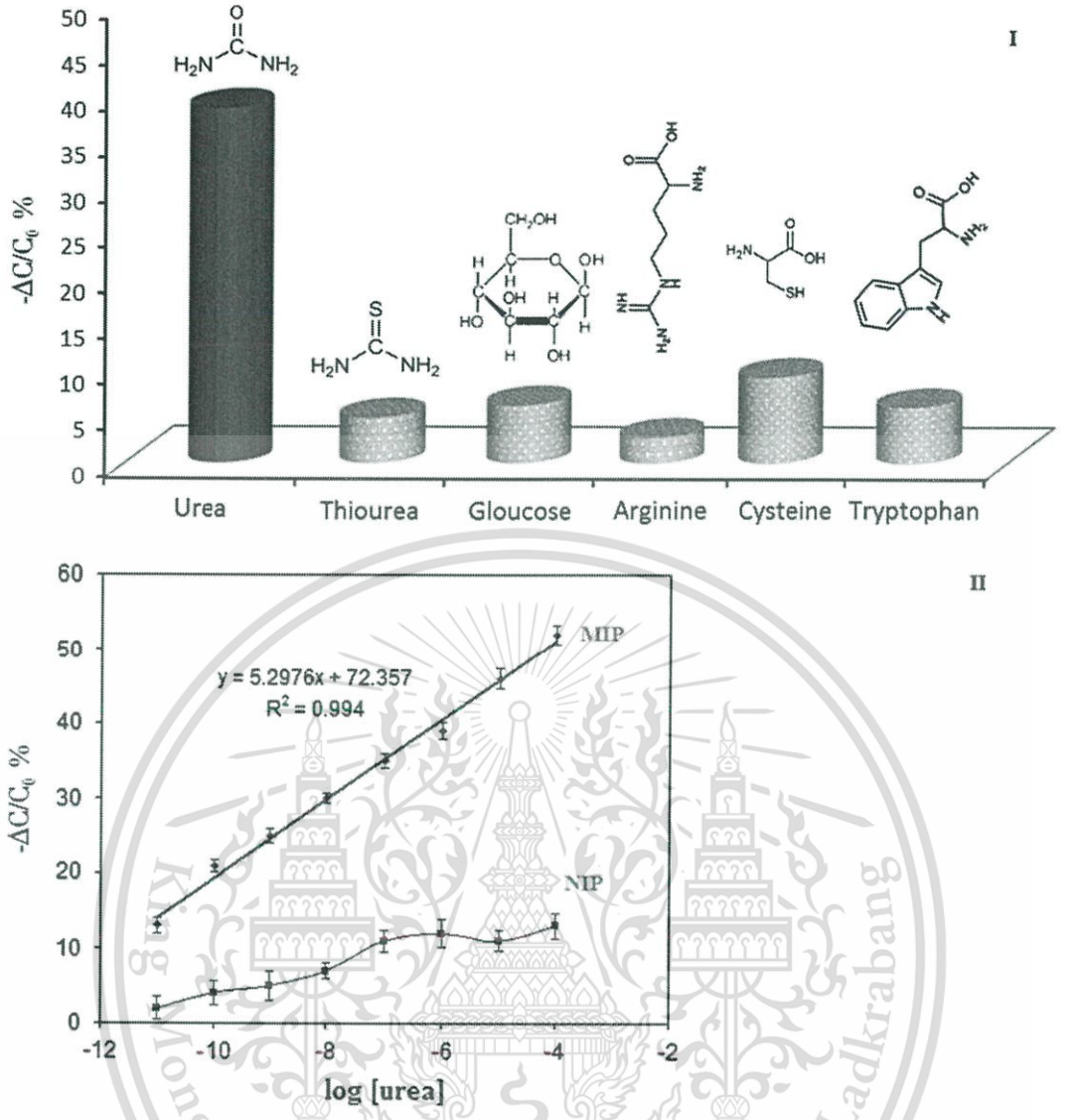

Figure 2.30 (I) The response of the nano-MIPs to urea and other compounds at the same condition, (II) calibration curve of the prepared nano-MIPs capacitive sensor [73].

CHAPTER 3

MOLECULARLY SELECTIVE PMMA-COATED ELECTRODES FABRICATION FOR UREA DETECTION

Overview - A simple fabrication method for molecularly imprinted electrochemical electrodes was developed for urea detection. The molecularly imprinted polymers (MIPs) were prepared by solvent evaporation on gold-coated electrodes using PMMA and urea as functional polymer and molecular templates, respectively. The fabricated electrodes were characterized by cyclic voltammetry (CV), amperometry, scanning electron microscopy (SEM), and Fourier transform infrared spectroscopy (FTIR). The urea detection was achieved by incubating the MIPs electrode in a test urea solution and measuring reduction in amperometric responses in the potassium ferrocyanide redox reaction. The performance of the electrodes was optimized by the preparation conditions, i.e. PMMA and urea concentrations, a drop-cast volume and an incubation time. The urea-sensing responses of the electrodes yielded two linearity ranges from 2.0×10^{-6} - 1.0×10^{-4} M and 1.0×10^{-4} - 1.0×10^{-1} M with the limit of detection of 8.0×10^{-7} M (S/N = 3). The MIPs electrodes also exhibited excellent reproducibility, repeatability and stability, as well as high selectivity to urea and were further applied to detect urea in human blood serum samples with success.

3.1 Introduction

Detection of urea concentration is essential for agricultural and clinical chemistry, food science and environmental monitoring [124]. Particularly in clinical diagnostics, nitrogen concentration in human serum in the form of urea is called Blood Urea Nitrogen or BUN, which is an indication for kidney failure or liver

malfunction. A typical level of urea nitrogen in human serum is 5 – 20 mg/dl (1.8 ~ 7.1 mM) [125]. Many methods exist for the determination of urea concentration such as colorimetry [12], luminescence [126], fluorometry [127] and high-performance liquid chromatography [128]. However, these methods often require a long analysis time and complicated sample preparation or measurement processes. Urease-based urea biosensors are generally regarded as a directly specific technique to quantify urea by measuring ammonium ions, the reaction product, using a potentiometric method. Nonetheless, enzyme-based sensor has a limitation in its stability and activity [18]. These hinder upscale fabrication and commercialization. In addition, urease may also catalyze the amido-hydrolysis by other compounds such as formamide, acetamide, and N-hydroxyurea. Furthermore, the activity of urease could be inhibited by other ions such as sodium, potassium, and fluoride [32]. More importantly, glutamate dehydrogenase is additionally required for better urea detection. This is because ammonium ions which are the product of urea hydrolysis are unstable and easily dispersed in the environment. Glutamate dehydrogenase, therefore, is utilized to catalyze the reaction between ammonium ions, α-ketoglutarate (α-KG) and nicotinamide adenine di-nucleotide (NADH) [13,14] producing L-glutamate with simultaneous oxidation NADH to NAD^+ which is then generated electrons are transferred to electrode.

To circumvent the above mentioned problem, molecularly imprinted polymers (MIPs) have attracted many interests when applied as selective membranes for non-enzymatic biosensors which are of high stability and low cost [129,130]. In order to prepare MIPs, a functional polymer and molecular templates are co-deposited on the surface of an electrode. The molecular template is next removed from the polymer matrix leaving molecular cavities functioning as selective binding sites for a specific target molecule. Many techniques such as polymerization [32–34], sol-gel synthesis [35–37], electrodeposition [38,39], and solvent evaporation [40,41] may be employed for co-deposition of a polymer and a molecular template.

Detection of urea using MIPs is still in its infancy. To the best of our knowledge, there are only three publications in this specific field. Chitosan was used for synthesizing MIPs for electrochemical urea detection with high selectivity, stability, repeatability and reproducibility were achieved [17]. This chitosan-based MIPs was later improved by incorporating CdS quantum dots, and the detection limit of the resulting sensor was extended as low as a picomolar level [18]. T. Alizadeh and A. Akbari [73] reported the nano-sized molecularly imprinted polymers (nano-MIPs) for a capacitive urea-sensor. This sensor demonstrated a detection limit as low as 5 picomolars and a very wide linear range of 1×10^{-11} - 1×10^{-4} M. Although these published works show splendid sensor performances, the obtained sensors are fabricated with complicated methods.

The response of electrochemical MIPs electrodes to target molecules may be classified into two strategies for molecular detection. One is the measurement of an increase of charge or electron transfer from chemical reactions between a polymeric membrane and a template molecule, leading to higher response signals [67,131]. The other is the obstruction of charge transfer to the surface of the electrode by the template molecules that are bound into the cavities, and results in reduction of response signals [71,72]. For the latter, the measuring process of MIPs sensor is similar to that of the biochemical detection method via enzyme inhibition due to exposure of enzymes to certain target molecules and the response is obtained from the reduction of their activities [74,75]. This approach has been demonstrated on MIPs by incubating the MIPs-coated electrode in a test solution before measuring the response in an electrolyte solution, such as Potassium ferrocyanide [26,132].

In this chapter, we report a simple fabrication method of MIPs electrode using a solvent evaporation technique for urea detection. Poly(methyl methacrylate) (PMMA) and urea were used as the functional polymer and the molecule template, respectively. They were drop-cast onto a gold-coated electrode on a printed-circuit board. The polymeric membrane was then exposed to UV irradiation to strengthen

the coated membrane by photo-polymerization. Removal of urea template by large loop CV finally resulted in a sensing membrane. Our fabricated urea-sensing electrodes were characterized by cyclic voltammetry (CV), amperometry, scanning electron microscopy (SEM), and Fourier transform infrared spectroscopy (FTIR). The sensitivity, selectivity, repeatability and reproducibility of the fabricated electrodes were investigated. Furthermore, the ability of these fabricated urea detection electrodes were demonstrated in a serum sample.

3.2 Materials and methods

3.2.1 Chemicals and reagents

Urea, methyl carbamate, glutamic acid, sodium chloride (NaCl), uric acid (UA), ascorbic acid (AA), dopamine (DA), creatinine (Cr), and human serum were purchased from Sigma-Aldrich. Poly(methyl methacrylate) (PMMA) and dimethylformamide (DMF) were bought from Acros organics. Potassium ferrocyanide ($K_4Fe(CN)_6$), potassium nitrate (KNO_3), sodium dihydrogen phosphate (NaH_2PO_4) and disodium hydrogen phosphate (Na_2HPO_4) were ordered from Ajax Finechem. Thiourea and ammonia were purchased from CARLO ERBA. All chemicals were of analytical grade. De-ionized (DI) water (Resistivity >18 MΩ/cm) was used throughout the experiments.

3.2.2 Apparatus

All electrochemical measurements were performed by a Metrohm PGSTAT 302N - High Performance Potentiostat/Galvanostat in a 50 mM $K_4Fe(CN)_6$ solution containing 0.1 M phosphate buffer (pH 7.0) at room temperature (25°C). The 3-electrode system was employed, consisting of an Ag/AgCl (3 M KCl) electrode as the reference electrode, a gold rod as the auxiliary electrode, and a gold disk electrode (3 mm in diameter), MIPs and non-molecularly imprinted polymers (NIPs)-modified gold electrodes were used as the working electrodes. The coated MIPs film was characterized to confirm the functional group of the target molecules by FTIR

spectroscopy using a Spectrum Tw TM FT-IR spectrophotometer with an attenuated total reflectance (ATR) device from PerkinElmer, Inc. The surface morphology of PMMA-Urea/Au, MIPs/Au, and NIPs/Au were characterized by scanning electron microscopy (SEM, EVO MA10, Zeiss) and the cross-section of MIPs layer coated on gold electrode was characterized by field-emission scanning electron microscopy (FE-SEM, JSM-7800F Prime, JEOL).

Figure 3.1 Gold disk electrodes with gold rod on the printed circuit boards.

3.2.3 The fabrication of the MIPs-modified gold electrodes

The printed circuit boards with gold-coated electrodes were made to order by Seagate Circuit Co., Ltd. (Bangkok, Thailand). The bare electrodes were firstly cleaned with ethanol followed by DI water in ultrasonic bath for 5 min each. After that, the electrodes were pretreated in 50 mM $K_4Fe(CN)_6$ solution containing 0.1 M phosphate buffer by cyclic voltammetric between -0.3 to +0.6 V (Vs. Ag/AgCl) at the scan rate of 0.05 V/s. Schematic of the fabrication procedure was illustrated in Figure 3.2. The polymer-urea solution was prepared by dissolving 250 mg (2.5 wt%) of PMMA and 40 mg (0.4 wt%) of urea in 10 ml DMF and ultrasonicating the mixture for 10 min. The electrode surface was coated by drop-casting 1.5 µl of the PMMA-urea

solution and curing with UV radiation (Stratagene UV Stratalinker 1800, 254 nm UV light bulbs with the power of 3 mW/cm^2.) for 15 min [133]. The urea molecular templates were removed from the polymer film to produce the sensing membrane by large loop cyclic voltammetric scans [68] in 50 mM $K_4Fe(CN)_6$ solution containing 0.1 M phosphate buffer using potential cycling between -0.3 to +1.0 V. The NIPs electrodes were fabricated employing the above process but without the addition of urea template molecules.

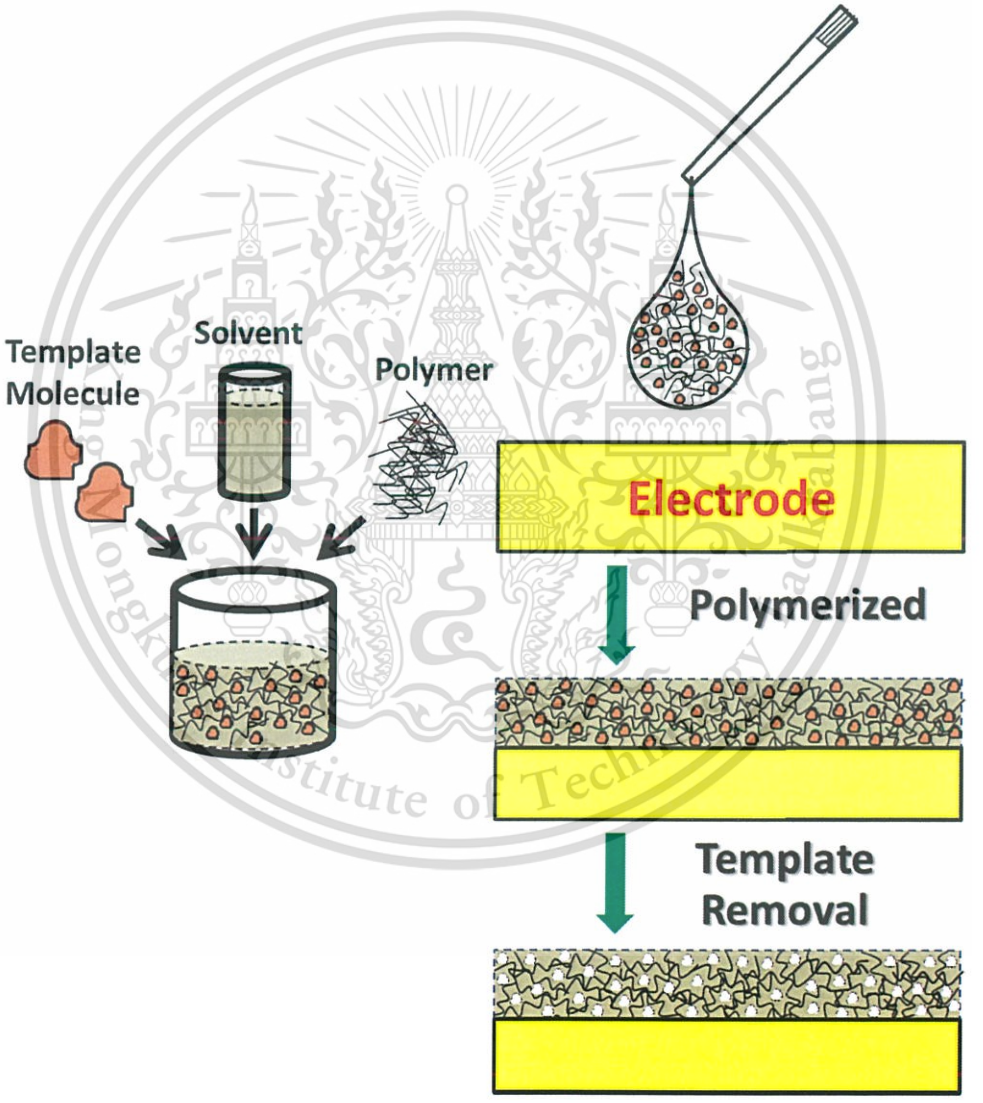

Figure 3.2 Fabrication process of MIPs sensor for urea detection.

3.2.4 Electrochemical measurements

The MIPs modified electrode was incubated in a 5 ml urea solution (at a specified concentration) for 20 min and then immersed in a 50 mM $K_4Fe(CN)_6$ solution containing 0.1 M phosphate buffer for electrochemical measurements. The CV characteristics of MIPs and NIPs electrodes were investigated in a potential range of -0.3 to +0.6 V at a scan rate of 0.05 V/s. Chronoamperometry was employed to assess the sensing performance of all electrodes at a fixed potential of 0.30 V and a measurement time of 900 s.

3.3 Results and discussion

3.3.1 Characterization of MIPs-modified gold electrodes

3.3.1.1 Surface morphology of modified electrodes

The material structure and surface morphology characteristics of different modified electrodes were determine by SEM. The morphology of PMMA/gold electrode (NIPs/Au) shown in Figure 3.3 (A) demonstrates mixed characteristics of PMMA microspheres and film which the observed cracks were due to tensile stresses in the polymer matrix [134]. Figure 3.3 (B) shows that the more homogeneous microstructure of PMMA-urea layer before urea removal (PMMA-urea/Au), the urea-polymer composite layer has a flatten surface indicated that urea is well dispersed in the PMMA matrix [134]. After removal of urea templates from the polymer composite layer (MIPs/Au), the surface morphology of imprinted layer on the electrode surface was showed in Figure 3.3 (C). This exhibited that the urea molecules were successfully removed from the PMMA-Urea/Au electrode [135]. However, the SEM image only showed the morphology of pore on MIPs surface layer. From the knowledge base, the urea template cavity on polymer structure is in nano size [136]. Figure 3.3(D) shows a SEM cross-section image of the MIPs layer on the gold electrode which confirms that the thickness of polymer layer was approximately 1 μm.

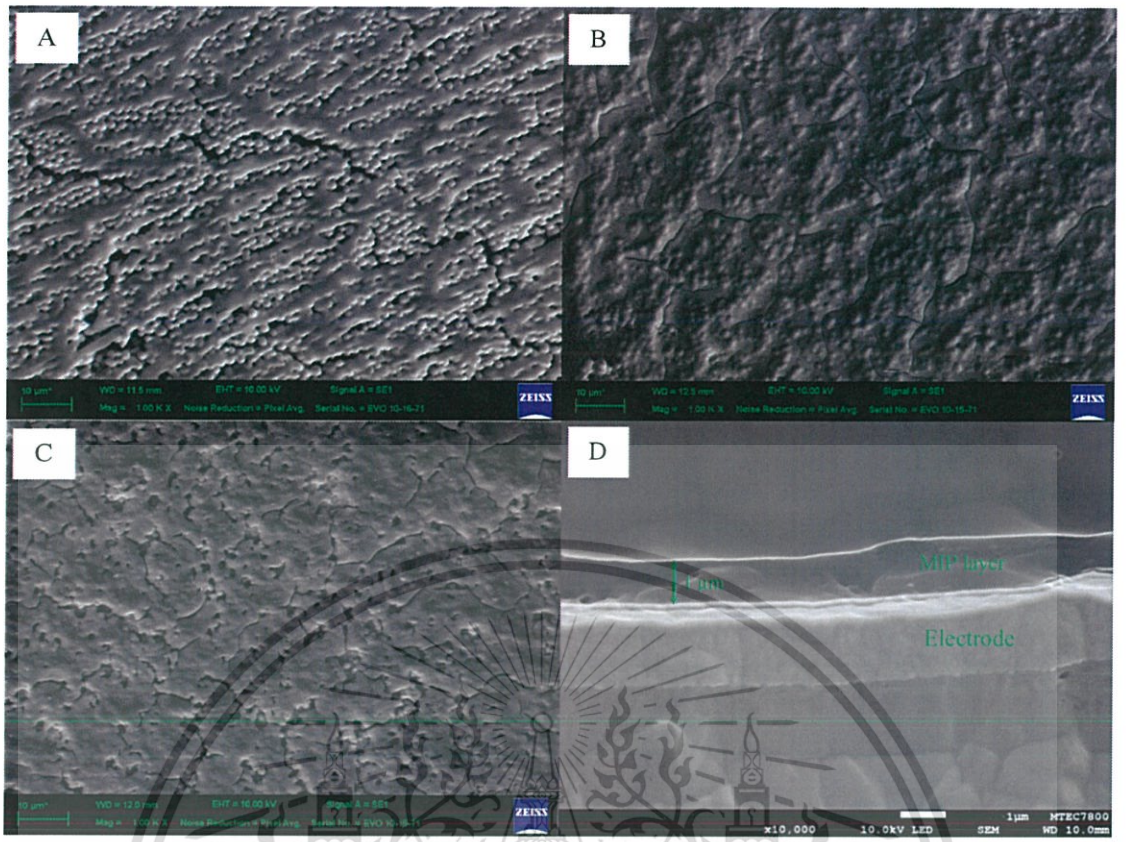

Figure 3.3 SEM images of PMMA/Au electrode (NIPs/Au) (A), PMMA-urea/Au electrode before template removal (PMMA-urea/Au) (B), PMMA-urea/Au electrode after template removal (MIPs/Au) (C), and cross-section of the MIPs layer on the gold electrode (D).

3.3.1.2 Electrochemical measurement of modified electrodes

The urea templates were removing by large loop cyclic voltammetric scans as showed in Figure 3.4. The results show that the current response of the MIPs sensor increasingly depends on the number of scans. Figure 3.5 displays the cyclic voltammetry characteristics of the electrodes at different fabrication stages in a 50 mM $K_4Fe(CN)_6$ solution containing 0.1 M phosphate buffer and schematic of the proposed mechanism for the MIPs sensor. A bare gold electrode (Au) illustrates clear redox peaks of $K_4Fe(CN)_6$ which refer to the Fe^{2+}/Fe^{3+} redox reactions.

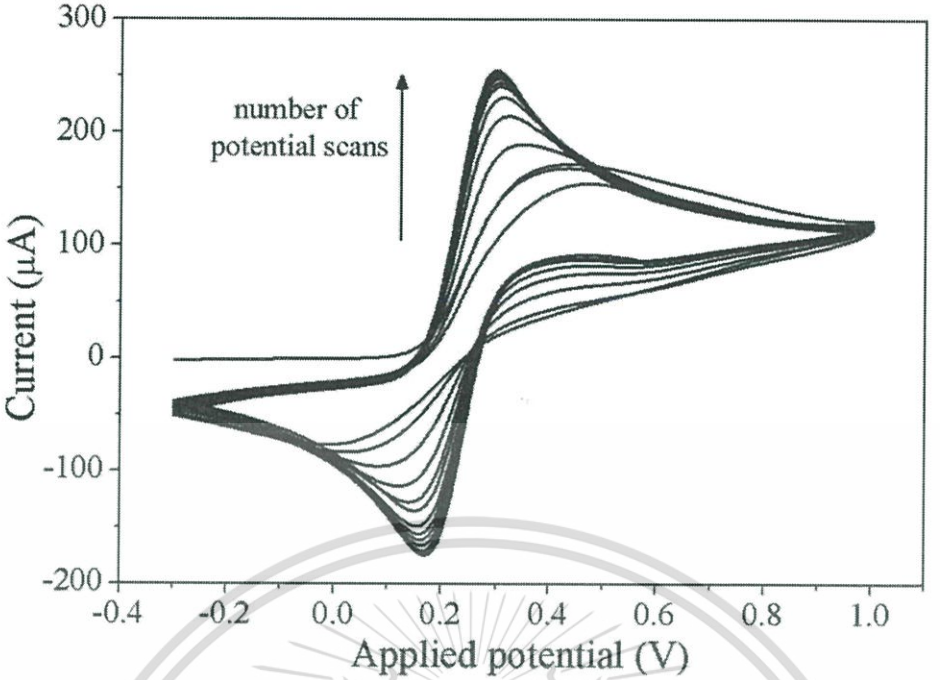

Figure 3.4 Cyclic voltammograms for urea template removal from PMMA-urea/Au electrode in 50 mM $K_4Fe(CN)_6$ solution containing 0.1 M phosphate buffer (pH 7.0) with large loop scans from -0.3 to 1.0 V.

For the gold electrode coated with the PMMA–urea composite layer (PMMA-Urea/Au), the redox peaks are barely observed. This indicates that the polymer-urea layer obstructed the electron transfer at the surface of PMMA-Urea/Au electrode. After removal of urea templates the sensor (MIPs/Au) exhibits a distinctive increase in the redox currents when compared to the PMMA-Urea/Au electrode. It should be noted that the response currents of the MIPs/Au electrode are only half of the bare Au electrode. This suggested that the PMMA membrane became more porous after the urea molecules were displaced, leaving some parts of the electrode to be electroactive. The results are in accordance to the SEM images of the electrode surface. For the gold electrode coated the PMMA layer (NIPs/Au), the current signals are nearly the same as that of the PMMA-urea/Au electrode but with lower current.

This was likely due to less cavities of the pure polymer layer which resulted in decreasing electron transfer [137].

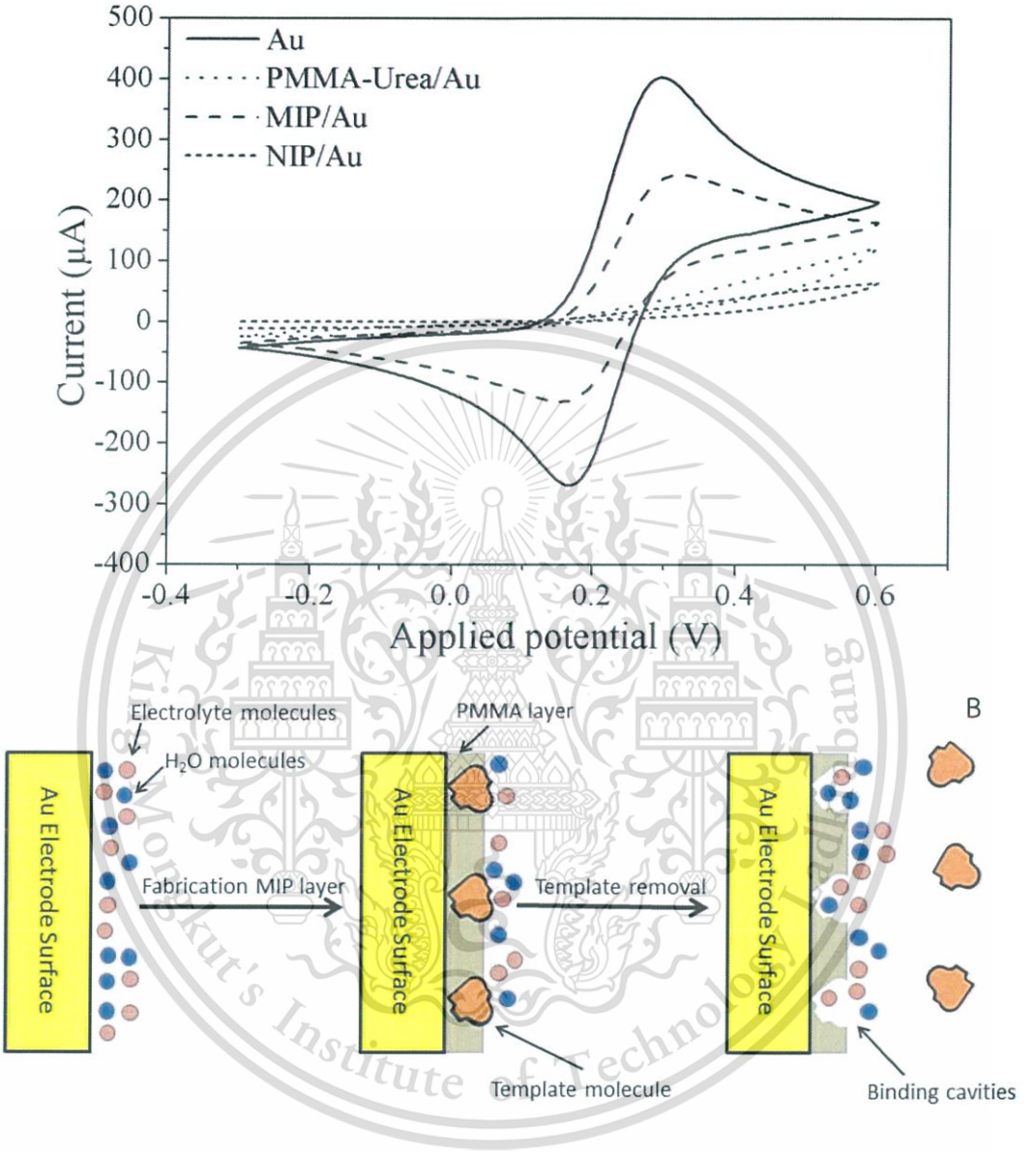

Figure 3.5 (A) Cyclic voltammograms of bare gold electrode (Au), gold electrode drop-cast with PMMA-urea solution before urea template removal (PMMA-Urea/Au), PMMA-Urea/Au electrode after urea template removal (MIPs/Au), and PMMA/Au electrode (NIPs/Au), in 50 mM $K_4Fe(CN)_6$ solution containing 0.1 M phosphate buffer pH 7.0. (B) Schematic of the proposed mechanism for the MIPs sensor.

3.3.1.3 Validation of template removal by FTIR

FTIR spectroscopy was applied to confirm the template removal by characterizing the PMMA-urea coating layer before and after the removal of urea, as shown in Figure 3.6. After the gold electrode was coated by the PMMA-urea solution and cured with UV radiation, the observed IR absorption peaks implying the existence of urea at around 3432 and 3331 cm^{-1}, corresponding to the characteristic of N–H stretching, and around 1682 and 1629 cm^{-1} for the forming of strong hydrogen bonds of bending NH_2 [138]. But after removal of the urea molecules from the coating layer, the IR absorption peaks of urea disappear. Moreover, on closer inspection, the absorption bands of urea for the C=O stretching around 1597 cm^{-1} and C=O bending around 557 cm^{-1} are not noted for the MIPs layer after the template removal [138].

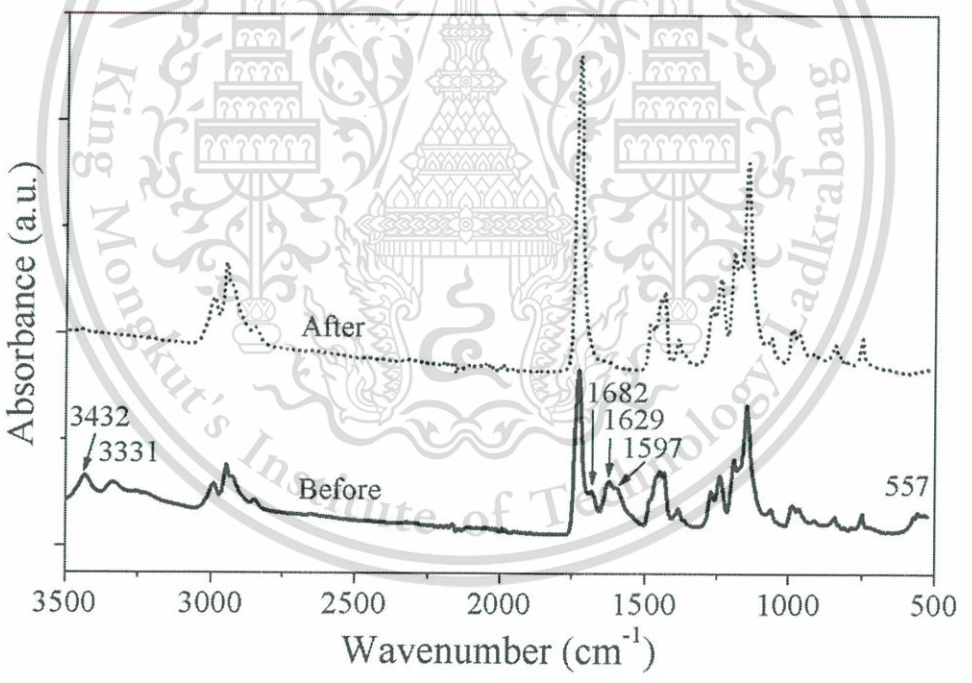

Figure 3.6 FTIR spectra of PMMA-urea/Au electrode before and after template removal.

3.3.2 Optimization of MIPs modified electrodes

3.3.2.1 Volumes of the PMMA-urea composite solution

The thickness of the polymer membrane is significant factor that determines the performance of the fabricated MIPs electrodes. In drop-casting, the volume of the PMMA-urea composite solution has the most effect on the thickness of the MIPs film. Figure 3.7 shows the difference in amperometric current responses ($I_b - I_u$). Where I_b is the current signal of the MIPs electrode in $K_4Fe(CN)_6$ solution containing 0.1 M phosphate buffer, and I_u is the response current of the MIPs electrode in the same solution after 20 min incubation in 1.0×10^{-5} M urea solution. The MIPs electrode was prepared by different drop-cast volumes (1.0, 1.5, 2.0, 2.5, and 3 µl) of the PMMA-urea composite solution at the fixed concentrations of 2.5 wt% PMMA and 0.4 wt% urea. The maximum current difference was obtained in the volume range of 1.5 – 2.0 µl. For the smaller volume range, the current difference drops sharply. In this case, the thickness of the polymer films may be insufficient, possibly resulting in cracks and leakage current between the solution and the electrode. For larger volume, the current response also decreases rapidly. Here the excessive thickness of the polymer films should result in lower porosity of the film and disrupt the ion exchange channel.

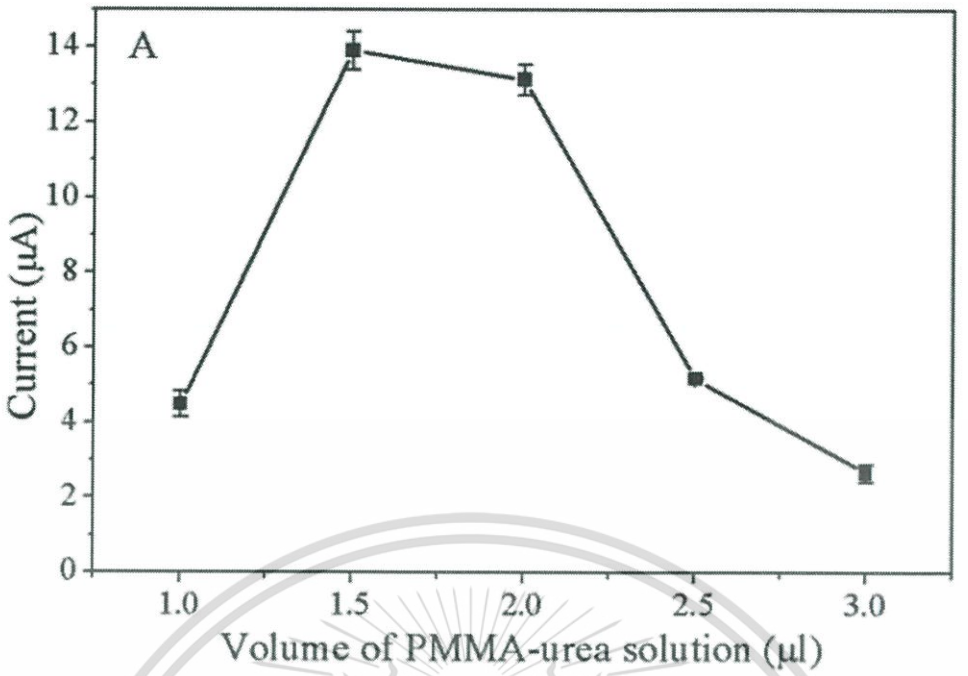

Figure 3.7 The effect of volume of the PMMA-urea solution for the MIPs fabrication.

3.3.2.2 Concentration of PMMA

The concentration of PMMA as the functional polymer in MIPs films should exhibit a similar effect to the volume of the PMMA-urea solution, regarding the thickness of the MIPs films. In addition, PMMA concentration may affect other properties such as uniformity of the films. Figure 3.8 shows the current response of the electrode fabricated with different PMMA concentrations (0.5, 1.5, 2.5, 3.5, and 4.5 wt%). In these cases, the urea concentration and the drop-cast volume were fixed at 0.4 wt% and 1.5 μl, respectively. The response was investigated in 1.0×10^{-5} M urea. The best current response was obtained in the PMMA concentration range of 2.5 – 3.5 wt%. The current response decreases rapidly outside this range. This PMMA concentration range for the drop-cast volume of 1.5 μl should result in the optimal thickness and film quality.

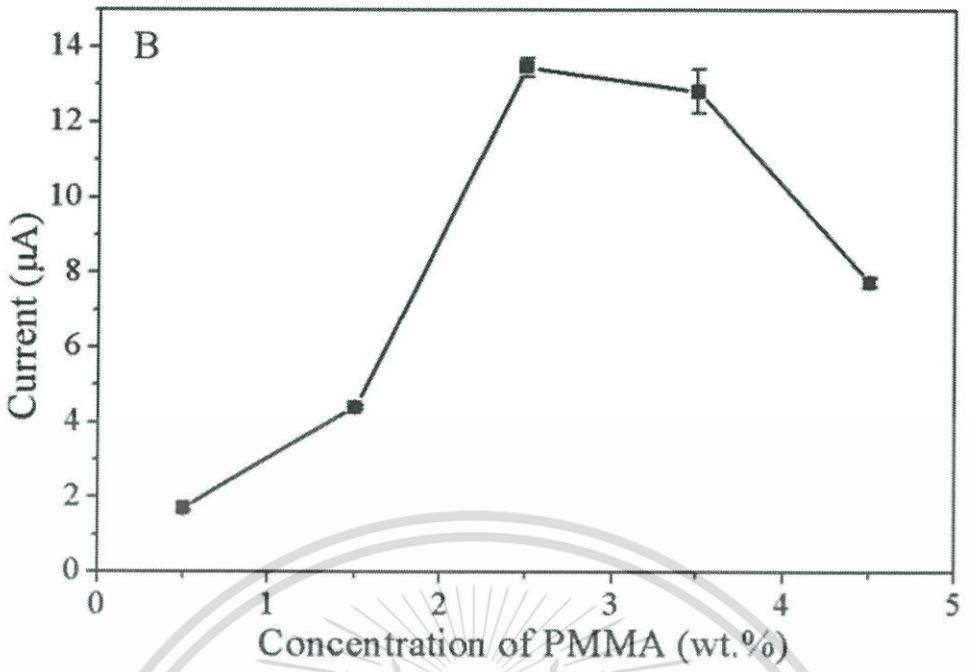

Figure 3.8 The effect of the PMMA concentration for the MIPs fabrication.

3.3.2.3 Concentration of the urea template

The concentration of template molecules affects the density of the molecular recognition cavities. As shown in Figure 3.9 the optimal response of the MIPs electrodes was obtained in the concentration of the urea template between 0.4 - 0.5 %wt. In these cases, the PMMA concentration and the drop-cast volume were fixed at 2.5 wt% and 1.5 μl, respectively. Outside this optimal range of the urea concentration, the current response gradually decreases. The effect of the template concentration is therefore less critical than those of the PMMA concentration and the drop-cast volume. This is consistent with the picture of three-dimensional molecularly selective porous membrane rather than two-dimensional molecular recognition surface. The three-dimensional percolating network of the molecular cavities should be less affected by the template concentration.

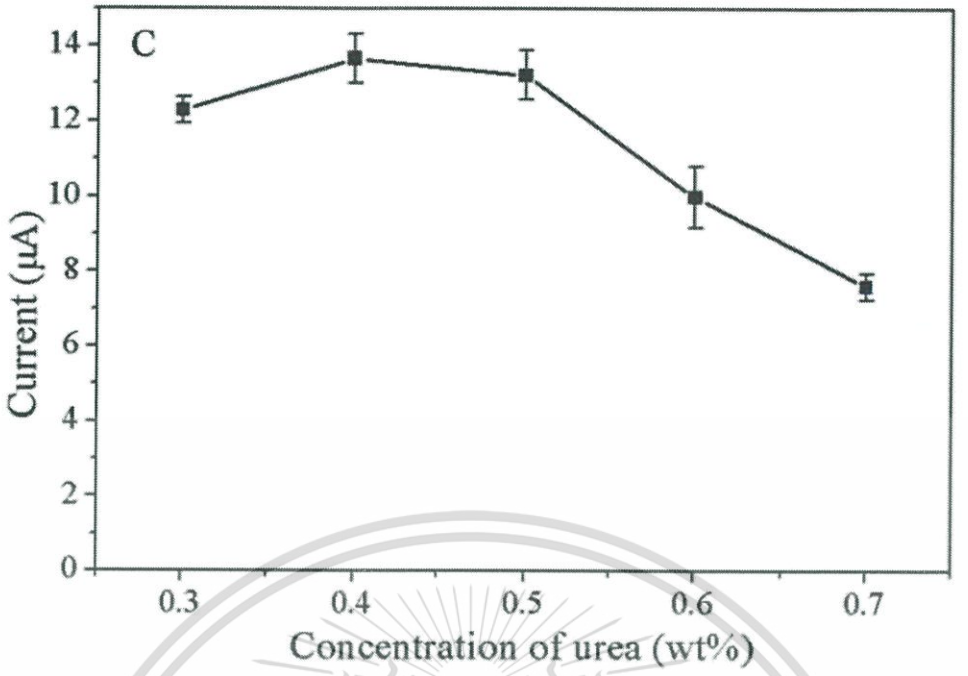

Figure 3.9 The effect of the urea template concentration for MIPs fabrication.

3.3.2.4 Urea incubation time

The effect of the time required for incubating the MIPs-coated electrode in 5 ml of the 1.0×10^{-5} M urea solutions is illustrated in Figure 3.10. In these cases, the electrode was fabricated with 2.5 wt% PMMA, 0.4 wt% urea, and the drop-cast volume of 1.5 μl. The current response slowly increases as the incubation time is prolonged and reaches a saturation level after 20 min. For this interaction volume, the optimal incubation time is, therefore 20 min.

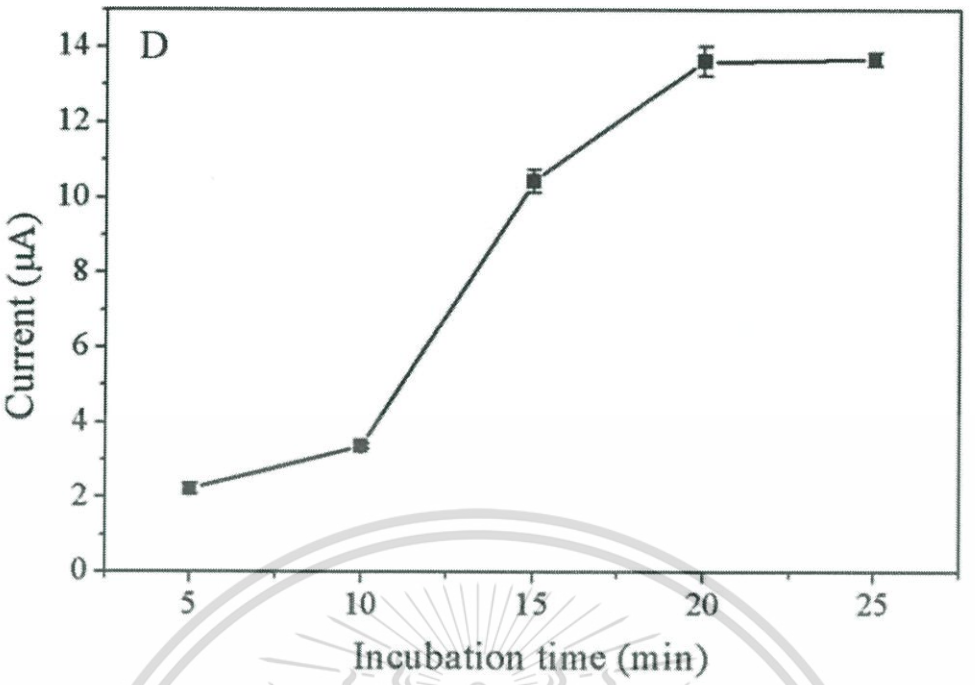

Figure 3.10 The effect of the incubation time for the MIPs fabrication.

3.3.3 Determination of aqueous urea samples

Amperometric responses of the MIPs and the NIPs electrodes were investigated for different concentrations of urea in aqueous solutions as shown in Figure 3.11. The MIPs electrodes were fabricated with 2.5 wt% PMMA, 0.4 wt% urea, and the drop-cast volume of 1.5 μl. The NIPs electrodes were fabricated with the same conditions but without urea. The incubation time was 20 min. The results indicate that the response of the MIPs electrode is distinctively higher than that of the NIPs which displays no current response throughout the whole urea concentration range. The response of the MIPs electrode shows two ranges of linearity for urea detection. The linear range for the lower concentration yields the sensitivity of 12.48 μA per pUrea (the logarithm of urea concentration) for 2.0×10^{-6} to 1.0×10^{-4} M (R^2 = 0.998). The linear range of the higher concentration yields the sensitivity of 2.11 μA per pUrea for 1.0×10^{-4} to 1.0×10^{-1} M (R^2 = 0.983). The limit of detection (LOD) for urea is found to be 8.0×10^{-7} M (S/N = 3). These linear ranges are

in good agreement with the target concentration range for urea detection in clinical diagnostics which confirms the success of the MIPs sensor proposed in this work.

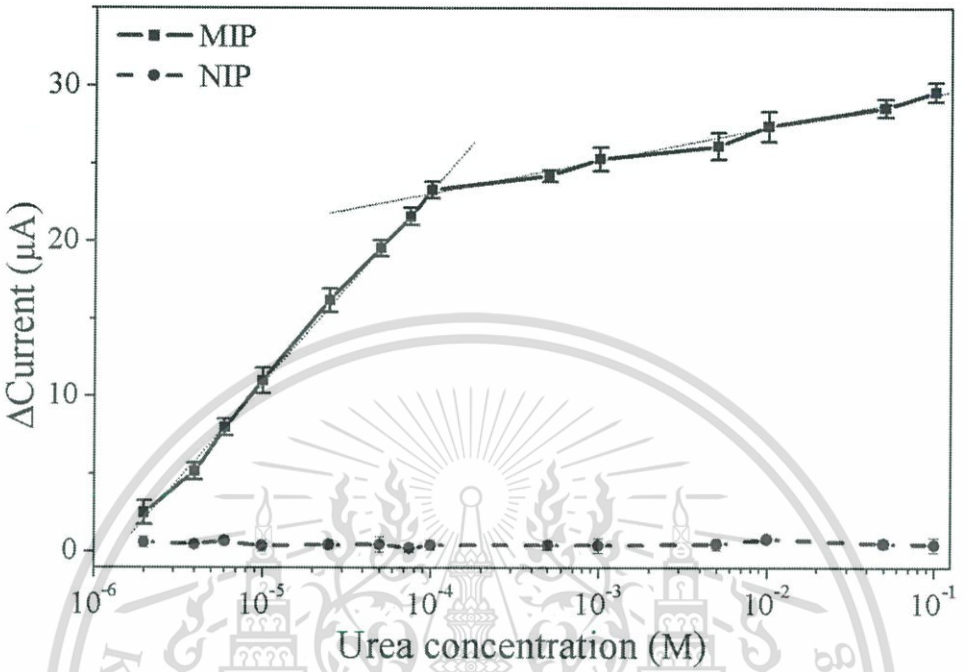

Figure 3.11 Amperometric responses of MIPs and NIPs electrodes at different urea concentrations.

The two linear ranges in the amperometric response of the MIPs-modified electrodes may be explained by the different molecular interaction mechanisms. At low concentration of urea (2.0×10^{-6} to 1.0×10^{-4} M), hydrogen adsorption is the main mode of interaction between the target molecules and the binding sites (as shown in Figure 3.12). In contrast, the response of the MIPs electrodes at higher urea concentration (1.0×10^{-4} to 1.0×10^{-1} M), should result from the domination of the Van Der Waals force between the target molecules and the binding sites over saturated hydrogen bonding adsorption [72]. It is generally known that the recognition of the MIPs sensor depends on the functional groups, size and shape

selection. Although the Van Der Waals force is a weak intermolecular force, but the shape of a molecular template tremendously helps enhancing MIPs selectivity [68].

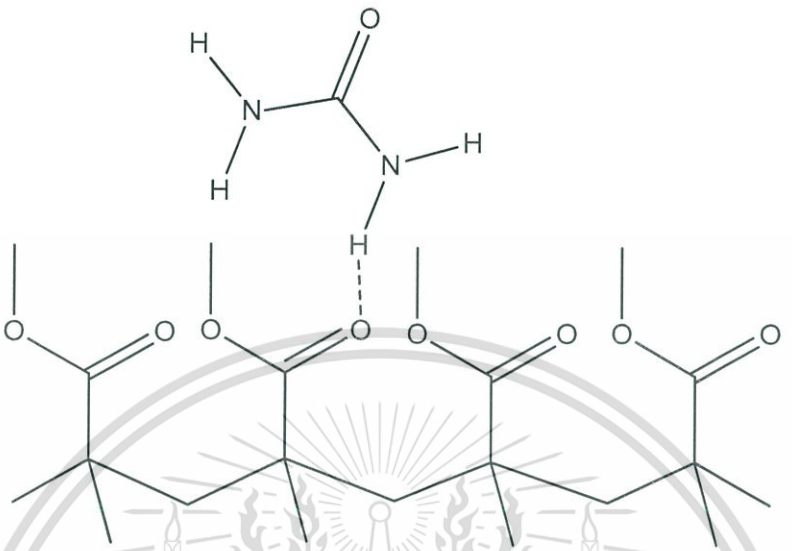

Figure 3.12 Schematic of the PMMA and urea interaction.

3.3.4 Selectivity of the MIPs-modified electrodes

The selectivity of the MIPs electrode to the urea target molecule was investigated by measuring the current response of interference species e.g., thiourea, methyl carbamate, glutamic acid, ammonia, potassium nitrate, and sodium chloride. These molecules were selected due to the similarity in the functional group, molecular shape and size to urea. Figure 3.13 displays the amperometric responses of the MIPs electrodes to urea and other interfering molecules at the concentration of 1.0×10^{-5} M.

The results illustrate the highest current response of urea than the other interfering molecules. Particularly, thiourea which is similar molecular structure to urea shows the decrease in current response of 40% due to the sulfur atom (S) has the larger size than oxygen atom (O) in urea. In addition, the higher electronegativity of oxygen than sulfur makes the polarity of –C=O group in urea higher than –C=S

group in thiourea resulting in the stronger interaction taken place in the cavity sites of MIPs [32].

The current response for methyl carbamate was about half for urea due to this molecule consist of only one amide group. In addition, the reduction of the current response obtained from this molecule can be also explained by the different in size between methyl carbamate and urea. The larger size of methyl carbamate allows this molecule to interact with some part of the PMMA in the cavity sites. As a consequence, the electrocatalytic molecule can pass through the surface electrode resulting in the decrease of the current response. For glutamic acid that has the similar behavior with methyl carbamate but larger molecular size, the current response was decreased even lower than methyl carbamate. These results indicate that the functional group is more effective than the molecular size in the selectivity of the MIPs sensor. The chemical substances consisting of amide functional group can be bonded with –C=O group of PMMA by hydrogen adsorption therefore urea and thiourea with two amide groups have the current response higher than methyl carbamate and glutamic acid. For different molecular sizes, the large molecules cause the decrease of the decrease of the current response.

In case of ammonia, the significant reduction of current response comparing to that of urea is observed. However, the current response shows the similar level comparing to methyl carbamate and glutamic acid. This suggested that the ammonia molecule which is smaller molecular size than urea can makes hydrogen bonding with PMMA, existing space in the binding cavities of the MIPs sensing membrane. This situation allows electroactive pass through the surface electrode, as a consequence, the reduction of the current response of ammonia is presented.

For potassium nitrate and sodium chloride that do not have the amide group and have the higher polarity than urea, the current responses are barely observed. This result can be attributed that the polarity does not have the affect on the

selectivity of the MIPs sensor. Our technique confirms the capability to sense urea and similar molecules.

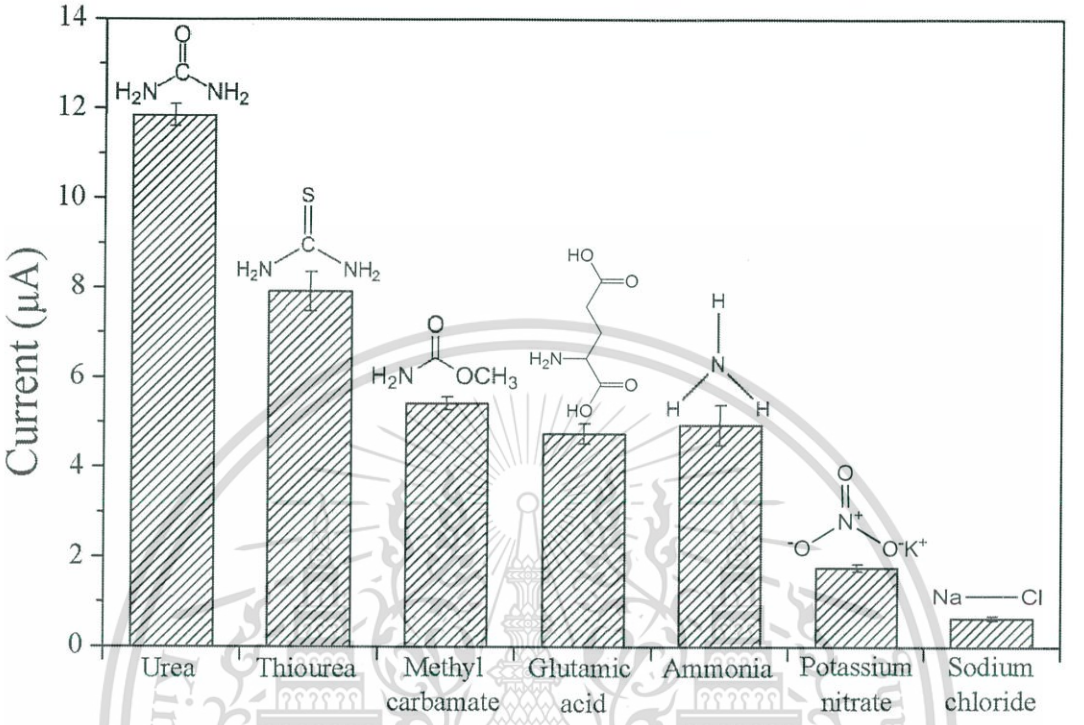

Figure 3.13 The selectivity of the MIPs-modified electrode to urea and other molecules at the same condition.

More importantly, the potential applications for the fabricated urea sensors were tested in human serum. The responses of the sensor were investigated with urea in the presence of interfering molecules (AA, Cr, UA and DA) in serum samples. For healthy people, the highest level of AA, Cr, UA and DA are 2.85×10^{-5}, 1.33×10^{-4}, 4.2×10^{-4},and 7.9×10^{-8} M, respectively [17]. The interference tests were done in triplicate in the solutions containing 1.0×10^{-5} M urea and interfering molecules at the respective concentration levels of 1-fold, 10-fold and 100-fold (1.0×10^{-5} M, 1.0×10^{-4} M and 1.0×10^{-3} M) higher than the natural concentrations of coexisting molecules in serum. Figure 3.14 shows the interference ratio ($\Delta I_P/\Delta I_O$) where ΔI_O is the response current of the MIPs electrode to 1.0×10^{-5} M urea, and ΔI_P is that of

the MIPs electrode to the coexisting molecules with 1.0×10^{-5} M urea. The relative standard deviation (RSD) of the current ratios ranged between 0.5 - 4.2 %. This indicated that the coexistence concentration might not affect the urea detection signal and this MIPs urea electrode exhibits high selectivity which will be useful and can be applied for detecting urea in serum samples.

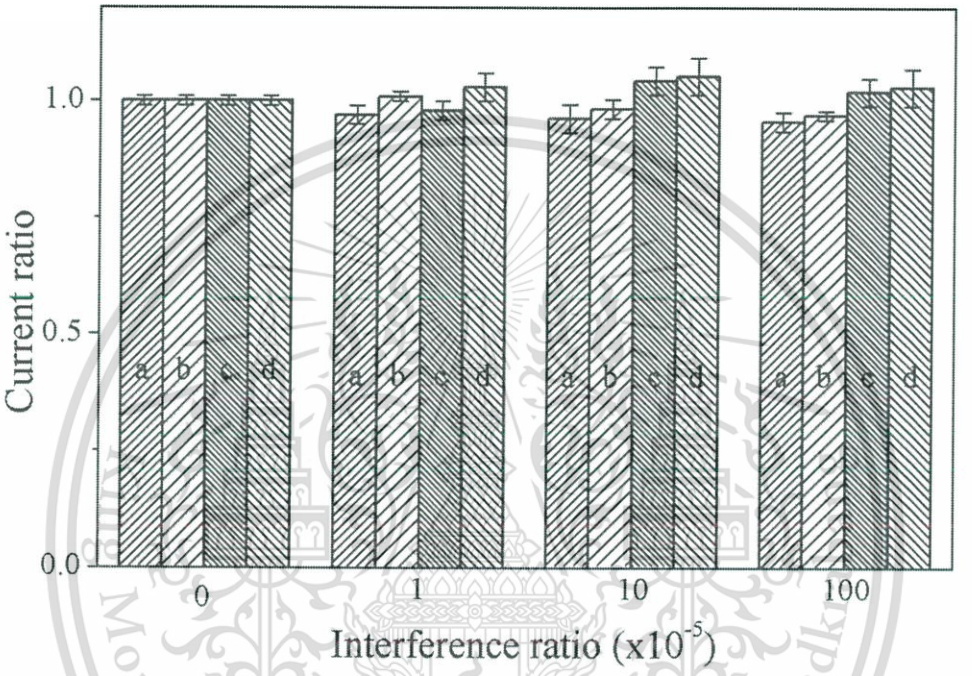

Figure 3.14 Effects of interference ratio on current ratio of various coexisting molecules UA (a), AA (b), Cr (c), and DA (d) at the concentrations of 0 M, 1-fold (1.0×10^{-5} M), 10-fold (1.0×10^{-4} M), 100-fold (1.0×10^{-3} M) in 1.0×10^{-5} M urea solutions.

3.3.5 Reproducibility, Repeatability and Stability of the MIPs electrodes

Reproducibility of the MIPs sensor was determined by testing identically fabricated MIPs electrodes (n=10) in 1.0×10^{-5} M urea solutions. The relative standard deviation (RSD) of 3.4 % was obtained as showed in Figure 3.15. This

demonstrates that the MIPs electrodes fabricated by the solvent evaporation technique were of good reproducibility.

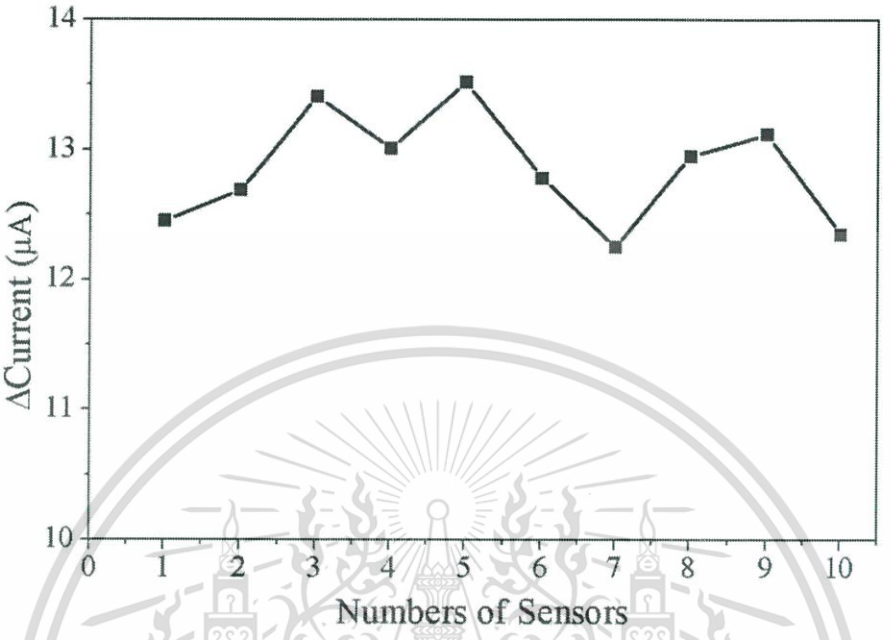

Figure 3.15 The current response for reproducibility of the MIPs electrodes.

Repeatability of the MIPs electrodes was investigated for three repetitions of the measurements in 1.0×10^{-5} M urea solutions by 10 identical electrodes. The RSD of 1.4 % was obtained as showed in Figure 3.16, showing a high repeatability.

Storage stability of the MIPs electrodes was investigated by monitoring the amperometric responses of the electrodes in 1.0×10^{-5} M urea solutions after a period of three months storage at room temperature (25°C in dry form). The retained response of the fabricated electrodes was 94% after three months of storage as showed in Figure 3.17. Due to PMMA has the glass transition temperature (T_g) is 105°C, therefore the MIPs electrodes can be storage at ambient conditions. This confirms an excellent long-term storage stability of the MIPs-modified electrode in comparison to standard urease-based biosensors.

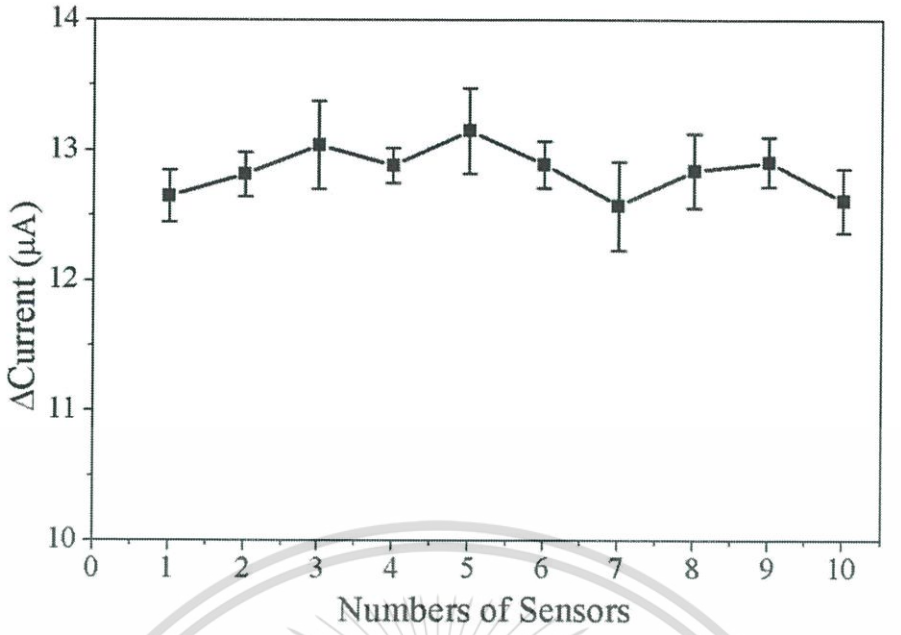

Figure 3.16 The current response for repeatability of the MIPs electrodes.

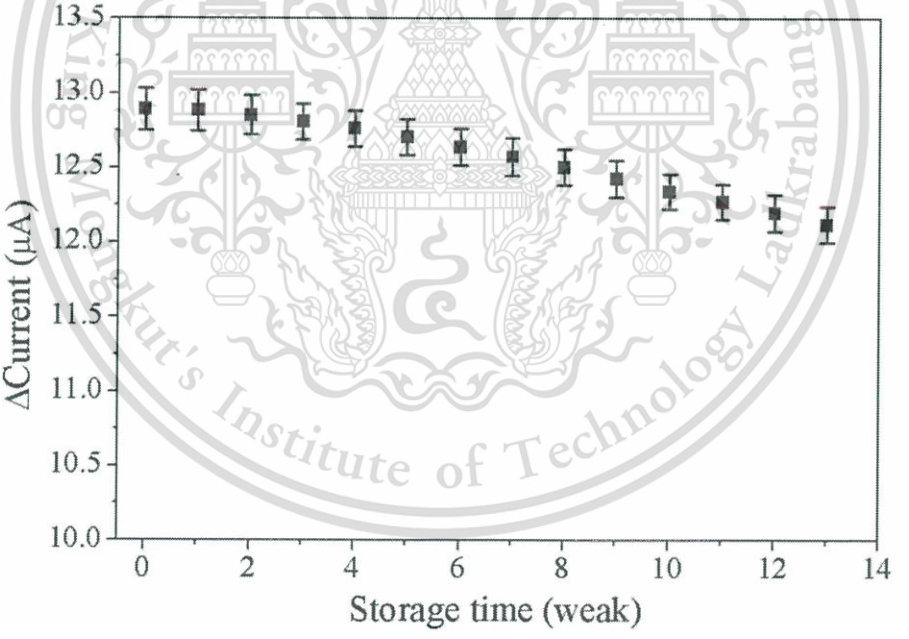

Figure 3.17 The current response for storage stability of the MIPs electrodes.

3.3.6 Determination of urea in real sample

In order to demonstrate the application of MIPs urea electrode for clinical analysis, urea in human serum samples were analyzed by the standard addition method for the recovery test. The urea at different concentrations (1.0×10^{-5}, 1.0×10^{-4}, 1.0×10^{-3} M) were added in the serum sample and were measured by the MIPs urea electrode. The experiments carried out triplicately and the recoveries of the MIPs urea sensors ranged from 95.4% - 105.6% as shown in Table 3.1. In addition the sensor shows possibility to detect urea in real blood serum samples.

Table 3.1 Recovery test for urea in human blood serum samples.

Measurement times	Urea concentration (M)		Recovery (%)
	Added	Found[a]	
1st measurement	1.0×10^{-5}	$0.98 \times 10^{-5} \pm 0.15$	98.1
	1.0×10^{-4}	$1.03 \times 10^{-4} \pm 0.23$	103.3
	1.0×10^{-3}	$1.05 \times 10^{-3} \pm 0.25$	105.2
2nd measurement	1.0×10^{-5}	$0.95 \times 10^{-5} \pm 0.24$	95.4
	1.0×10^{-4}	$0.96 \times 10^{-4} \pm 0.31$	96.3
	1.0×10^{-3}	$1.04 \times 10^{-3} \pm 0.14$	104.2
3th measurement	1.0×10^{-5}	$1.02 \times 10^{-5} \pm 0.15$	102.5
	1.0×10^{-4}	$1.03 \times 10^{-4} \pm 0.16$	103.6
	1.0×10^{-3}	$1.05 \times 10^{-3} \pm 0.25$	105.6

[a] Average of five measurements ± standard deviation.

CHAPTER 4

NON-ENZYMATIC UREA SENSOR USING MOLECULARLY IMPRINTED POLYMERS SURFACE MODIFIED BASED-ON ION-SENSITIVE FIELD EFFECT TRANSISTOR (ISFET)

Overview - A novel molecularly imprinted electrochemical sensor based on ISFET device has been developed for urea detection sensor. The molecularly imprinted polymers (MIPs) were prepared by photopolymerization on the surface of ISFET device using PMMA and urea as the functional polymer and molecular template, respectively. The fabricated sensors were characterized by potentiometry and UV-Vis spectroscopy. The preparation conditions were optimized for performance of the sensors, i.e. drop-cast volume and incubation time. The MIPs modified ISFET sensors has linear range response from 0.1 - 100 mM with the limit of detection of 0.1 mM (S/N = 3). The MIPs modified ISFET sensors also exhibit excellent reproducibility, repeatability and stability, as well as high selectivity to urea and were further applied to detect urea in human blood serum samples with success.

4.1 Introduction

Urea concentration is considerable indicator in agricultural chemistry, food science and environmental monitoring. Moreover, a urea has great significance in clinical diagnostics, i.e. Blood Urea Nitrogen or BUN. This is related to the concentration of nitrogen in the human serum in form of urea and indicator of the kidney function [6]. Typical urea concentration for urea nitrogen in serum is 5 - 20 mg/dl (1.8 - 7.1 mM/L) [139]. Urea determination has many methods such as gas chromatography, calorimetry and fluorimetric. These methods have disadvantages in complicated, expensive and time consuming. Nowadays, an electrochemical method

for urea biosensor has been widely studied due to simplicity, low cost and high sensitivity [14]. Ion-sensitive field effect transistors (ISFET) is electrochemical biosensor has been interested in development to wide range application devices such as glucose [93], triglycerides [94], creatinine [95] galactose and polyphenol [96] . The advantages of ISFET based biosensor are small size, high sensitivity, high level of activity, low cost and rapid response time [124]. The ISFET was first introduced by Bergveld in 1970 [80]. And then, in 1980 ISFET based enzyme biosensor was described by Caras and Janata [92]. The analytical technique for urea biosensor based on ISFET is enzymatic hydrolysis of urea causes pH changes in the system [9]. However enzyme has limitations such as: enzyme activity, enzyme stability and the environment of using [18].

Recently, molecularly imprinting technique has been developed for non-enzymatic sensor in electrochemical sensing for organic compounds. The advantages over biological recognition including, stability, low cost, long lifetime, high sensitivity and widely applied in sensor development [72,129]. Preparation of molecularly imprinted polymers (MIPs), the molecular template and functional polymer are mixed in solutions to form a complex. The polymer-template solution is co-deposited on the surface of an electrode. After that, the molecular template was removed from the polymer matrix, leaving molecular cavities has complementary to the template in size, shape, and functional groups [135]. The response of MIPs sensor to target molecules may be similarly enzymatic mechanisms into two strategies for molecular detection. One is response higher occurred the chemical reaction between polymeric membrane and template molecule, generated a charge or electron [67]. The other is the template molecules that are embedded into the molecular cavities which similar to the inhibition of enzymatic activities [74,75], obstruction for charge transfer to the surface of the electrode is the cause of the reduction of the response signal [71]. This approach has been presented for MIPs sensor by incubating the sensor in a sample solution before measuring the response in an electrolyte [135].

In this chapter, we reported a novel molecularly imprinted sensor based-on the ISFET device for urea detection. Urea was used as the molecule template and poly(methyl methacrylate) (PMMA) used as the functional polymer. The ISFET sensing area was coated by drop-casting of the PMMA-urea solution and exposed to UV irradiation for photopolymerization. Urea molecular templates were removed by immersion in DI water. The sensor was characterized by potentiometry and UV-Vis spectroscopy. The sensitivity, selectivity, repeatability and reproducibility of the fabricated sensor have been investigated.

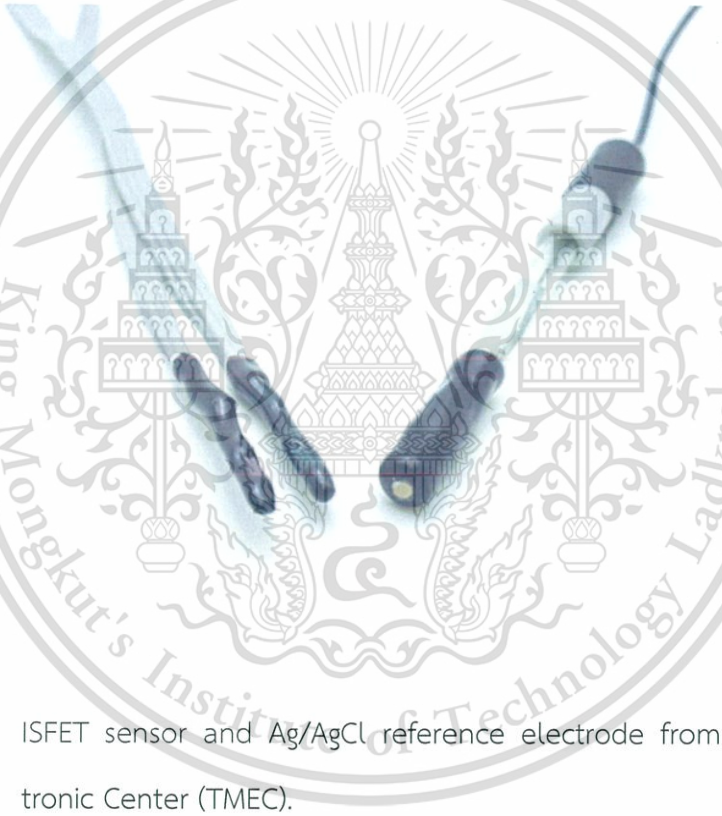

Figure 4.1 ISFET sensor and Ag/AgCl reference electrode from Thai Microelectronic Center (TMEC).

4.2 Materials and methods

4.2.1 Chemicals and reagents

All chemicals and reagent were used analytical grade and de-ionized (DI) water (Resistivity >18 MΩ/cm) was used in all experiments. Urea, methyl carbamate, glutamic acid, Sodium Chloride (NaCl), uric acid (UA), ascorbic acid (AA), dopamine

(DA), creatinine (Cr) human serum and sodium chloride (NaCl) were purchased from Sigma-Aldrich, poly(methyl methacrylate) (PMMA) from Acros organics, dimethylformamide (DMF) from Labscan Asia. Potassium nitrate (KNO_3), sodium dihydrogen phosphate (NaH_2PO_4) and disodium hydrogen phosphate (Na_2HPO_4) were ordered from Ajax Finechem, and pH buffer solution from CARLO ERBA Reagents.

4.2.2 ISFET device and measurement

The ISFET devices obtained from Thai Microelectronic Center (TMEC). The ISFET microdevice has gate area 100 × 2000 μm^2 and has silicon nitride (Si_3N_4) as sensing membrane. In addition, electrical and chemical specifications were shown as Table 4.1. For the electrochemical measurement, the ISFET and MIPs modified ISFET were used as working electrode, while an Ag/AgCl (3 M of KCl) was used as reference electrode. The ISFET response characteristic was determined at gate-source voltage (V_{GS}) variations by using a constant drain-source current (I_{DS} = 30 μA) and constant drain-source voltage (V_{DS} = 300 mV). Schematic of the electrical power using constant current-constant voltage circuits was illustrated in Figure 4.2. The voltage response was measured by microprocessor number ADuC847 from Analog Devices, Inc. with A/D (analog to digital) 24 bit. This circuit was operated and recorded all data via a serial port (RS-232) connection to the computer, by using a Labview software program.

The pH sensitivity and calibration curves of ISFET sensor have been measured with standard pH buffer solution. The MIPs modified electrode was incubated in 5 ml urea solution for 5 min and then measured the voltage response of the MIPs sensor in phosphate buffer solution pH 7.0. [135].

Table 4.1 Specification of ISFET sensor.

Specification	Value
Physical specification	
sensing membrane	SiO_2/Si_3N_4
chip dimensions	L=6mm, W=2mm
gate length	2,000 μm
gate width	100 μm
Electrical specification	
operational drain voltage, V_d	0.3 V
operational drain current, Id	30 μA
threshold voltage, V_{th}	0.5 V – 2.0 V
(V_d= 0.3 V pH = 7)	
leakage current, I_l	10 nA
(V_{REF} = 3 V pH = 7)	
Chemical specification	
sensitivity, S	40-50 mV/pH

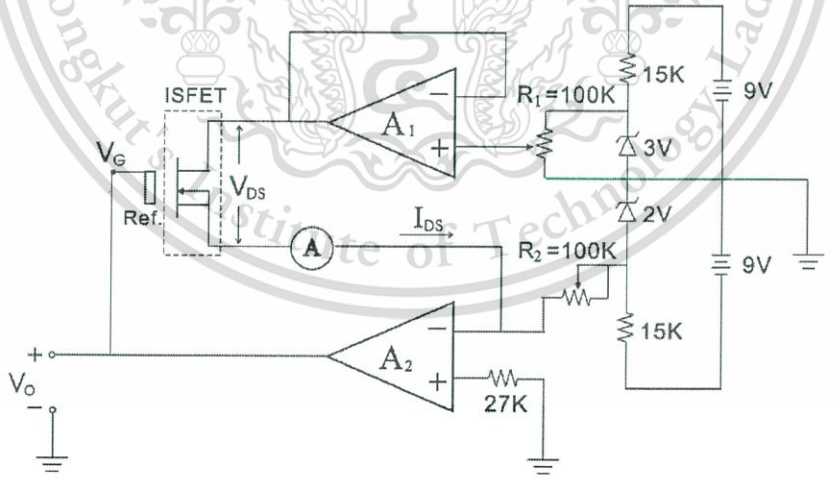

Figure 4.2 Schematic of constant current-constant voltage circuits [140].

4.2.3 ISFET surface modification

The ISFET surface was cleaned with ethanol and DI water in ultrasonic bath for 5 min in each step. The polymer-urea solution was prepared by dissolve 2.5 wt% of PMMA and 0.4 wt% of urea in 10 ml of DMF and sonication for 10 min. The ISFET surface area of 6 mm^2 was coated by 1 µl of mixture solution and curing with ultraviolet radiation (Stratagene UV Stratalinker 1800) for 15 min. After the polymer-urea layer on ISFET surface was immersed in DI water for 1 h to remove the urea template molecules form the polymer layer then the MIPs membrane was produced.

Validation of urea template removal for MIPs membrane on the ISFET sensor cannot determine by a direct method such as FT-IR, due to a small surface area of the ISFET sensor. Therefore, the template removal characteristic of the MIPs membrane was investigated by UV-Vis spectroscopy (T92+ UV-VIS spectrophotometer from PG Instruments Ltd.) which is an indirect method. The PMMA-urea coating layer on the ISFET sensor was immersed in DI water and then measurement DI water before and after washing PMMA-urea coating layer [26].

4.3 Results and discussion

4.3.1 Characterization of MIPs modified ISFET sensors

4.3.1.1 Electrochemical measurement

The pH sensitivity of ISFET sensors at different fabrication stages were tested in pH buffer solutions (4, 7, 10). The sensitivities of different fabricated ISFET devices were shown as the slope of characteristic curves displayed in Figure 4.3. The PMMA-urea/ISFET sensor has lower sensitivity than Si_3N_4/ISFET sensor because of the polymer-urea layer obstructs the charges that pass through to the electrodes of device affected to high voltage. After the urea template molecule removal, the surface of sensor becomes to porous membrane so the MIPs/ISFET sensor exhibits an

increased sensitivity. However, the response voltage level of the MIPs/ISFET sensor is higher than the Si_3N_4/ISFET sensor [71,135].

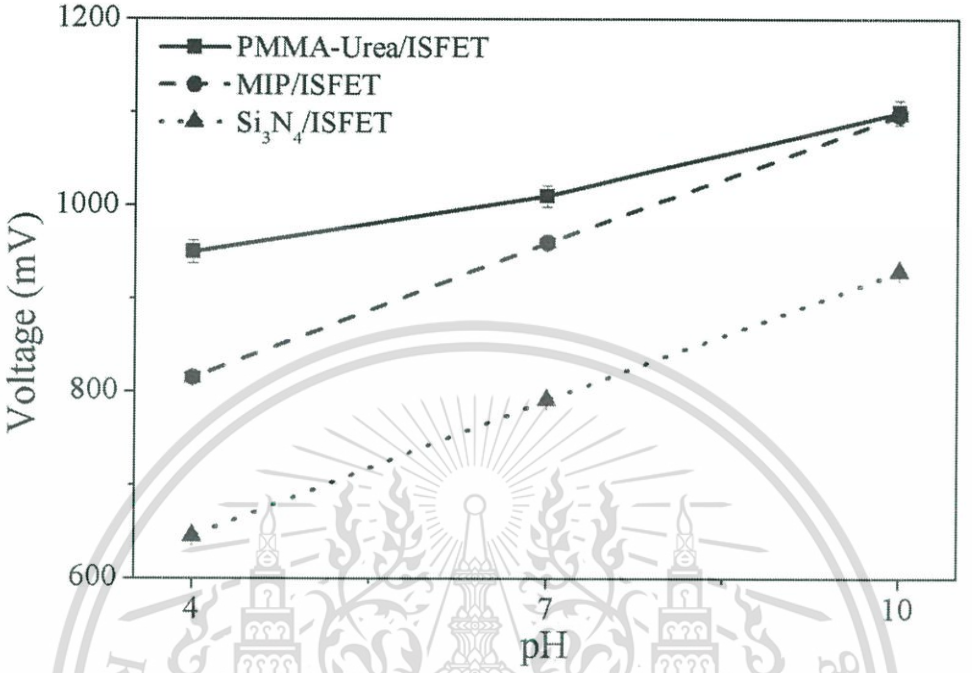

Figure 4.3 The voltage and pH characteristic of fabricated sensors, PMMA-urea/ISFET (solid line), MIPs/ISFET (dash line) and Si_3N_4/ISFET (dot line) in pH buffer solutions.

4.3.1.2 Characterization of removal template

The UV-Vis absorption spectroscopy was applied to confirm the template removal characteristic of DI water before and after washing PMMA-urea coating layer. Figure 4.4 shows UV-Vis spectra of DI water and elution solution. The reference solution i.e. DI water has no absorption peak between 200 - 900 nm, while the elution after washing coating layer has the absorption peak of urea could be found at 230 nm. The reason is due to the urea template molecules have been removed from the polymer matrix.

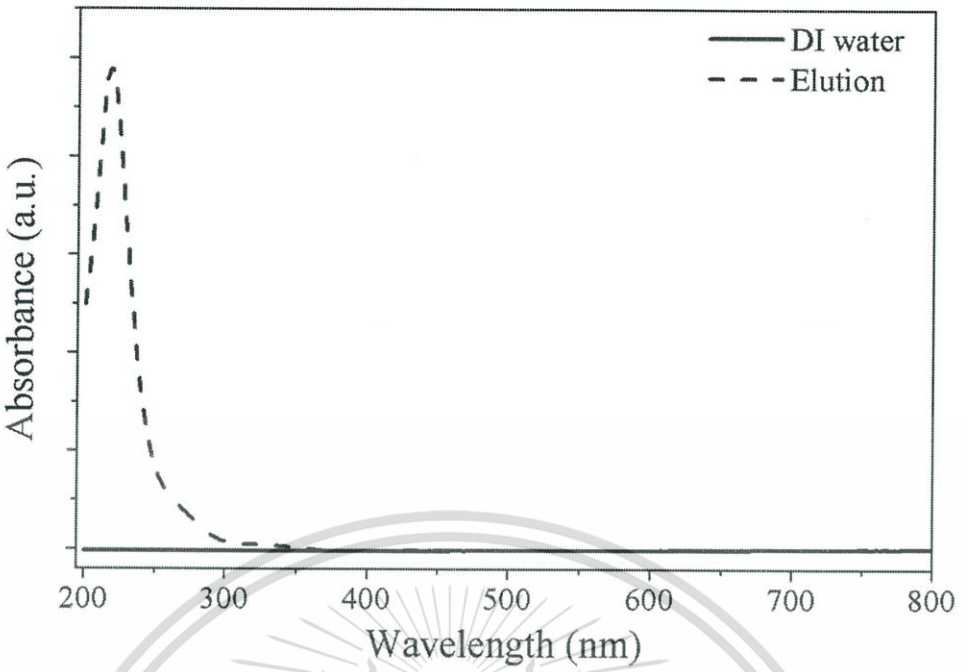

Figure 4.4 UV-Vis absorption spectra of DI water and elution solution.

4.3.2 Optimization of MIPs modified ISFET sensor

4.3.2.1 Optimization of the volume of the polymer-urea composite solution

The performance of the MIPs modified ISFET depends on the thickness of the polymer membrane. This is consistent with the drop-cast volume of the polymer-urea composite solution. Figure 4.5 shows the voltage response of MIPs modified ISFET sensor to 1 mM urea. The volume of PMMA-urea composite solution at 1.0 µl obtains maximum response. When the volume of PMMA-urea composite solution less than 1.0 µl, the response voltage was decreased because the polymer film may cracks while urea template molecule was removed. If the volume of composite solution more than 1.0 µl, the urea template molecule cannot completely remove from polymer matrix caused by the film thickness [26,135].

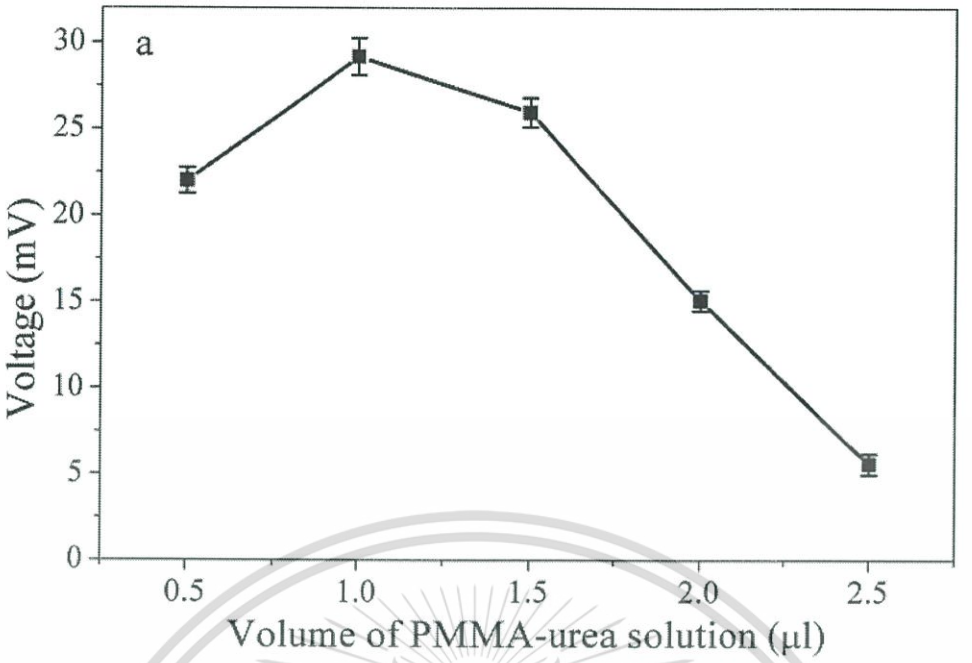

Figure 4.5 The effect of volume of the PMMA-urea solution for the MIPs fabrication.

4.3.2.2 Effect of the incubation time

Investigation the effect of incubation time to the output response of the sensor, the MIPs modified ISFET sensor was studied in 1 mM urea solution for 1, 3, 5, 10 and 15 min at room temperature. Figure 4.6 shows the voltage response with the incubation time. When the incubation time is increased the voltage is increased and saturated after 5 min. Therefore, the optimal of incubation time is 5 min.

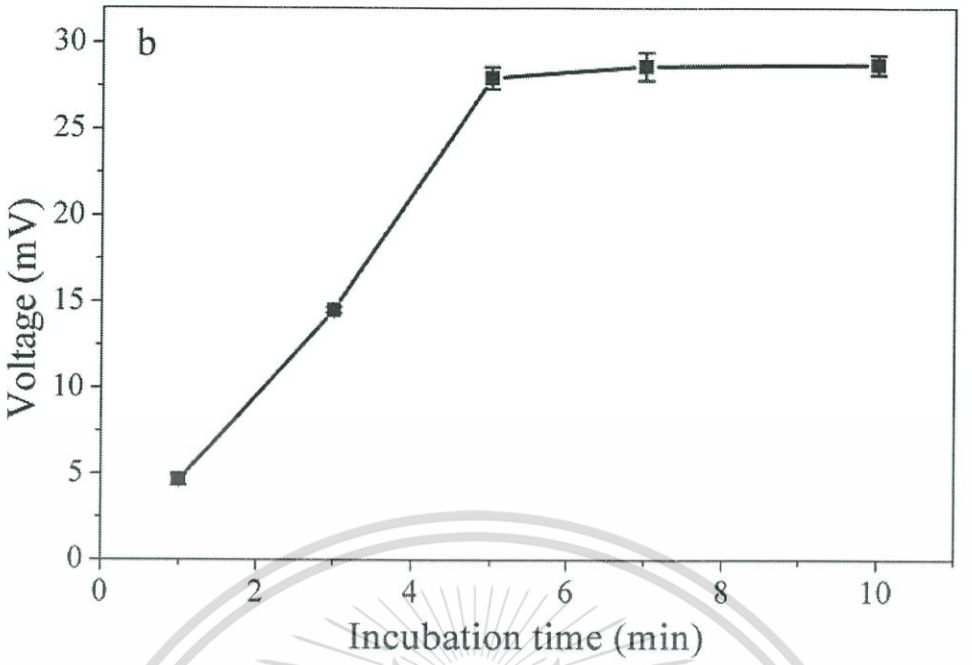

Figure 4.6 The effect of inclubation time for the MIPs measurement.

4.3.3 Determination of aqueous urea samples

The electrochemical responses of the MIPs and NIPs modified ISFET sensors have been investigated in urea solution at different concentrations (from 0.1 mM – 1.0 M) as shown in Figure 4.7. The results represent the obviously highest response of the MIPs sensor, while the NIPs sensor has no trend response for all urea concentration ranges. The response of the MIPs sensor to urea was found to be linearity in the range of 0.1 - 100 mM, with the sensitivity of 18.4 mV/pUrea (R^2 = 0.992). The limit of detection (LOD) for urea is 0.1 mM (S/N = 3).

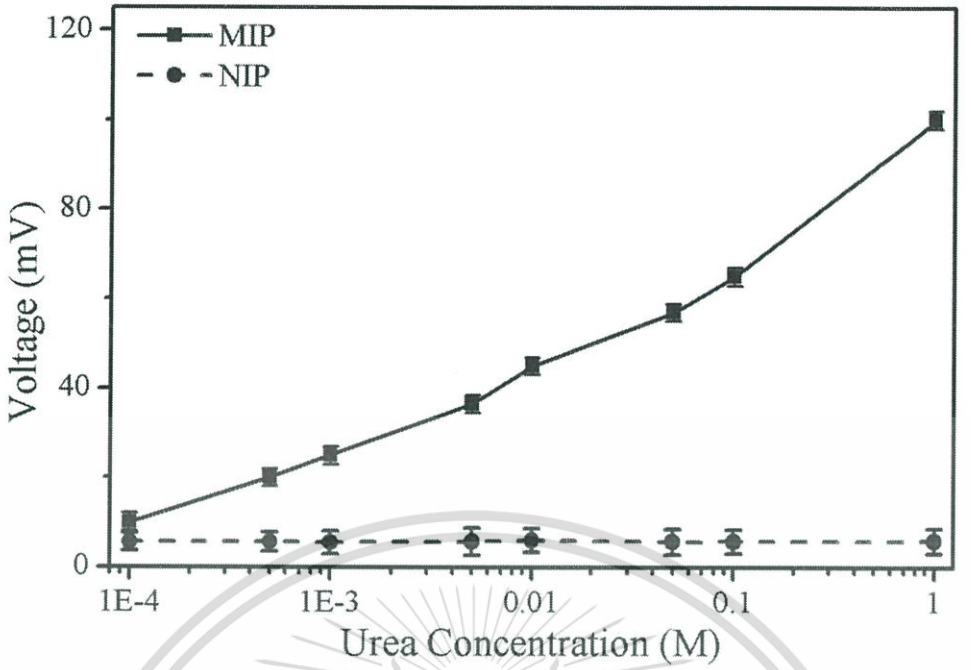

Figure 4.7 Voltage response of MIPs (solid line) and NIPs (dash line) modified ISFET sensors in different urea concentrations.

4.3.4 Selectivity of the MIPs modified ISFET sensors

Specific recognition to the urea target molecule has been important for developing the MIPs modified ISFET sensor. In order to check the selectivity of molecularly imprinted sensor, methyl carbamate, glutamic acid, potassium nitrate and sodium chloride were chosen for interference studies, which molecules methyl carbamate, glutamic acid and potassium nitrate have a similar structure to urea, and sodium chloride has interaction type to urea in the blood sample. Figure 4.8 displays the voltage response of MIPs modified ISFET sensor to urea and four substrates at concentration of 1 mM for all solutions. The result shows that the voltage response of urea has higher than four other interfering molecules. It can imply that the molecular cavities from removal template molecule on surface of fabricated MIPs modified ISFET sensor has highly specific to urea molecules.

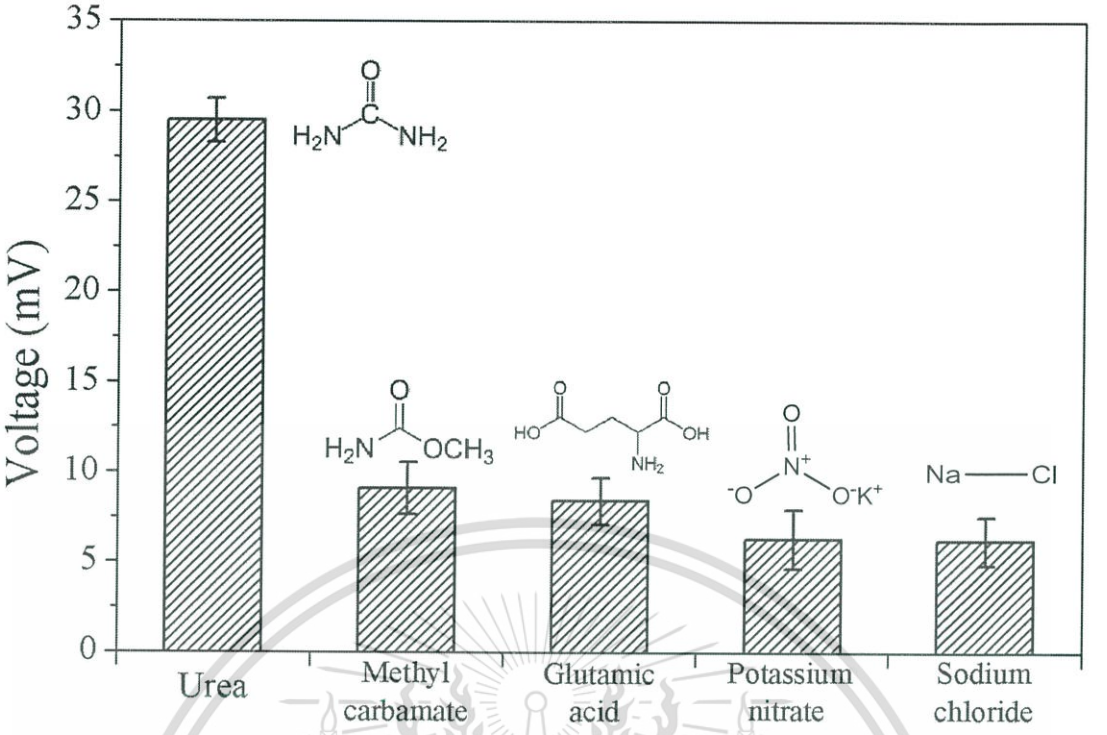

Figure 4.8 The voltage response of MIPs-modified ISFET sensor to urea and other molecules.

The potential applications for the fabricated urea sensors were tested in human serum. The responses of the sensor were evaluated with urea in the presence of interfering molecules (AA, Cr, UA and DA) in serum samples. The interference tests were done in 1 mM urea and interfering molecules at the concentration levels of 1, 5, and 10 mM containing 1 mM urea. Figure 4.9 shows the interference ratio ($\Delta V_P/\Delta V_O$) where ΔV_O is the voltage output of the MIPs electrode to 1 mM urea, and ΔV_P is that of the MIPs electrode to the coexisting molecules with 1 mM urea. The relative standard deviation (RSD) of the voltage ratios ranged between 1.3 – 4.5 %. This indicated that the coexistence concentration might not affect the urea detection signal and this MIPs modified ISFET sensor exhibits high selectivity which will be useful and can be applied for detecting urea in serum samples.

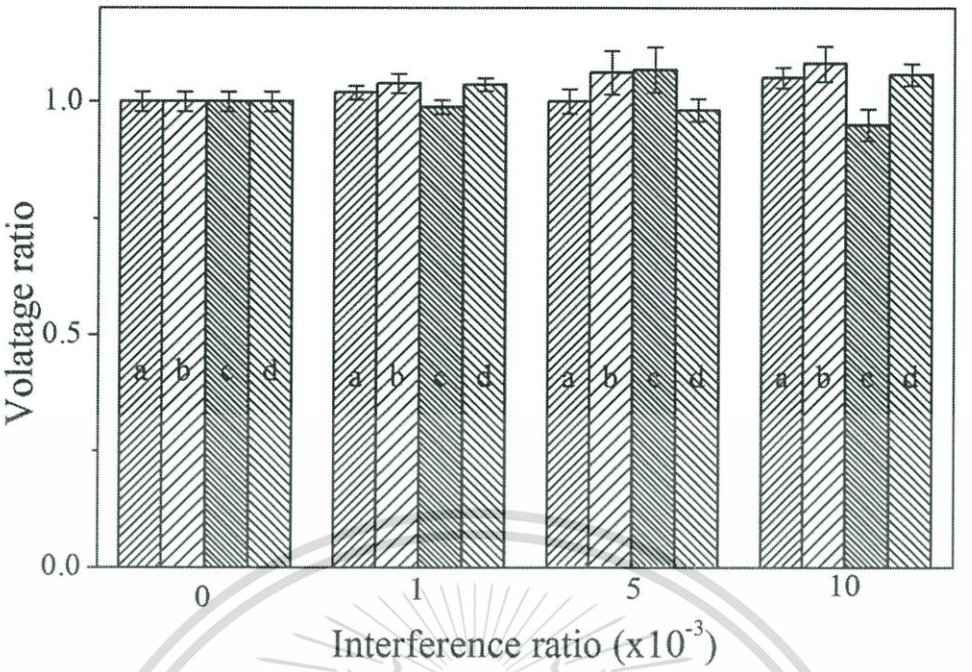

Figure 4.9 Effects of interference ratio on voltage ratio of various coexisting molecules UA (a), AA (b), Cr (c), and DA (d) at the concentrations of 0 M, 1-fold (1 mM), 5-fold (5 mM), 10-fold (10 mM) in 1 mM urea solutions.

4.3.5 Reproducibility, Repeatability, and Stability of the MIPs modified ISFET sensors

Reproducibility of the fabricated sensor was determined by using 1 mM urea with ten MIPs modified ISFET sensors which prepared at same conditions. The relative standard deviation (RSD) of voltage response was calculated to be 3.4%, represented that the MIPs modified ISFET sensors are a good reproducibility [129].

Repeatability of the MIPs modified ISFET sensor was defined by using ten same fabricated sensors measured in 1 mM urea for 3 times. The RSD of 2.5% was observed for a good repeatability [129].

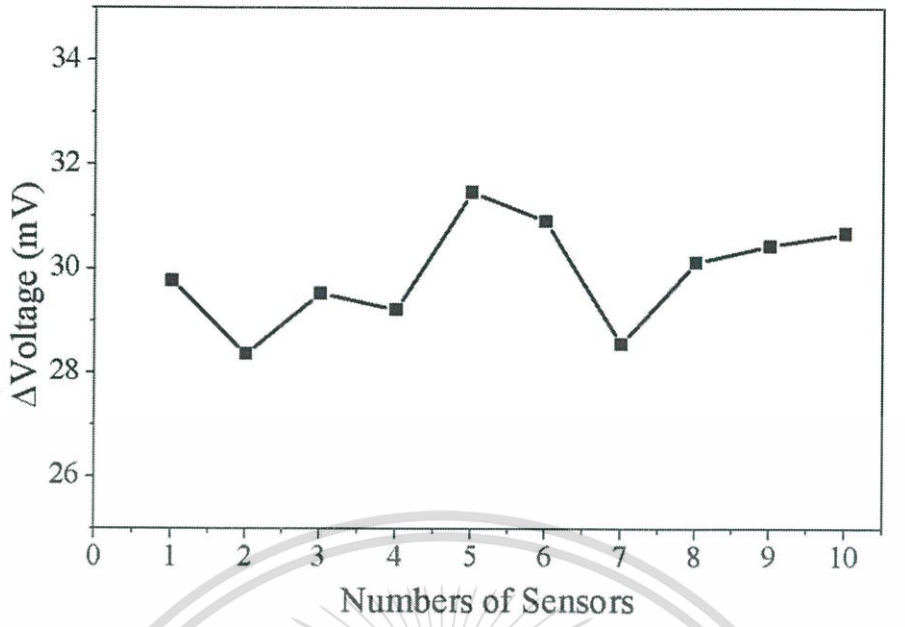

Figure 4.10 The voltage output for reproducibility of the MIPs electrodes.

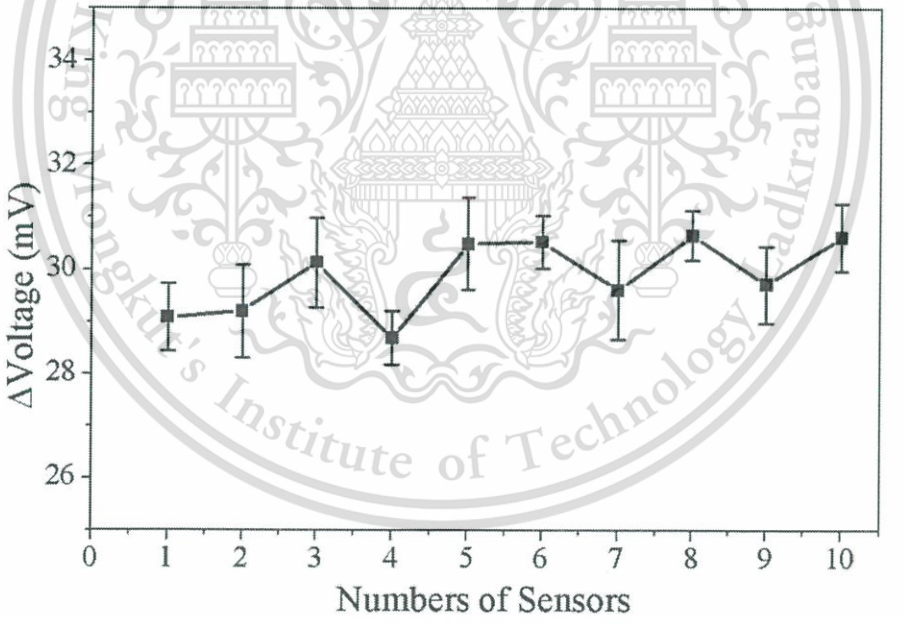

Figure 4.11 The voltage output for repeatability of the MIPs electrodes.

Storage stability of the MIPs modified ISFET sensor has been investigated by comparing the voltage response of 1 mM urea for a period of two months at room temperature. The response of the sensors has retained 95% after two months. The result was indicated that our novel MIPs modified ISFET sensor has excellent long-term storage stability.

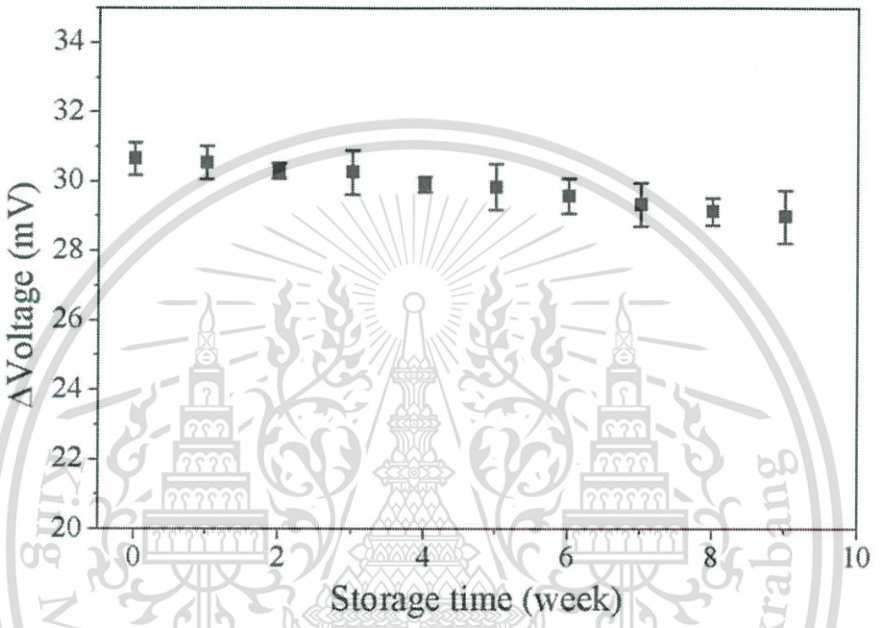

Figure 4.12 The voltage output for storage stability study of the MIPs electrodes.

4.3.6 Determination of urea in real sample

The MIPs modified ISFET sensors were applied to measure the urea in the blood human serum for clinical analysis, urea in human serum samples were determined by the standard addition method for the recovery test. The serum sample with three different urea additions was measured and obtained the recoveries ranged from 95.3% - 104.9% as shown in Table 4.2. In addition, the sensor shows the possibility to detect urea in real blood serum samples.

Table 4.2 Recovery test for urea in human blood serum samples.

Measurement times	Urea concentration (mM)		Recovery (%)
	Added	Found[a]	
1st measurement	1.0	0.96 ± 0.12	96.3
	5.0	5.06 ± 0.17	101.3
	10.0	10.36 ± 0.52	103.6
2nd measurement	1.0	1.05 ± 0.11	104.7
	5.0	5.01 ± 0.19	100.3
	10.0	9.93 ± 0.54	99.3
3th measurement	1.0	0.95 ± 0.09	95.3
	5.0	5.04 ± 0.18	100.8
	10.0	10.49 ± 0.47	104.9

[a] Average of three measurements ± standard deviation.

CHAPTER 5

CONCLUSIONS AND OUTLOOK

This thesis demonstrates a successful MIPs urea sensor fabricated using a simple method on the gold-coated electrodes and ISFET sensors. The PMMA-based MIPs sensors are synthesized by solvent-assisted drop casting technique. The urea-sensing responses of the MIPs sensors on gold-coated electrode yield two linearity ranges from 2 - 100 μM and 0.1 - 100 mM with the limit of detection is 0.8 μM (S/N = 3). For the urea measurement in the human blood serum, the MIPs urea sensor obtained the recoveries range between 95.4% - 105.6%. The MIPs modified ISFET sensors have linear range response from 0.1 - 100 mM with the limit of detection is 0.1 mM (S/N = 3). In order to measure urea in the human blood serum, the MIPs modified ISFET sensors have the recovery range between 95.3 - 104.9 %. The MIPs sensors also exhibited high reproducibility, repeatability, as well as high selectivity to urea with storage stability in ambient conditions. This work, we have filed a patent number applicant 1501000653 in the title of "Polymeric selective membranes for non-enzymatic detection of urea and organic compounds".

The electrochemical sensors with the urea-MIPs membrane are promising to develop for clinical diagnostic assay. The MIPs urea sensor should be developed to the portable device for urea measurement in the blood samples. The blood cells are mainly red blood cells, white blood cells and plaletes that affect to the electrochemical detection. Consequently, it is necessary to separate blood cells and collect only plasma or serum to detect BUN. To separate blood cells, we need to perform in close system, therefore the microfluidic, which is the fluid manipulation in micro/nano scale, is promising to integrate with the MIPs sensors [141–144]. Such a diagnostic tool will be a very useful for either scientific purposes or medical.

Refference

1. Grieshaber D, MacKenzie R, Vörös J, Reimhult E. 2008, "Electrochemical Biosensors - Sensor Principles and Architectures." **Sensors**, 8(3): 1400–1458.
2. Revilla M, Alexander J, Glibert PM. 2005, "Urea analysis in coastal waters: comparison of enzymatic and direct methods." **Limnol Oceanogr Methods**, 3(7): 290–299.
3. Wilson MS. 2005, "Electrochemical Immunosensors for the Simultaneous Detection of Two Tumor Markers." **Anal Chem**, 77(5): 1496–1502.
4. D'Orazio P. 2003, "Biosensors in clinical chemistry." **Clin Chim Acta**, 334(1–2): 41–69.
5. Sahney R, Anand S, Puri BK, Srivastava AK. 2006, "A comparative study of immobilization techniques for urease on glass-pH-electrode and its application in urea detection in blood serum." **Anal Chim Acta**, 578(2): 156–161.
6. Rajesh, Bisht V, Takashima W, Kaneto K. 2005, "A novel thin film urea biosensor based on copolymer poly(N-3-aminopropylpyrrole-co-pyrrole) film." **Surf Coat Technol**, 198(1–3): 231–236.
7. Rajesh, Bisht V, Takashima W, Kaneto K. 2005, "An amperometric urea biosensor based on covalent immobilization of urease onto an electrochemically prepared copolymer poly (N-3-aminopropyl pyrrole-co-pyrrole) film." **Biomaterials**, 26(17): 3683–3690.
8. Luppa PB, Sokoll LJ, Chan DW. 2001, "Immunosensors—principles and applications to clinical chemistry." **Clin Chim Acta**, 314(1–2): 1–26.
9. Soldatkin AP, Montoriol J, Sant W, Martelet C, Jaffrezic-Renault N. 2003, "A novel urea sensitive biosensor with extended dynamic range based on recombinant urease and ISFETs." **Biosens Bioelectron**, 19(2): 131–135.
10. Singhal R, Gambhir A, Pandey MK, Annapoorni S, Malhotra BD. 2002, "Immobilization of urease on poly(N-vinyl carbazole)/stearic acid Langmuir–

Blodgett films for application to urea biosensor." **Biosens Bioelectron**, 17(8): 697–703.

11. Taylor AJ, Vadgama P. 1992, "Analytical Reviews in Clinical Biochemistry: The Estimation of Urea." **Ann Clin Biochem Int J Biochem Med**, 29(3): 245–64.
12. Francis PS, Lewis SW, Lim KF. 2002, "Analytical methodology for the determination of urea: current practice and future trends." **TrAC Trends Anal Chem**, 21(5): 389–400.
13. Ali A, Ansari AA, Kaushik A, Solanki PR, Barik A, Pandey MK, et al. 2009, "Nanostructured zinc oxide film for urea sensor." **Mater Lett**, 63(28): 2473–2475.
14. Kaushik A, Solanki PR, Ansari AA, Sumana G, Ahmad S, Malhotra BD. 2009, "Iron oxide-chitosan nanobiocomposite for urea sensor." **Sens Actuators B Chem**, 138(2): 572–580.
15. Mondal S, Sangaranarayanan MV. 2013, "A novel non-enzymatic sensor for urea using a polypyrrole-coated platinum electrode." **Sens Actuators B Chem**, 177: 478–486.
16. Bianchi RC, Silva ER da, Dall'Antonia LH, Ferreira FF, Alves WA. 2014, "A Nonenzymatic Biosensor Based on Gold Electrodes Modified with Peptide Self-Assemblies for Detecting Ammonia and Urea Oxidation." **Langmuir**, 30(38): 11464–11473.
17. Chen Y-P, Liu B, Lian H-T, Sun X-Y. 2011, "Preparation and Application of Urea Electrochemical Sensor Based on Chitosan Molecularly Imprinted Films." **Electroanalysis**, 23(6): 1454–1461.
18. Lian H-T, Liu B, Chen Y-P, Sun X-Y. 2012, "A urea electrochemical sensor based on molecularly imprinted chitosan film doping with CdS quantum dots." **Anal Biochem**, 426(1): 40–46.
19. Hulanicki A, Glab S, Ingman F. 2009, "Chemical sensors: definitions and classification." **Pure Appl Chem**, 63(9): 1247–1250.

20. Thevenot DR, Tóth K, Durst RA, Wilson GS. 1999, "Electrochemical Biosensors: Recommended Definitions and Classification." **Pure Appl Chem**, 71(12): 2333–2348.

21. Nakamura H, Karube I. 2003, "Current research activity in biosensors." **Anal Bioanal Chem**, 377(3): 446–468.

22. Clark LC, Lyons C. 1962, "Electrode Systems for Continuous Monitoring in Cardiovascular Surgery." **Ann N Y Acad Sci**, 102(1): 29–45.

23. Wulff G, Sarhan A. 1972, "The use of polymers with enzyme-analogous structures for the resolution of racemates." **Angew Chem Int Ed Engl**, 11(4): 341.

24. Wulff G, Sarhan A, Zabrocki K. 1973, "Enzyme-analogue built polymers and their use for the resolution of racemates." **Tetrahedron Lett**, 14(44): 4329–4332.

25. O'Shannessy DJ, Ekberg B, Andersson LI, Mosbach K. 1989, "Recent advances in the preparation and use of molecularly imprinted polymers for enantiomeric resolution of amino acid derivatives." **J Chromatogr A**, 470(2): 391–399.

26. Lian W, Liu S, Yu J, Xing X, Li J, Cui M, et al. 2012, "Electrochemical sensor based on gold nanoparticles fabricated molecularly imprinted polymer film at chitosan–platinum nanoparticles/graphene–gold nanoparticles double nanocomposites modified electrode for detection of erythromycin." **Biosens Bioelectron**, 38(1): 163–169.

27. Schirhagl R, Latif U, Podlipna D, Blumenstock H, Dickert FL. 2012, "Natural and Biomimetic Materials for the Detection of Insulin." **Anal Chem**, 84(9): 3908–3913.

28. Haupt K. 2003, "Molecularly imprinted polymers: the next generation." **Anal Chem**, 75(17): 376A–383A.

29. Vasapollo G, Sole RD, Mergola L, Lazzoi MR, Scardino A, Scorrano S, et al. 2011, "Molecularly Imprinted Polymers: Present and Future Prospective." **Int J Mol Sci**, 12(9): 5908–5945.

30. Cheong WJ, Yang SH, Ali F. 2013, "Molecular imprinted polymers for separation science: A review of reviews." **J Sep Sci**, 36(3): 609–628.

31. Mafu LD, Msagati TAM, Mamba BB. 2013, "Ion-imprinted polymers for environmental monitoring of inorganic pollutants: synthesis, characterization, and applications." **Environ Sci Pollut Res**, 20(2): 790–802.

32. Alizadeh T. 2010, "Preparation of molecularly imprinted polymer containing selective cavities for urea molecule and its application for urea extraction." **Anal Chim Acta**, 669(1–2): 94–101.

33. Alizadeh T, Ganjali MR, Zare M, Norouzi P. 2010, "Development of a voltammetric sensor based on a molecularly imprinted polymer (MIP) for caffeine measurement." **Electrochimica Acta**, 55(5): 1568–1574.

34. Athikomrattanakul U, Katterle M, Gajovic-Eichelmann N, Scheller FW. 2011, "Preparation and characterization of novel molecularly imprinted polymers based on thiourea receptors for nitrocompounds recognition." **Talanta**, 84(2): 274–279.

35. Marx S, Zaltsman A, Turyan I, Mandler D. 2004, "Parathion Sensor Based on Molecularly Imprinted Sol–Gel Films." **Anal Chem**, 76(1): 120–126.

36. Jiang X, Tian W, Zhao C, Zhang H, Liu M. 2007, "A novel sol–gel-material prepared by a surface imprinting technique for the selective solid-phase extraction of bisphenol A." **Talanta**, 72(1): 119–125.

37. Li F, Li J, Zhang S. 2008, "Molecularly imprinted polymer grafted on polysaccharide microsphere surface by the sol–gel process for protein recognition." **Talanta**, 74(5): 1247–1255.

38. Gholivand MB, Karimian N. 2015, "Fabrication of a highly selective and sensitive voltammetric ganciclovir sensor based on electropolymerized molecularly imprinted polymer and gold nanoparticles on multiwall carbon nanotubes/glassy carbon electrode." **Sens Actuators B Chem**, 215: 471–479.

39. Cieplak M, Szwabinska K, Sosnowska M, Chandra BKC, Borowicz P, Noworyta K, et al. 2015, "Selective electrochemical sensing of human serum albumin by semi-covalent molecular imprinting." **Biosens Bioelectron**, 74: 960–966.

40. Huang C-Y, Tsai T-C, Thomas JL, Lee M-H, Liu B-D, Lin H-Y. 2009, "Urinalysis with molecularly imprinted poly(ethylene-co-vinyl alcohol) potentiostat sensors." **Biosens Bioelectron**, 24(8): 2611–2617.

41. Khadro B, Sanglar C, Bonhomme A, Errachid A, Jaffrezic-Renault N. 2010, "Molecularly imprinted polymers (MIP) based electrochemical sensor for detection of urea and creatinine." **Procedia Eng**, 5: 371–374.

42. Stevenson D. 1999, "Molecular imprinted polymers for solid-phase extraction." **TrAC Trends Anal Chem**, 18(3): 154–158.

43. Qiao F, Sun H, Yan H, Row KH. 2006, "Molecularly Imprinted Polymers for Solid Phase Extraction." **Chromatographia**, 64(11–12): 625–634.

44. Dias ACB, Figueiredo EC, Grassi V, Zagatto EAG, Arruda MAZ. 2008, "Molecularly imprinted polymer as a solid phase extractor in flow analysis." Talanta, 76(5): 988–996.

45. Byrne ME, Park K, Peppas NA. 2002, "Molecular imprinting within hydrogels." **Adv Drug Deliv Rev**, 54(1): 149–161.

46. Alvarez-Lorenzo C, Concheiro A. 2004, "Molecularly imprinted polymers for drug delivery." **J Chromatogr B**, 804(1): 231–245.

47. Cunliffe D, Kirby A, Alexander C. 2005, "Molecularly imprinted drug delivery systems." **Adv Drug Deliv Rev**, 57(12): 1836–1853.

48. Lavignac N, Allender CJ, Brain KR. 2004, "Current status of molecularly imprinted polymers as alternatives to antibodies in sorbent assays." **Anal Chim Acta**, 510(2): 139–145.

49. Zimmerman SC, Lemcoff NG. 2004, "Synthetic hosts via molecular imprinting—are universal synthetic antibodies realistically possible?" **Chem Commun**, 2004(1): 5–14.

50. Fernández-González A, Guardia L, Badía-Laíño R, Díaz-García ME. 2006, "Mimicking molecular receptors for antibiotics – analytical implications." **TrAC Trends Anal Chem**, 25(10): 949–957.

51. Wei S, Jakusch M, Mizaikoff B. 2006, "Capturing molecules with templated materials—Analysis and rational design of molecularly imprinted polymers." **Anal Chim Acta**, 578(1): 50–58.

52. Blanco-López MC, Lobo-Castañón MJ, Miranda-Ordieres AJ, Tuñón-Blanco P. 2004, "Electrochemical sensors based on molecularly imprinted polymers." **TrAC Trends Anal Chem**, 23(1): 36–48.

53. Henry OYF, Cullen DC, Piletsky SA. 2005, "Optical interrogation of molecularly imprinted polymers and development of MIP sensors: a review." **Anal Bioanal Chem**, 382(4): 947–956.

54. Su C, Zhang C, Lu G, Ma C. 2010, "Nonenzymatic Electrochemical Glucose Sensor Based on Pt Nanoparticles/Mesoporous Carbon Matrix." **Electroanalysis**, 22(16): 1901–1905.

55. Van Dorst B, Mehta J, Bekaert K, Rouah-Martin E, De Coen W, Dubruel P, et al. 2010 "Recent advances in recognition elements of food and environmental biosensors: A review." **Biosens Bioelectron**, 26(4): 1178–1194.

56. Hedborg E, Winquist F, Lundström I, Andersson LI, Mosbach K. 1993, "Some studies of molecularly-imprinted polymer membranes in combination with field-effect devices." **Sens Actuators Phys**, 37–38: 796–799.

57. Nopper D, Lammershop O, Wulff G, Gauglitz G. 2003, "Amidine-based molecularly imprinted polymers—new sensitive elements for chiral chemosensors." **Anal Bioanal Chem**, 377(4): 608–613.

58. Latif U, Rohrer A, Lieberzeit PA, Dickert FL. 2011, "QCM gas phase detection with ceramic materials—VOCs and oil vapors." **Anal Bioanal Chem**, 400(8): 2457–2462.

59. Jenik M, Schirhagl R, Schirk C, Hayden O, Lieberzeit P, Blaas D, et al. 2009, "Sensing Picornaviruses Using Molecular Imprinting Techniques on a Quartz Crystal Microbalance." **Anal Chem**, 81(13): 5320–5326.

60. Hayden O, Mann K-J, Krassnig S, Dickert FL. 2006, "Biomimetic ABO Blood-Group Typing." **Angew Chem Int Ed**, 45(16): 2626–2629.

61. Andaç M, Mirel S, Şenel S, Say R, Ersöz A, Denizli A. 2007, "Ion-imprinted beads for molecular recognition based mercury removal from human serum." **Int J Biol Macromol**, 40(2): 159–166.

62. Otero-Romaní J, Moreda-Piñeiro A, Bermejo-Barrera P, Martin-Esteban A. 2008, "Synthesis, characterization and evaluation of ionic-imprinted polymers for solid-phase extraction of nickel from seawater." **Anal Chim Acta**, 630(1): 1–9.

63. Tsoi Y-K, Ho Y-M, Leung KS-Y. 2012, "Selective recognition of arsenic by tailoring ion-imprinted polymer for ICP-MS quantification." **Talanta**, 89: 162–168.

64. Kriz D, Mosbach K. 1995, "Competitive amperometric morphine sensor based on an agarose immobilised molecularly imprinted polymer." **Anal Chim Acta**, 300(1–3): 71–75.

65. Kitade T, Kitamura K, Konishi T, Takegami S, Okuno T, Ishikawa M, et al. 2004, "Potentiometric Immunosensor Using Artificial Antibody Based on Molecularly Imprinted Polymers." **Anal Chem**, 76(22): 6802–6807.

66. Kröger S, Turner APF, Mosbach K, Haupt K. 1999, "Imprinted Polymer-Based Sensor System for Herbicides Using Differential-Pulse Voltammetry on Screen-Printed Electrodes." **Anal Chem**, 71(17): 3698–3702.

67. Sadeghi S, Motaharian A. 2013, "Voltammetric sensor based on carbon paste electrode modified with molecular imprinted polymer for determination of sulfadiazine in milk and human serum." **Mater Sci Eng C**, 33(8): 4884–4891.

68. Özcan L, Şahin Y. 2007, "Determination of paracetamol based on electropolymerized-molecularly imprinted polypyrrole modified pencil graphite electrode." **Sens Actuators B Chem**, 127(2): 362–369.

69. Luo X, Vidal GD, Killard AJ, Morrin A, Smyth MR. 2007, "Nanocauliflowers: A Nanostructured Polyaniline-Modified Screen-Printed Electrode with a Self-Assembled Polystyrene Template and Its Application in an Amperometric Enzyme Biosensor." **Electroanalysis**, 19(7–8): 876–883.

70. Wu H, Wang J, Kang X, Wang C, Wang D, Liu J, et al. 2009, "Glucose biosensor based on immobilization of glucose oxidase in platinum nanoparticles/graphene/chitosan nanocomposite film." **Talanta**, 80(1): 403–406.

71. Gong J-L, Gong F-C, Zeng G-M, Shen G-L, Yu R-Q. 2003, "A novel electrosynthesized polymer applied to molecular imprinting technology." **Talanta**, 61(4): 447–453.

72. Wang Z, Li H, Chen J, Xue Z, Wu B, Lu X. 2011, "Acetylsalicylic acid electrochemical sensor based on PATP–AuNPs modified molecularly imprinted polymer film." **Talanta**, 85(3): 1672–1679.

73. Alizadeh T, Akbari A. 2013, "A capacitive biosensor for ultra-trace level urea determination based on nano-sized urea-imprinted polymer receptors coated on graphite electrode surface." **Biosens Bioelectron**, 43: 321–327.

74. Du D, Huang X, Cai J, Zhang A. 2007, "Comparison of pesticide sensitivity by electrochemical test based on acetylcholinesterase biosensor." **Biosens Bioelectron**, 23(2): 285–289.

75. Viswanathan S, Radecka H, Radecki J. 2009, "Electrochemical biosensor for pesticides based on acetylcholinesterase immobilized on polyaniline deposited on vertically assembled carbon nanotubes wrapped with ssDNA." **Biosens Bioelectron**, 24(9): 2772–2777.

76. Haupt K, Mosbach K. 2000, "Molecularly Imprinted Polymers and Their Use in Biomimetic Sensors." **Chem Rev**, 100(7): 2495–2504.

77. Maloy JT. 1983, "Factors affecting the shape of current-potential curves." **J Chem Educ**, 60(4): 285.

78. Silva SM, Bond AM. 2003, "Contribution of migration current to the voltammetric deposition and stripping of lead with and without added supporting electrolyte at a mercury-free carbon fibre microdisc electrode." **Anal Chim Acta**, 500(1–2): 307–321.

79. Nicholson RS, Shain I. 1964, "Theory of Stationary Electrode Polarography Single Scan and Cyclic Methods Applied to Reversible, Irreversible, and Kinetic Systems." **Anal Chem**, 36(4): 706–723.

80. Bergveld P. 1970, "Development of an Ion-Sensitive Solid-State Device for Neurophysiological Measurements." **IEEE Trans Biomed Eng**, BME-17(1): 70–71.

81. Matsuo T, Wise KD. 1974, "An Integrated Field-Effect Electrode for Biopotential Recording." **IEEE Trans Biomed Eng**, BME-21(6): 485–487.

82. Koch S, Woias P, Meixner LK, Drost S, Wolf H. 1999, "Protein detection with a novel ISFET-based zeta potential analyzer." **Biosens Bioelectron**, 14(4): 413–421.

83. Yuqing M, Jianguo G, Jianrong C. 2003, "Ion sensitive field effect transducer-based biosensors." **Biotechnol Adv**, 21(6): 527–534.

84. Chiang J-L, Chou J-C, Chen Y-C. 2002, "Sensitivity and hysteresis properties of a-WO3,Ta2O5, and a-Si:H gate ion-sensitive field-effect transistors." **Opt Eng**, 41(8): 2032–2038.

85. Chou JC, Wang YF. 2001, "Temperature Characteristics of a-Si:H Gate ISFET." **Mater Chem Phys**, 70(1): 107–111.

86. Chou J-C, Weng C-Y, Tsai H-M. 2002, "Study on the temperature effects of Al2O3 gate pH-ISFET." **Sens Actuators B Chem**, 81(2–3): 152–157.

87. Yin L-T, Chou J-C, Chung W-Y, Sun T-P, Hsiung S-K. 2001, "Characteristics of silicon nitride after O_2 plasma surface treatment for pH-ISFET applications." **IEEE Trans Biomed Eng**, 48(3): 340–344.

88. Chou JC, Wang YF. 2002, "Preparation and study on the drift and hysteresis properties of the tin oxide gate ISFET by the sol–gel method." **Sens Actuators B Chem**, 86(1): 58–62.

89. Lahav M, Kharitonov AB, Willner I. 2001, "Imprinting of Chiral Molecular Recognition Sites in Thin TiO_2 Films Associated with Field-Effect Transistors: Novel Functionalized Devices for Chiroselective and Chirospecific Analyses." **Chem – Eur J**, 7(18): 3992–3997.

90. Bergveld P. 2003, "Thirty years of ISFETOLOGY: What happened in the past 30 years and what may happen in the next 30 years." **Sens Actuators B Chem**, 88(1): 1–20.

91. Yates DE, Levine S, Healy TW. 1974, "Site-binding model of the electrical double layer at the oxide/water interface." **J Chem Soc Faraday Trans 1**, 70: 1807–1818.

92. Caras S, Janata J. 1980, "Field effect transistor sensitive to penicillin." **Anal Chem**, 52(12): 1935–1937.

93. Park K-Y, Choi S-B, Lee M, Sohn B-K, Choi S-Y. 2002, "ISFET glucose sensor system with fast recovery characteristics by employing electrolysis." **Sens Actuators B Chem**, 83(1–3): 90–97.

94. Vijayalakshmi A, Tarunashree Y, Baruwati B, Manorama SV, Narayana BL, Johnson REC, et al. 2008, "Enzyme field effect transistor (ENFET) for estimation of triglycerides using magnetic nanoparticles." **Biosens Bioelectron**, 23(11): 1708–1714.

95. Premanode B, Toumazou C. 2007, "A novel, low power biosensor for real time monitoring of creatinine and urea in peritoneal dialysis." **Sens Actuators B Chem**, 120(2): 732–735.

96. Sasaki Y, Ogawa J, Tani T. 2012, "Simple and convenient measurement of enzyme reaction by high sensitive signal accumulation ISFET biosensor (AMIS Sensor) and Micro Bioactivity Analyzer." **Biocatal Agric Biotechnol**, 1(3): 259–261.

97. Sibbald A, Covington AK, Carter RF. 1984, "Simultaneous on-line measurement of blood K+, Ca2+, Na+, and pH with a four-function ChemFET integrated-circuit sensor." **Clin Chem**, 30(1): 135–137.

98. Zayats M, Raitman OA, Chegel VI, Kharitonov AB, Willner I. 2002, "Probing Antigen–Antibody Binding Processes by Impedance Measurements on Ion-Sensitive Field-Effect Transistor Devices and Complementary Surface Plasmon Resonance Analyses: Development of Cholera Toxin Sensors." **Anal Chem**, 74(18): 4763–4773.

99. Kim D-S, Jeong Y-T, Park H-J, Shin J-K, Choi P, Lee J-H, et al. 2004, "An FET-type charge sensor for highly sensitive detection of DNA sequence." **Biosens Bioelectron**, 20(1): 69–74.

100. Habibi M, Fanaei M, Emami Z. 2015, "A double gate DNA FET based on solution processed ZnO nano layers for high sensitivity and low cost oligonucleotide hybridization detection." **Microelectron Eng**, 131: 29–35.

101. Wolf B, Brischwein M, Baumann W, Ehret R, Kraus M. 1998, "Monitoring of cellular signalling and metabolism with modular sensor-technique: The PhysioControl-Microsystem (PCM®)." **Biosens Bioelectron**, 13(5): 501–509.

102. Guilbault GG, Montalvo JG. 1969, "Urea-specific enzyme electrode." **J Am Chem Soc**, 91(8): 2164–2165.

103. Guilbault GG, Montalvo JG. 1970, "Enzyme electrode for the substrate urea." **J Am Chem Soc**, 92(8): 2533–2538.

104. Koncki R. 2007, "Recent developments in potentiometric biosensors for biomedical analysis." **Anal Chim Acta**, 599(1): 7–15.

105. Guilbault GG, Shu FR. 1972, "Enzyme electrodes based on the use of a carbon dioxide sensor Urea and L-tyrosine electrodes." **Anal Chem**, 44(13): 2161–2166.

106. Guilbault GG, Tarp M. 1974, "A specific enzyme electrode for urea." **Anal Chim Acta**, 73(2): 355–365.

107. Koncki R, Chudzik A, Walcerz I. 1999, "Urea determination using pH–enzyme electrode." **J Pharm Biomed Anal**, 21(1): 51–57.

108. Volotovsky V, Nam YJ, Kim N. 1997, "Urease-based biosensor for mercuric ions determination." **Sens Actuators B Chem**, 42(3): 233–237.

109. Soldatkin AP, Volotovsky V, El'skaya AV, Jaffrezic-Renault N, Martelet C. 2000, "Improvement of urease based biosensor characteristics using additional layers of charged polymers." **Anal Chim Acta**, 403(1–2): 25–29.

110. Melo JV de, Cosnier S, Mousty C, Martelet C, Jaffrezic-Renault N. 2002, "Urea Biosensors Based on Immobilization of Urease into Two Oppositely Charged Clays (Laponite and Zn–Al Layered Double Hydroxides)." **Anal Chem**, 74(16): 4037–4043.

111. Miyahara Y, Moriizumi T, Ichimura K. 1985, "Integrated enzyme fets for simultaneous detections of urea and glucose." **Sens Actuators**, 7(1): 1–10.

112. Karbue I, Tamiya E, Dicks JM, Gotoh M, Research. 1986, "A microsensor for urea based on an ion-selective field effect transistor." **Anal Chim Acta**, 185: 195–200.

113. Hanazato Y, Nakako M, Shiono S. 1986, "Multi-enzyme electrode using hydrogen-ion-sensitive field-effect transistors." **IEEE Trans Electron Devices**, 33(1): 47–51.

114. Schoot BH van der, Bergveld P. 1987, "The pH-static enzyme sensor." **Anal Chim Acta**, 199: 157–160.

115. Nakamoto S, Ito N, Kuriyama T, Kimura J. 1988, "A lift-off method for patterning enzyme-immobilized membranes in multi-biosensors." **Sens Actuators**, 13(2): 165–172.

116. Sant W, Pourciel ML, Launay J, Do Conto T, Martinez A, Temple-Boyer P. 2003, "Development of chemical field effect transistors for the detection of urea." **Sens Actuators B Chem**, 95(1–3): 309–314.

117. Bertocchi P, Compagnone D, Palleschi G. 1996, "Amperometric ammonium ion and urea determination with enzyme-based probes." **Biosens Bioelectron**, 11(1): 1–10.

118. Eggenstein C, Borchardt M, Diekmann C, Gründig B, Dumschat C, Cammann K, et al. 1999, "A disposable biosensor for urea determination in blood based on an ammonium-sensitive transducer." **Biosens Bioelectron**, 14(1): 33–41.

119. Pijanowska DG, Torbicz W. 1997, "pH-ISFET based urea biosensor." **Sens Actuators B Chem**, 44(1–3): 370–376.

120. Tymecki Ł, Zwierkowska E, Koncki R. 2005, "Strip bioelectrochemical cell for potentiometric measurements fabricated by screen-printing." **Anal Chim Acta**, 538(1–2): 251–256.

121. Verma N, Singh M. 2003, "A disposable microbial based biosensor for quality control in milk." **Biosens Bioelectron**, 18(10): 1219–1224.

122. Verma N, Singh M. 2005, "Biosensors for heavy metals." **Biometals**, 18(2): 121–129.

123. Puig-Lleixà C, Jiménez C, Alonso J, Bartrolí J. 1999, "Polyurethane–acrylate photocurable polymeric membrane for ion-sensitive field-effect transistor based urea biosensors." **Anal Chim Acta**, 389(1–3): 179–188.

124. Dhawan G, Sumana G, Malhotra BD. 2009, "Recent developments in urea biosensors." **Biochem Eng J**, 44(1): 42–52.

125. Tyagi M, Tomar M, Gupta V. 2013, "NiO nanoparticle-based urea biosensor." **Biosens Bioelectron**, 41: 110–115.

126. Huang C-P, Li Y-K, Chen T-M. 2007, "A highly sensitive system for urea detection by using CdSe/ZnS core-shell quantum dots." **Biosens Bioelectron**, 22(8): 1835–1838.

127. Liu S, Shi F, Chen L, Su X. 2014, "Dopamine functionalized CuInS2 quantum dots as a fluorescence probe for urea." **Sens Actuators B Chem**, 191: 246–251.

128. Veloso ACA, Teixeira N, Ferreira IM. 2002, "Separation and quantification of the major casein fractions by reverse-phase high-performance liquid chromatography and urea–polyacrylamide gel electrophoresis: Detection of milk adulterations." **J Chromatogr A**, 967(2): 209–218.

129. Xing X, Liu S, Yu J, Lian W, Huang J. 2012, "Electrochemical sensor based on molecularly imprinted film at polypyrrole-sulfonated graphene/hyaluronic acid-multiwalled carbon nanotubes modified electrode for determination of tryptamine." **Biosens Bioelectron**, 31(1): 277–283.

130. Zhao L, Zhao F, Zeng B. 2013, "Electrochemical determination of methyl parathion using a molecularly imprinted polymer–ionic liquid–graphene composite film coated electrode." **Sens Actuators B Chem**, 176: 818–824.

131. Kong L, Jiang X, Zeng Y, Zhou T, Shi G. 2013, "Molecularly imprinted sensor based on electropolmerized poly(o-phenylenediamine) membranes at reduced graphene oxide modified electrode for imidacloprid determination." **Sens Actuators B Chem**, 185: 424–431.

132. Aghaei A, Milani Hosseini MR, Najafi M. 2010, "A novel capacitive biosensor for cholesterol assay that uses an electropolymerized molecularly imprinted polymer." **Electrochimica Acta**, 55(5): 1503–1508.

133. Sepeur S, Kunze N, Werner B, Schmidt H. 1999, "UV curable hard coatings on plastics." **Thin Solid Films**, 351(1–2): 216–219.

134. Devikala S, Kamaraj P, Arthanareeswari M. 2013, "Conductivity and Dielectric Studies of PMMA Composites." **Chem Sci Trans**, 2(S1): S129–S134.

135. Lian W, Liu S, Yu J, Li J, Cui M, Xu W, et al. 2013, "Electrochemical sensor using neomycin-imprinted film as recognition element based on chitosan-silver nanoparticles/graphene-multiwalled carbon nanotubes composites modified electrode." **Biosens Bioelectron**, 44: 70–76.

136. Alizadeh T, Rezaloo F. 2013, "A new chemiresistor sensor based on a blend of carbon nanotube, nano-sized molecularly imprinted polymer and poly methyl methacrylate for the selective and sensitive determination of ethanol vapor." **Sens Actuators B Chem**, 176: 28–37.

137. Chen J, Huang H, Zeng Y, Tang H, Li L. 2015, "A novel composite of molecularly imprinted polymer-coated PdNPs for electrochemical sensing norepinephrine." **Biosens Bioelectron**, 65: 366–374.

138. Yue D, Jia Y, Yao Y, Sun J, Jing Y. 2012, "Structure and electrochemical behavior of ionic liquid analogue based on choline chloride and urea." **Electrochimica Acta**, 65: 30–36.

139. Singh M, Verma N, Garg AK, Redhu N. 2008, "Urea biosensors." **Sens Actuators B Chem**, 134(1): 345–351.

140. Fung CD, Cheung PW, Ko WH. 1986, "A generalized theory of an electrolyte-insulator-semiconductor field-effect transistor." **IEEE Trans Electron Devices**, 33(1): 8–18.

141. Shevkoplyas SS, Yoshida T, Munn LL, Bitensky MW. 2005, "Biomimetic Autoseparation of Leukocytes from Whole Blood in a Microfluidic Device." **Anal Chem**, 77(3): 933–937.

142. Davis JA, Inglis DW, Morton KJ, Lawrence DA, Huang LR, Chou SY, et al. 2006," Deterministic hydrodynamics: Taking blood apart." **Proc Natl Acad Sci**, 103(40): 14779–14784.

143. Hou HW, Bhagat AAS, Lee WC, Huang S, Han J, Lim CT. 2011, "Microfluidic Devices for Blood Fractionation." **Micromachines**, 2(3): 319–343.

144. Hong C-C, Lin C-C, Hong C-L, Lin Z-X, Chung M-H, Hsieh P-W. 2016, "Handheld analyzer with on-chip molecularly-imprinted biosensors for electrical detection of propofol in plasma samples." **Biosens Bioelectron**, 86: 623–629.

VITA

Name-Surename	:	Yossawat Rayanasukha
Date of birth	:	24 June 1987
Province	:	Nakhon Ratchasima
Education	:	B.Sc. (Applied Physics), Faculty of Science, King Mongkut's Institute of Technology Ladkrabang, Bangkok (2008)

International Publications

1. W. Bunjongpru, A. Sungthong, S. Porntheeraphat, **Y. Rayanasukha**, A. Pankiew, W. Jeamsaksiri, A. Srisuwan, W. Chaisriratanakul, E. Chaowicharat, N. Klunngien, C. Hruanun, A. Poyai, and J. Nukeaw, "Very low drift and high sensitivity of nanocrystal-TiO2 sensing membrane on pH-ISFET fabricated by CMOS compatible process," Applied Surface Science, vol. 267, pp. 206–211, 2013.
2. **Yossawat Rayanasukha**, Supanit Porntheeraphat, Win Bunjongpru, Narathon Khemasiri, Apirak Pankiew, Wutthinan Jeamsaksiri, Awirut Srisuwan, Woraphan Chaisriratanakul, Charndet Hruanun, Amporn Poyai and Jiti Nukeaw, "High Sensitive Nanocrystal Titanium Nitride EG-FET pH Sensor", Advanced Materials Research, vol. 802, pp 232-236, 2014.
3. Narathon Khemasiri, Chanunthorn Chananonnawathorn, Mati Horprathum, **Yossawat Rayanasukha**, Darinee Phromyothin, Win Bunjongpru, Supanit Porntheeraphat and Jiti Nukeaw, "High Performance Metal Surface Coating using Ta2O5 Thin Film Prepared by D.C. Magnetron Sputtering", Advanced Materials Research, vol. 802, pp 242-246, 2014.
4. **Y. Rayanasukha**, S. Pratontep, S. Porntheeraphat, W. Bunjongpru, and J. Nukeaw "Non-Enzymatic Urea Sensor using Molecularly Imprinted Polymers Surface Modified based-on Ion-Sensitive Field Effect Transistor (ISFET)", Surface and Coatings Technology, vol. 306, pp.147-150, 2016.

International Conferences

1. Thanakorn Jiemsakul, Opas Trithaveesak, Win Bunjongpru, **Yossawat Rayanasukha**, Supanit Porntheeraphat, Charndet Hruanun, Amporn Poyai, Jiti Nukeaw, "A ISFETs integrated microchannel device for detection solution concentration" , International Conference on Flow Injection Analysis 140, 2010, Pattaya, Thailand.
2. Supanit Porntheeraphat, Win Bunjongpru, Praphaphan Wipatawit, Amporn Poyai, Jiti Nukeaw, **Yossawat Rayanasukha**, Witsaroot Sripumkhai, Amornrat Lekwichai , 2010, "Thermal Sensor Array for Temperature Profile and Flow rates Measurement in Fluidic PDMS Microchannel", International Conference on Flow Injection Analysis, 140, 2010, Pattaya, Thailand.
3. Panwadee Wattanasin, **Yossawat Rayanasukha**, Win Bunjongpru, Benchapol Tunhoo, Supanit Porntheeraphat, Nuchutha Thamsumet, Piyawan Phansi, Kanchana Uraisina, and Duangjai Nacapricha, "A Membraneless Unit for Measuring Calcium Carbonate with pH-ISFET Detection via Vaporization of CO2", The International Congress for Innovation in Chemistry (PERCH-CIC 2011), 2011, Pattaya, Thailand.
4. **Yossawat Rayanasukha**, Supanit Porntheeraphat, Win Bunjongpru, Narathon Khemasiri, Apirak Pankiew, Wutthinan Jeamsaksiri, Awirut Srisuwan, Woraphan Chaisriratanakul, Charndet Hruanun, Amporn Poyai and Jiti Nukeaw, "High Sensitive Nanocrystal Titanium Nitride EG-FET pH Sensor", International Conference on Engineering, Applied Sciences and Technology (ICEAST 2013), 2013, Bangkok, Thailand.
5. Narathon Khemasiri, Chanunthorn Chananonnawathorn, Mati Horprathum, **Yossawat Rayanasukha**, Darinee Phromyothin, Win Bunjongpru, Supanit Porntheeraphat and Jiti Nukeaw, "High Performance Metal Surface Coating using Ta2O5 Thin Film Prepared by D.C. Magnetron Sputtering", International Conference on Engineering, Applied Sciences and Technology (ICEAST 2013), 2013, Bangkok, Thailand.

6. Supanat Sasipongpana, Nongluck Houngkanhang, **Yossawat Rayanasukha**, Seerong Prichanont, Sirapat Pratontep, Pornpimol Sritongkam, "AChE/agarose gel Coated on ISFET for Methyl-Parathion Sensors", Siam Physics Congress 2015 (SPC 2015), 2015, Krabi, Thailand.
7. Piyawan Leepheng, Sirikan Thongboon, Chanchana Thanachayanont, Sirapat Pratontep, Suppanat Sasipongpana, **Yossawat Rayanasukha**, Pornpimol Sritongkam, Nongluck Houngkanhang, "Imprinted expended gate Field-Effect transistor for pesticide detection", Siam Physics Congress 2015 (SPC 2015), 2015, Krabi, Thailand.
8. **Yossawat Rayanasukha**, Supanat Sasipongpana, Nongluck Houngkanhang, Supanit Porntheeraphat, Jiti Nukeaw, Seerong Prichanont, Chanchana Thanachayanont, Pornpimol Sritongkam, and Sirapat Pratontep, "Nanostructured coating for selective chemical sensing", Advanced Materials for Electronics Application (AMEA 2015), 2015, Pathumthani, Thailand.
9. **Yossawat Rayanasukha**, Sirapat Pratontep, Supanit Porntheeraphat and Jiti Nukeaw, "Non Enzymatic Urea Sensor using Molecular Imprinted Polymer (MIP) Surface Modification", The 19th International Conference on Surface Modification of Materials by Ion Beams (SMMIB-19), 2015, Chiang Mai, Thailand.
10. Supanat Sasipongpana, **Yossawat Rayanasukha**, Seeroong Prichanont, Chanchana Thanachayanont, Supanit Porntheeraphat, Nongluck Houngkamhang, "Extended–gate field effect transistor (EGFET) for carbaryl pesticide detection based on enzyme inhibition assay", International Conference on Science and Technology of Emerging Materials (STEMa2016), 2016, Pattaya, Thailand.

Patents and Petty Patents

1. Jiti Nukeaw, Sirapat Pratontep, Supanit Porntheeraphat, Sirajit Vuttivong, **Yossawat Rayanasukha**, "Hybrid Nanomaterial Composite for Prevention of Fungal and Rehabilitation of Tree Wounds", petty patent number 11211.

2. Jiti Nukeaw, Sirapat Pratontep, Supanit Porntheeraphat, **Yossawat Rayanasukha** et al., "Polymeric Selective Membranes for Non-Enzymatic Detection of Urea and Organic Compounds", patent number applicant 1501000653
3. Jiti Nukeaw, Sirapat Pratontep, Supanit Porntheeraphat, **Yossawat Rayanasukha** et al., "Artemisinin Detection Devices using Metal-Salophen complex Material for Electrocatalyst", patent number applicant 1501002871

Applied Surface Science 267 (2013) 206–211

Contents lists available at SciVerse ScienceDirect

Applied Surface Science

journal homepage: www.elsevier.com/locate/apsusc

Very low drift and high sensitivity of nanocrystal-TiO_2 sensing membrane on pH-ISFET fabricated by CMOS compatible process

W. Bunjongpru[a,c], A. Sungthong[e,*], S. Porntheeraphat[a,b], Y. Rayanasukha[c], A. Pankiew[a,c], W. Jeamsaksiri[a], A. Srisuwan[a], W. Chaisriratanakul[a], E. Chaowicharat[a], N. Klunngien[a], C. Hruanun[a], A. Poyai[a], J. Nukeaw[c,d]

[a] Thai Microelectronics Center (TMEC), Chachoengsao 24000, Thailand
[b] Photonics Technology Laboratory (PTL), NECTEC, NSTDA, Thailand Science Park, Patumthani 12120, Thailand
[c] College of Nanotechnology, King Mongkut's Institute of Technology Ladkrabang, Bangkok 10520, Thailand
[d] ThEP Center, CHE, 328 Si-Ayutthaya Rd., Bangkok 10400, Thailand
[e] Rajanagarindra Rajabhat University, Chachoengsao 24000, Thailand

ARTICLE INFO

Article history:
Received 30 September 2011
Received in revised form 26 October 2012
Accepted 29 October 2012
Available online 9 November 2012

ABSTRACT

High sensitivity and very low drift rate pH sensors are successfully prepared by using nanocrystal-TiO_2 as sensing membrane of ion sensitive field effect transistor (ISFET) device fabricated via CMOS process. This paper describes the physical properties and sensing characteristics of the TiO_2 membrane prepared by annealing Ti and TiN thin films that deposited on SiO_2/p-Si substrates through reactive DC magnetron sputtering system. The X-ray diffraction, scanning electron microscopy and Auger electron spectroscopy were used to investigate the structural and morphological features of deposited films after they had been subjected to annealing at various temperatures. The experimental results are interpreted in terms of the effects of amorphous-to-crystalline phase transition and subsequent oxidation of the annealed films.

The electrolyte–insulator–semiconductor (EIS) device incorporating Ti—O—N membrane that had been obtained by annealing of TiN thin film at 850 °C exhibited a higher sensitivity (57 mV/pH), a higher linearity (1), a lower hysteresis voltage (1 mV in the pH cycle of 7 → 4 → 7 → 10 → 7), and a smaller drift rate (0.246 mV/h) than did those devices prepared at the other annealing temperatures. Furthermore, this pH-sensing device fabrication process is fully compatible with CMOS fabrication process technology.

1. Introduction

Ion sensitive field effect transistor (ISFET) was first invented by Piet Bergveld in 1970 [1]. ISFET was developed from Metal oxide semiconductor field effect transistor (MOSFET) by removing the metal gate and leaving the gate dielectric intact. This gate dielectric or so-called "sensitive membrane" is used to sense the concentration of the hydrogen ions in a solution. The gate is replaced by an external reference electrode to monitor the sensor output signal [2]. In addition, Fog et al. reported properties of a number of metal oxides for pH measurements, i.e. Ta_2O_5 [3], Al_2O_3 [4] and TiO_2 [5] for instant.

TiO_2 thin film, in particular, is of interest for many research groups due to the various properties such as high refractive index, high dielectric constant, chemically stable, and water insoluble [6].

In the past years, it has been studied about the activity of TiO_2 which lattice is substituted of several metal ions, such as Fe, Cr, Pt, Ta, etc. However, several serious problems have been pointed out about the chemical stability. In 2004, Suda et al. studied the doped TiO_2 with nitrogen (N). They found that the crystalline structure of deposited film has changed from TiO_2 to TiN when the nitrogen concentration ratio increased. Based on these results, it was found that the $TiO_{2-x}N_x$ films have anatase crystalline structure with nitrogen doped into TiO_2 oxygen sites, which leads to different properties [7].

This paper reports the studies of TiO_2 film prepared from two different initial films; Ti and TiN by dc magnetron sputtering in CMOS process line. After depositing the films on prepared Si wafers, the deposited films were annealed at various temperatures from 450 to 850 °C in nitrogen furnace. The effect of initial films and annealing temperature were then characterized and analyzed in terms of their crystal structures, surface morphology and chemical composition. The pH sensitivity was later characterized by means of electrolyte–insulator–semiconductor (EIS) structure to find the optimal condition for incorporating TiO_2 film in the ISFET. These

* Corresponding author.
E-mail address: win.bunjongpru@nectec.or.th (W. Bunjongpru).

0169-4332/$ – see front matter © 2012 Elsevier B.V. All rights reserved.
http://dx.doi.org/10.1016/j.apsusc.2012.10.176

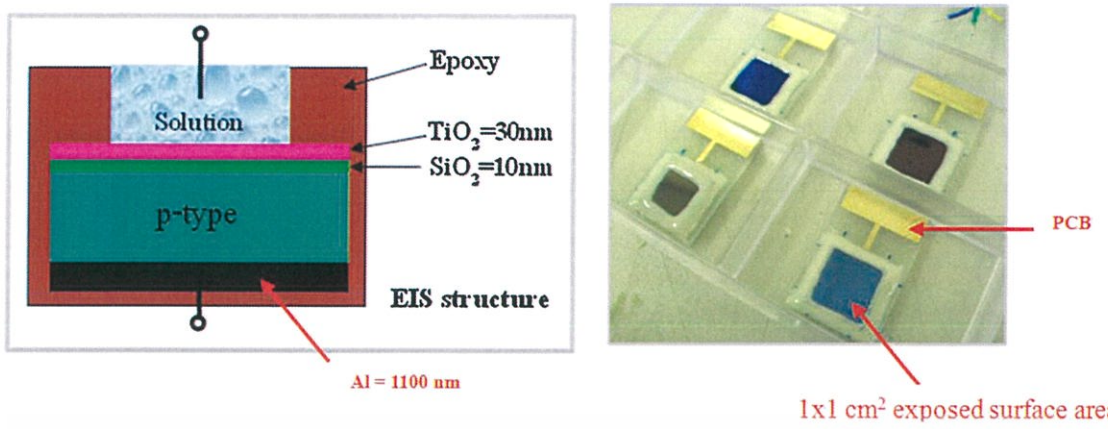

Fig. 1. EIS structure device for pH sensitivity characterization.

TiO_2-ISFET devices were successfully done compatible with CMOS fabrication process.

2. Experimental

2.1. Ti and TiN thin films growth

The Ti and TiN films studied in this report were grown on 6" p-type Si wafers with 100 crystal orientation. The resistivity of the wafers was 20–30 Ω cm. Initially thermal oxide of 10 nm was grown on the wafers then either Ti or TiN film was then sputtered on the wafers.

Ti thin film was grown with dc magnetron sputtering tool (model ILC-1051 from Anelva). The Ti target had purity of 99.999% with diameter of 342 mm. The chamber based pressure was below 1×10^{-7} mbar. The sputtering gas was Ar with purity of 99.999%. The Ar gas was supplied with 40 cm^3/min at pressure of 4×10^{-3} mbar with the chuck temperature controlled at 100 °C. The dc input power supplied to the system was set to 1.5 kW. The Ti film was grown to the thickness of 30 nm. The substrate chuck was not heated in the process while, the 30 nm of TiN was similarly grown on the other Si wafer. The N_2 with purity of 99.9999% was used as the sputtering gas and the reactive gas in the process. The N_2 flow rate of 40 cm^3/min was fed into the chamber at the pressure of 4×10^{-3} mbar. The dc input power supplied to the system was set to 6 kW.

Then prepared samples from both processes were annealed at temperature of 450, 550, 650, 750, 800, and 850 °C in N_2 atmosphere at 1 atm (Diffusion furnace model TMX 10,000 from Thermco system) for 30 min. The N_2 flow in furnace was controlled at 14 l/min.

2.2. Ti and TiN EIS devices fabrication

The pH sensitivity test of the films of interest, i.e. Ti/SiO_2/p-Si and TiN/SiO_2/p-S, were characterized by means of the capacitance–voltage (C–V) measurements on the electrolyte–insulator–semiconductor (EIS) structure as shown in Fig. 1. The characterization was done on the films with the annealing temperatures of 750, 800, and 850 °C at which the films were insulators. The backside Al film of 1100 nm thickness was then connected electrically with copper interconnect on printed circuit board (PCB) through bonding wires using special silver paste. The exposed area of the film on each EIS structure was 1 cm × 1 cm. Five EIS structure devices were taken from five parts of the p-Si wafer, i.e. center, right, left, top, and bottom.

2.3. Characterizations

Crystal structure, surface morphology and chemical composition were obtained with XRD (Model TTRAX 111 from Riagku), FESEM (model S4700 from Hitachi) and AUGER (PHI700 from ULVAC), respectively.

Additionally the C–V characterization of the films was done on the respective EIS structures using Agilent model B1500A with parallel capacitance-impedance model. The cable compensation was done before the measurement using open circuit compensation at the measurement frequency. The dc input voltage range was from −5 to 5 V. The small signal was set at 30 mV at the frequency of 1 kHz. The film thickness was calculated at the accumulation region of the C–V curve.

The pH sensitivity, linearity and hysteresis were obtained from C–V measurement of the EIS structures by submerging the structures in the buffer solutions with pH cycle of 7–4–7–10–7, respectively. Each cycle takes 5 min. The drift rate was calculated from the measurement of the EIS structure in a pH 7 buffer solution for 10 h continuously.

3. Results and discussion

3.1. Physical properties

With Glancing angle diffraction system, it was found that the titanium (Ti) thin film was amorphous before annealing and was crystallize after annealing at 550 and 650 °C in N_2 at 1 atm. The small XRD peaks exhibits at 27.92° and 27.50°, respectively in (1 0 1) plane corresponded to anatase-TiO_2 structure.

At higher annealing temperature of 750 °C, there existed XRD peaks at 36.63°, 41.85°, and 54.87° representing polycrystalline TiO_2 with rutile (R) crystal structure in (1 0 1), (1 1 1) planes and anatase crystal structure in (1 0 5) plane, respectively as shown in Fig. 2. The highest crystalline presence in the film was preferred of R (1 0 1) orientation. The XRD peaks shifted toward lower angles as the annealing temperatures were increased to 800 and 850 °C. By means of the oxygen incorporation, at higher temperature the oxygen atoms can more react with Ti atoms to form of TiO_2 crystal than at lower temperature that causes the expansion of crystal lattice [8,9]. This result agrees with the result from AES that found higher oxygen content at higher annealing temperature. Furthermore, FE-SEM also showed larger surface grain boundary at higher temperatures as shown in Fig. 3.

From the Beer–Lambert law, the lattice constant of TiO_2 increased as a result of higher possibility of oxygen atoms

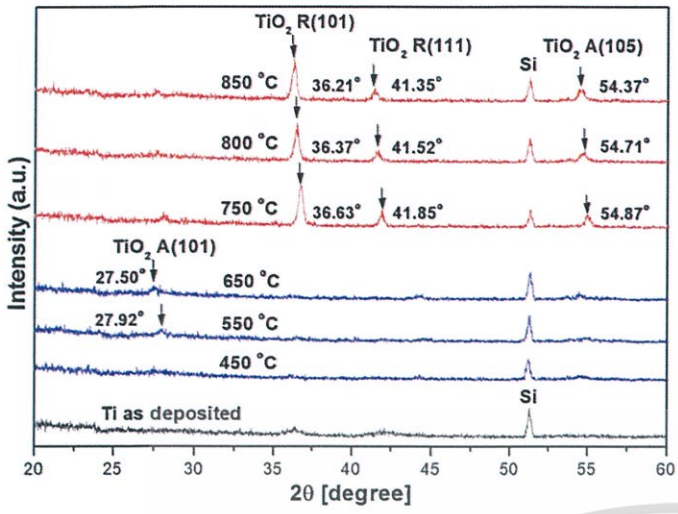

Fig. 2. XRD of Ti thin film before and after annealing with temperature of 450–850 °C.

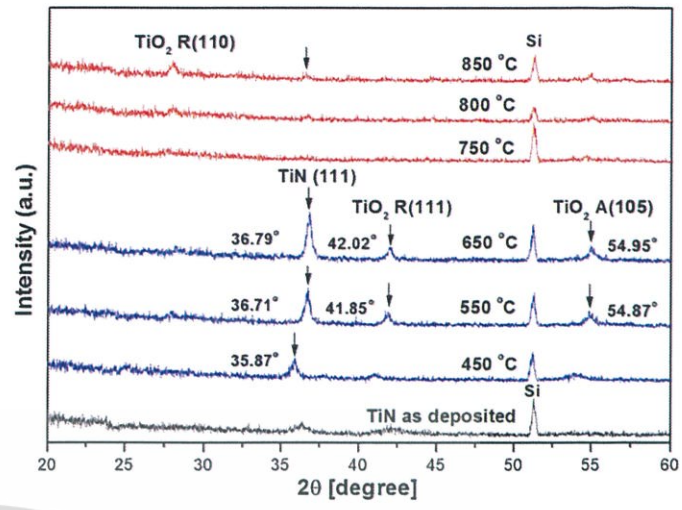

Fig. 5. The XRD pattern of TiN thin film before and after annealing with temperature of 450–850 °C.

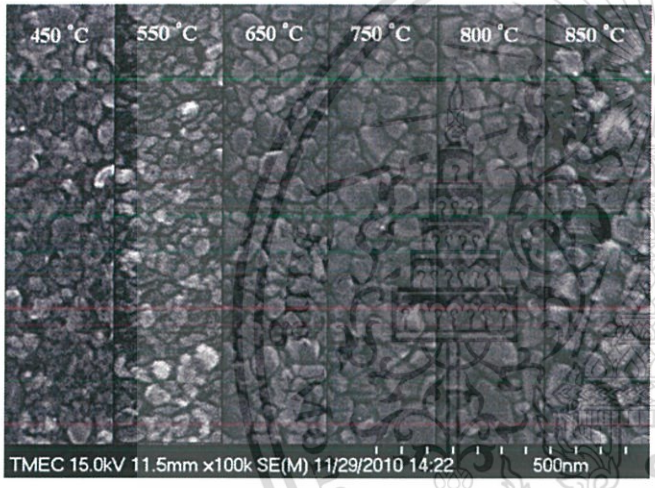

Fig. 3. Electron micrograph of surface topology on Ti thin film after annealing temperature at 450–850 °C.

reacting with Ti atoms at higher temperatures, and therefore, expansion of lattice crystal structure [8,9].

The Auger spectra corresponding to the Ti_{LMM}, Ti_{LMV}, N_{KLL} and O_{KLL} transitions is represented as a function of the annealing temperature as demonstrated in Fig. 4. Unfortunately, the typical overlap between the Auger transition of Ti_{LMM} (390 eV) and N_{KLL} (389 eV) appears. Therefore the Auger spectra of Ti and N cannot quantify the atomic concentration with precision. But the Auger spectra shape used to identify the different Ti compounds that appear along whole experiments.

Fig. 4(a and b) show the Auger spectra of annealed titanium films at 450 and 850 °C in N_2 environment furnace, respectively. The Ti_{LMM}, Ti_{LMV} and O_{KLL} transitions were compared to database that similar to the Auger spectra shape of titanium-oxide (TiO). They were considered as TiO is in different chemical states. The Ti peak was fitted with several components which were identified as Ti atoms in different oxidation states, namely TiO, Ti_2O_3, TiO_2 and Ti–OH.

For the sputtered titanium nitride (TiN) thin film, the XRD result shows amorphous phase of thin film before annealing. However after annealing at 450, 550 and 650 °C, there were XRD peaks at 35.87°, 36.71° and 36.79° represented TiN crystal with cubic structure in (1 1 1) plane as shown in Fig. 5. It was found that the XRD peak of TiN on (1 1 1) plane shifted toward higher angles as increased annealing temperature. This showed that the lattice constant of TiN on (1 1 1) plane decreased as a result of nitrogen vacancy [10]. At higher annealing temperatures, oxygen atoms were reacting with Ti atoms to form TiO_2 with R(1 1 1) and A(1 0 5) mixing with TiN(1 1 1).

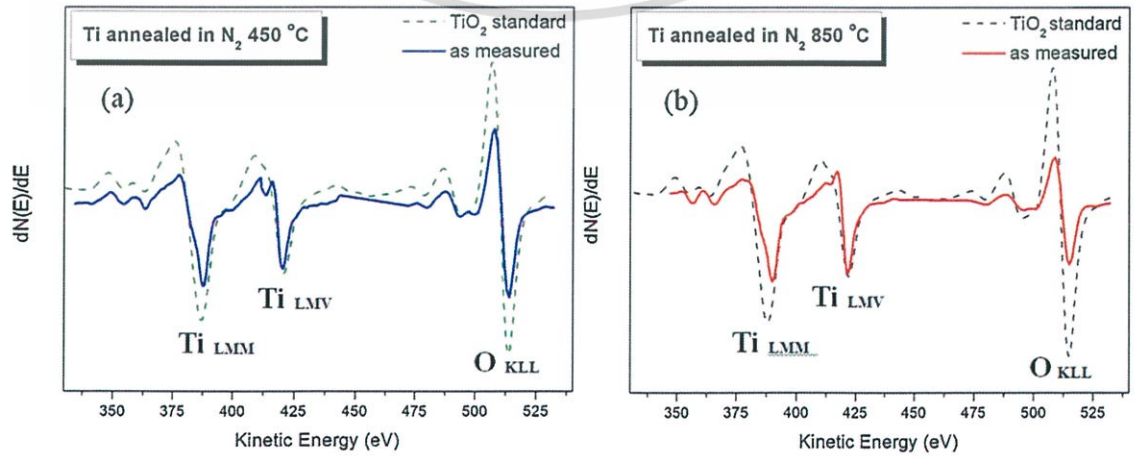

Fig. 4. Auger spectra of Ti thin films after annealing at 450 °C (a) and 850 °C (b).

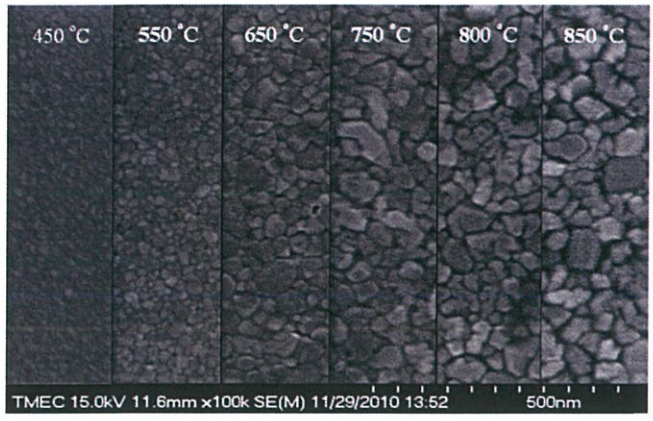

Fig. 6. Electron micrograph of surface topology of TiN thin film after annealing with temperature of 450–850 °C.

At higher annealing temperature in the range of 750–850 °C, there existed a phase change due to increasing amount of oxygen atoms able to react with Ti atoms resulting in TiO_2 with R (1 1 0) structure. At the same time, the TiN phase was reduced noticeably as exhibited in Fig. 5.

From the scanning electron micrograph (SEM) on the surface of TiN before and after annealing process, Fig. 6(a) shows the surface morphology of the N film as 450 °C annealing temperature that corresponded to amorphous phase from XRD peak. As the annealing temperature was increasing, the surface morphology showed the increasing of grain boundary as the increasing of annealing temperature and distinct phase contrast of different grain types mixing together as exhibited in dark and white shades (Fig. 6(b–f)). This was in agreement with XRD result identifying both TiN and TiO_2 crystals in the film.

In Fig. 7 shows the Auger spectra of annealed titanium nitride (TiN) films at 450 and 850 °C in N_2 environment furnace. In Fig. 7(a and b), the Ti_{LMM}, Ti_{LMV}, N_{KLL} and O_{KLL} transitions were compared to database and corresponded to the results of XRD. Their spectra were similar to the Auger spectra of titanium nitride (Ti—N) and titanium oxide (Ti—O). Therefore, the Auger spectra in Fig. 7(a) and Fig. 7(b) were considered as titanium-oxide-nitride (Ti—O—N).

3.2. Electrical properties

3.2.1. Dielectric constant

Physical layer thickness and corresponding equivalent oxide thickness (EOT) of MIS structures (Ti/SiO_2/p-Si, TiN/SiO_2/p-Si) are listed in Table 1. The EOT was calculated from the accumulation capacitance of *C–V* curves.

Table 1
Equivalent oxide thickness for gate stacks.

Physical thickness	Annealing temperature (°C)	EOT (nm)	Dielectric constant
10 nm SiO_2/30 nm Ti	750	11.82	24.74
	800	12.12	27.36
	850	11.74	24.92
10 nm SiO_2/30 nm TiN	750	11.24	19.44
	800	11.18	22.68
	850	11.12	22.79

Table 1 shows that the dielectric constant for the TiO_2/SiO_2 stacked layers range from 19.4 to 27.4, depending on the as-deposited stack layers, Ti/SiO_2 and TiN/SiO_2 stacks, and the annealing temperature. The dielectric constant of TiO_2 film prepared from Ti film was higher than the one prepared from TiN. This might be a result of TiO_2 film prepared from annealing TiN film having mixture of both TiN phase and TiO_2 phase. As a result, the dielectric constant was calculated to be lower than TiO_2 film prepared from annealing Ti film having only a single TiO_2 phase.

3.2.2. Sensing characterization

The pH sensitivity can be calculated by plotting the normalized *C–V* curve of the EIS-structure device (electrolyte-Insulator-Semiconductor) with TiO_2 layer, which were annealed at different temperatures. The measurement of sheet resistance of these films using 4-point probe found that the annealing Ti and TiN at temperature higher than 750 °C completely converted these films to insulator. The pH sensitivity of EIS devices, as tested in standard pH buffer solution of 4, 7, and 10, showed the shifting of flat-band-voltage as calculated at 0.6 of the Normalized *C–V* curve shown in Fig. 8. This phenomenon could be explained by examining the site-binding model [11].

Each *C–V* curve, from pH buffer solutions, was an average of 5 samples from different sites in a wafer. Fig. 8(a) was from annealed Ti film, and Fig. 8(b) was from annealed TiN film. The annealing temperatures of 750, 800, and 850 °C showed that a temperature, high enough to change phase of Ti and TiN film to TiO_2, produced pH sensitivity within similar range of 56–59 mV/pH with linearity close to 1.

Hysteresis is an effect of defects in dielectric films [12]. With annealing temperature of Ti and TiN films in the range of 750–850 °C, Table 1 shows that higher annealing temperature caused the hysteresis to decrease to 8 ± 4 mV and 2 ± 2 mV,

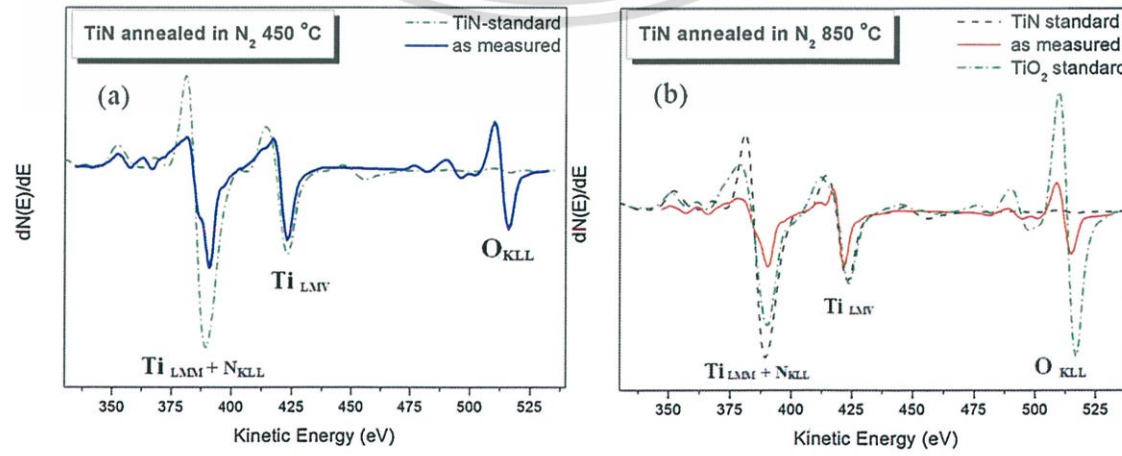

Fig. 7. Auger spectra of TiN thin films after annealing at 450 °C (a) and 850 °C (b).

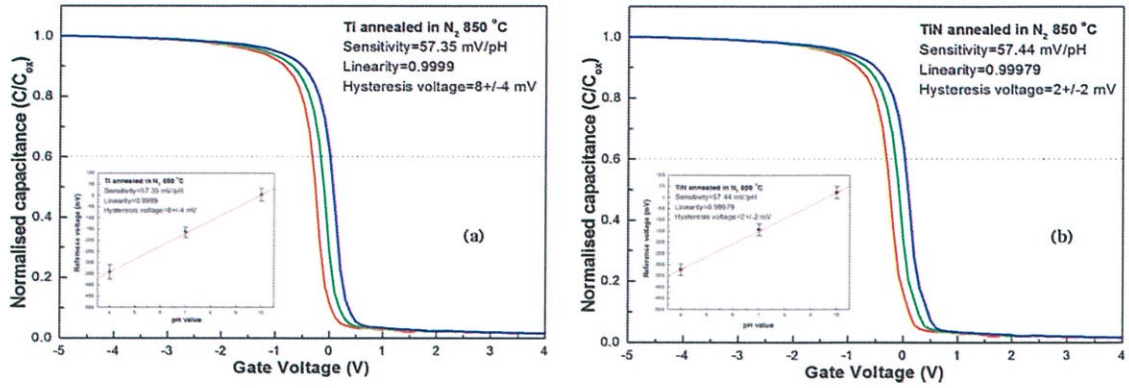

Fig. 8. *C–V* characteristics of EIS device with different TiO_2 films.
(a) Annealing Ti in Nitrogen atmosphere at temperatures of 850 °C.
(b) Annealing TiN in Nitrogen atmosphere at temperatures of 850 °C.

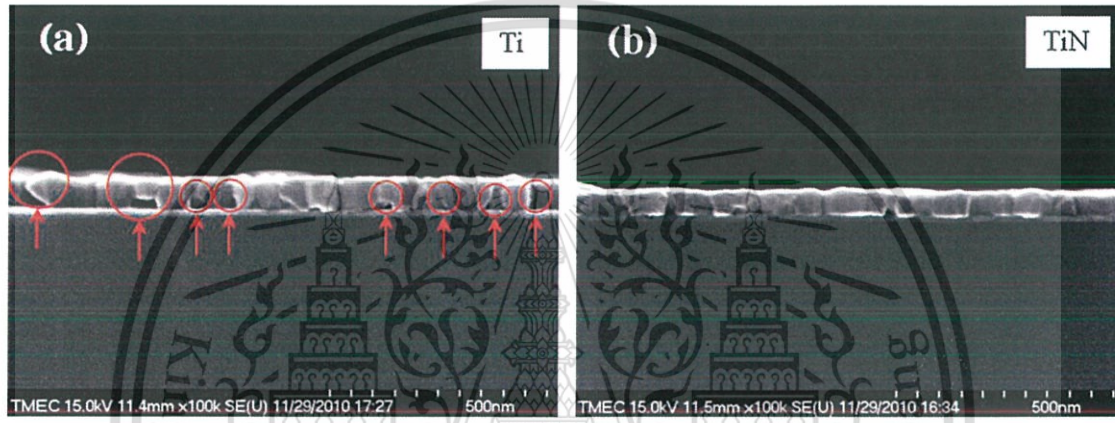

Fig. 9. Cross-sectional view from FE-SEM.
(a) Annealing Ti in Nitrogen atmosphere at 850 °C.
(b) Annealing TiN in Nitrogen atmosphere at 850 °C.

respectively (average from 5 sampling sites on a wafer). From the experiment, it was clear that TiO_2 boding from annealing Ti film had higher hysteresis than the one from annealing TiN film. These results were due to the better chemical stability of Ti—O—N than Ti—O boding.

By choosing the annealing temperature of 850 °C for both Ti and TiN films having lowest hysteresis rate, the drift rate of the nanocrystal-TiO_2 EIS devices was tested continuously in pH 7 buffer solution for 10 h. It found that the film from annealed TiN film was shown a very low drift rates of 0.246 mV/h. This result can explain by examining the cross-sectional views from FE-SEM. It was found that the interface of annealing Ti film (Fig. 9(a)) had higher number of defects than the annealed TiN film (Fig. 9(b)) which causes the drift in pH measurement. Fig. 10 showed the drift rate revealed from annealed-Ti and annealed-TiN at 850 °C annealing (Table 2).

To select an appropriate condition for fabricating TiO_2 suitable for the CMOS fabrication line, we considered the uniformity of TiO_2 film by examining the *C–V* characteristics from the Ti and TiN annealed at 750, 800, and 850 °C (Fig. 8). Then we compared different standard deviation (SD) of the measurement of flat-band-voltage in standard pH buffer solution of 4, 7, and 10, from 5 samples of EIS devices that were from 5 sampling sites on a wafer as shown in Fig. 11. The analysis could be separated into two parts.

Table 2
Sensing characterization.

Physical thickness	Annealing temperature (°C)	Sensitivity (mV/pH)	Linearity	Hysteresis (mV)
10 nm SiO_2/30 nm Ti	750	56.81	0.9997	13 ± 7
	800	59.75	0.9999	9 ± 9
	850	57.35	0.9999	8 ± 4
10 nm SiO_2/30 nm TiN	750	57.57	0.9995	17 ± 16
	800	58.83	0.9998	6 ± 5
	850	57.44	0.9998	2 ± 2

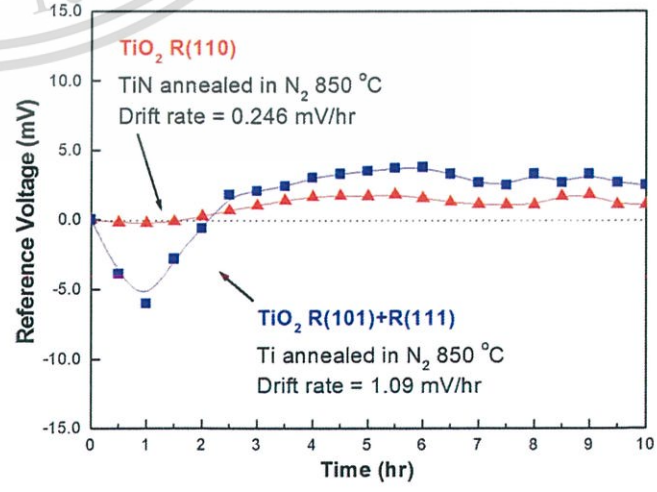

Fig. 10. Drift characteristics EIS device with different TiO_2 phase of sensing membranes.

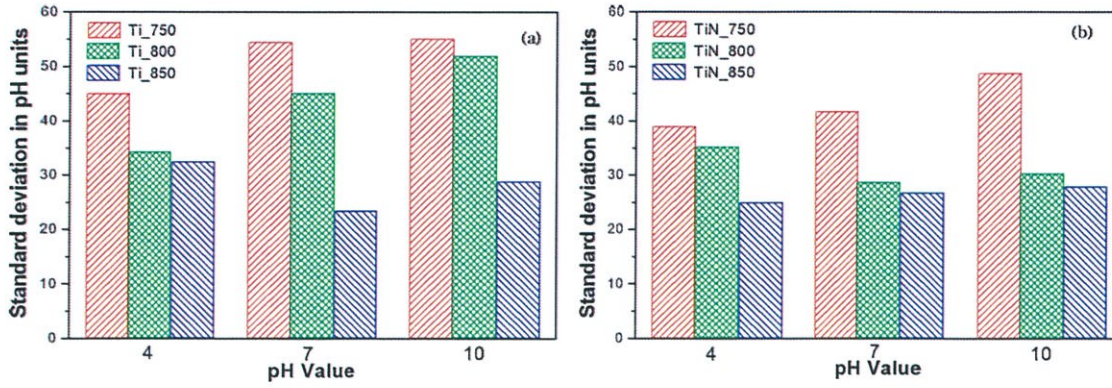

Fig. 11. Comparison of standard deviation in pH buffer solution 4, 7, and 10 of EIS devices prepared from annealed Ti and TiN at different temperatures from 5 sites on a wafer.

3.2.2.1. In the case of annealed Ti membrane/EIS device. The standard deviation determined from pH measuring of annealed-Ti EIS devices in buffer solutions of pH 4, 7 and 10 is increased as a function of pH value in every annealing temperature. However, for the same pH, the EIS device with higher annealing temperature showed lower standard deviation. The EIS device with Ti film annealed at 850 °C showed the lowest standard deviation of flat-band voltage as compared with measurement from acid and base which may cause of the chemical instability of annealed-Ti film.

3.2.2.2. In the case of annealed TiN membrane/EIS device. The standard deviation determined from pH measuring of annealed-TiN EIS devices in buffer solutions of pH 4, 7 and 10 is very different. The standard deviation is increased as a function of pH value determined from annealed-TiN-EIS at 750 °C and is decreased as a function of pH value determined from annealed-TiN-EIS at 800 °C. Only the EIS device with TiN film annealed at 850 °C showed the lowest standard deviation of flat-band voltage as compared with other devices and offered quite similar value for measurements from every pH values (acid, neutral, base). This reveals that the annealed-TiN film has more chemical stability due to crystalline structure, surface morphology, chemical composition and interface defect represented on the characterizations.

4. Conclusion

High-performance ISFET-pH devices incorporating nanocrystal-TiO_2 as sensing membrane have been developed compatible to CMOS fabrication process. The reactive dc magnetron sputtering was used to deposit 30 nm of Ti and TiN thin films on SiO_2/Si substrates with various annealing temperature in N_2 furnace. The presence of TiO_2 structures in annealed-Ti and annealed-TiN was confirmed by means of XRD, FE-SEM and AES analysis. In as deposited Ti and TiN, their phases were changed from amorphous-to-crystalline transition phase at high annealing temperature. The optimal condition was found to be an annealing temperature at 850 °C for both Ti and TiN thin films. At high temperature annealing of TiN thin film, the Ti—O—N composition was presented. The EIS device incorporating TiN film annealed at 850 °C exhibited a highest sensitivity (59 mV/pH), a good linearity (1), a very small hysteresis voltage (1 mV in the pH cycle $7 \rightarrow 4 \rightarrow 7 \rightarrow 10 \rightarrow 7$), and a low drift rate (0.246 mV/h) in pH 7 buffer solution for 10 h continuously. This result can be explained by the presence of a chemical stable of well-crystallized Ti—O—N and no interface defect with dielectric layer. The standard deviation flat-band-voltage of Ti—O—N EIS device revealed that this ISFET-pH device can be successfully fabricated with inline CMOS fabrication process.

Acknowledgements

This work has partially been supported by the National Nanotechnology Center (NANOTEC), NSTDA, Ministry of Science and Technology, Thailand, through its program of Center of Excellence Network.

References

[1] P. Bergveld, Development of an ion sensitive solid-state device for neurophysiological measurement, IEEE Transactions on Biomedical Engineering BME-17 (1970) 70–71.
[2] T. Mastsuo, K.D. Wise, IEEE Transactions on Biomedical Engineering 21 (1947) 485.
[3] P.V. Bobro, Y.A. Tarantov, S. Krause, W. Moritz, Sensors and Actuators B3 (1991) 75.
[4] H.V.D. Vlekkert, L. Bousse, N. De Rooij, Journal of Colloid and Interface Science 122 (1991) 75.
[5] A. Fog, R. Buck, Electronic semiconducting oxides as pH sensors, Sensors and Actuators 5 (1984) 137–146.
[6] J.B. Goodenough, A. Hamnett, Q. Madelung, in: L. Bornstein (Ed.), III-Semiconductors, Springer-Verlag, Berlin, Germany, 1984.
[7] Y. Suda, H. Kawasaki, T. Ueda, T. Ohshima, Thin Solid Films 453–454 (2004) 162–166.
[8] Z. Liu, G. Welsch, Literature survey on diffusivities of oxygen, Metallurgical and Materials Transactions A 19 (4) (2012) 1121–1125.
[9] Y. Koizumi, M. Kishimoto, Y. Minamino, H. Nakajima, Philosophical Magazine 88 (24) (2008).
[10] S. Zerkouta, S. Achoura, A. Mosserb, N. Tabetc, On the existence of superstructure in TiNx thin films, Thin Solid Films 441 (2003) 135–139.
[11] C.D. Fung, P.W. Cheung, W.H. Ko, A generalized theory of an electrolyte-insulator-semiconductor field-effect transistor, IEEE Transactions on Electron Devices 33 (1986) 8–18.
[12] T.-M. Pan, C.-D. Lee, M.-H. Wu, High-k Tm_2O_3 sensing membrane-based electrolyte-insulator-semiconductor for pH detection, Journal of Physical Chemistry 113 (2009) 21937–21940.

Advanced Materials Research Vol. 802 (2013) pp 232-236
© (2013) Trans Tech Publications, Switzerland
doi:10.4028/www.scientific.net/AMR.802.232

High Sensitive Nanocrystal Titanium Nitride EG-FET pH Sensor

Yossawat Rayanasukha[1,4,5,a], Supanit Porntheeraphat[2,5,b], Win Bunjongpru[1,3], Narathon Khemasiri[1,5], Apirak Pankiew[1,3], Wutthinan Jeamsaksiri[3], Awirut Srisuwan[3], Woraphan Chaisriratanakul[3], Charndet Hruanun[3], Amporn Poyai[3] and Jiti Nukeaw[1,4,5]

[1]College of Nanotechnology, King Mongkut's Institute of Technology Ladkrabang, Bangkok 10520, Thailand
[2]Photonics Technology Laboratory, National Electronics and Computer technology Center (NECTEC), NSDTA, Patumthani 12120, Thailand
[3]Thai Microelectronics Center, NECTEC, NSTDA, Chachoengsao 24000, Thailand
[4]ThEP Center, CHE, 328 Si Ayutthaya Rd., Bangkok 10400, Thailand
[5]Nanotec-KMITL Center of Excellence on Nanoelectronic Devices, Chalongkrung Rd., Ladkrabang, Bangkok 10520, Thailand

[a]Rayanasukha.Y@gmail.com, [b]supanit.porntheeraphat@nectec.or.th

Keywords: Titanium Nitride, Ion-Sensitive, EG-FET, Sputtering, Nanocrystal, pH sensing

Abstract. Solid state pH-sensor device with high efficiency has successfully prepared by using TiN thin film as sensing membrane of extended gate field effect transistor (EG-FET) device. This research has described the physical properties and sensing characteristics of TiN membrane thin film which deposited on SiO_2/Si substrate through reactive D.C. magnetron sputtering system. Thenanocrytal-TiNwith anatasestructure depended on substrate heating conditions was revealed from glancing angle x-ray diffraction. The I_{DS}-V_{GS} measurement in the standard buffer solutions showed that the sensitivity of fabricated TiN-EGFET pH deviceis 59.82mV/pH.

Introduction

The pH value is the significant parameter in wide applications for example chemistry, biochemistry, waste water, environmental and so on. The ion-sensitive filed effect transistor (ISFET) first published by Bergveld [1]has more advantages than traditional glass electrodes for instance: small size, rapid response, high input impedance, low output impedance and can develop as biochemical sensors [2]. An a-Si:H [2,3], Ta_2O_5 [2], a-WO_3[2], Al_2O_3[4], Si_3N_4[5], SnO_2[6], and TiO_2 [7] were fabricated as sensing membrane of ISFET. The extended gate filed effect transistor (EG-FET) was first introduced by Van Der Spiegel *et al.*[8] in 1983 with it's advantages over the ISFET in properties which of cheaper, simple structure and easier packaging.The EGFET composes of two component parts including sensing membrane and conventional metal oxide semiconductor filed effect transistor (MOSFET). Mainly a sensing membrane of pH-ISFET and pH-EGFET almost is the metal oxide which has a high sheet resistance although the sensing membrane of pH-EGFET should be a high conductivity material which can be transmitted electrical signal easily [9]. Therefore, metal oxide with electrical insulation property is not suitable for the sensing membrane of pH-EGFET. Chuo *et al.* [10]had introduced to ruthenium nitride sensing membrane for pH-EGFET and reviewed to other metal nitride used to sensing membrane of this structure.

In this work, the titanium nitride (TiN) thin films were prepared as external sensing membrane gate FET device. The TiN thin films were deposited on a silicon (Si) substrate by d.c. magnetron sputtering with different substrate heating temperatures. The sputtered TiN thin film and gate electrode for pH-EGFET device were determind. The sensitivity of the fabricated pH-EGFET device were characterized by current-voltage (I-V) measurement systems.

Experimental and Methodology

2.1 TiN Thin Film Deposition

The 50 nm of TiN thin fiilms were grown on p-type Si (100) substrates with different substrate heating temperatures of 250, 350 and 450°C, respectively.The resistivity of the Si substrate was 20-30 Ohm-cm. Initially the 10 nm of silicon oxide layer was grown on the substrate by thermal oxide process then TiN thin film was sputtered from a 99.999% purity of Ti target by d.c. magnetron sputtering system (model ILC-1051 from Anelva).The sputtering chamber base pressure was below 1×10^{-7} mbar. The N_2 gas with high purity of 99.9999% was used as the sputtering and the reactive gas in during process. The N_2 flow rate of 40cc/min was fed into the chamber at working pressure of 4×10^{-3} mbar. The D.C. input power supplied to the system was set to 6 kW.

2.2 TiN Thin Film Characterization

Crystalline structure, surface morphology and surface roughness of sputteredTiN grown at RT, 250, 350 and 450°C were obtained byGlancing Angle X-ray Diffraction (GAXRD) (model TTRAX 111 from Riagku). The sheet resistance of the sputtered thin films was determined using a four-point probe.

2.3 The pH Sensitivity Measurement

The current-voltage (I-V) characteristic of the fabricated devices was measured by usingAgilentB1500A Semiconductor Device Analyzer. The TiN-EGFET pH sensing device was prepared by connecting the TiN/SiO_2/p-Si device as the external gate electrode to a commercial MOSFET gate electrode as shown in Fig.1. For pH measurement, the Ag/AgCl electrode in KCl gel was prepared as the reference electrode as shown in Fig. 1. The TiN/SiO_2/p-Si device and Ag/AgCl reference electrode were immersed into standard buffer solutions with pH of 4, 7 and 10, respectively. The pH sensitivity of fabricated TiN-EGFET sensor device was calculated form I_{DS}-V_{GS} curve measurement.

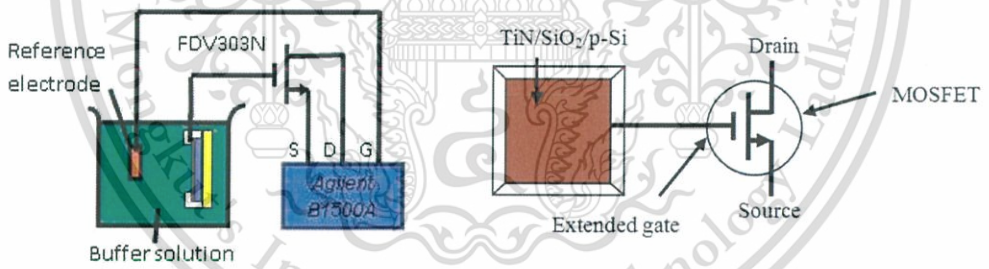

Figure. 1 The fabricated TiN-EGFET pH sensing device as the external gate electrode

Results and Discussions

3.1 Physical Properties of TiN Thin Film

The XRD exhibits the peaks at 2-theta of 36° and 42.2° corresponded to (111) and (200) of cubic-TiN crystal orientations as displayed in Fig. 2. This result reveals that the 50 nm thick ofsputtered film at RT was amorphous-TiN phase while, the crystallinity of TiN will grow with theincreasing of substrate heating temperature of 250 and 350°C. At the high temperature of 450°C, the residue oxygen atom in the sputtering process can incorporate with Ti atom to form TiO_2 which exhibits as a small peak at 2-theta of 38° agreed with (004) orientation of TiO_2 as shown in Fig. 2. At the high substrate temperature in the TiN deposition process, the oxygen atom can compoundwith Ti to form TiO_2 with anatase structure (004) at 38° [11].

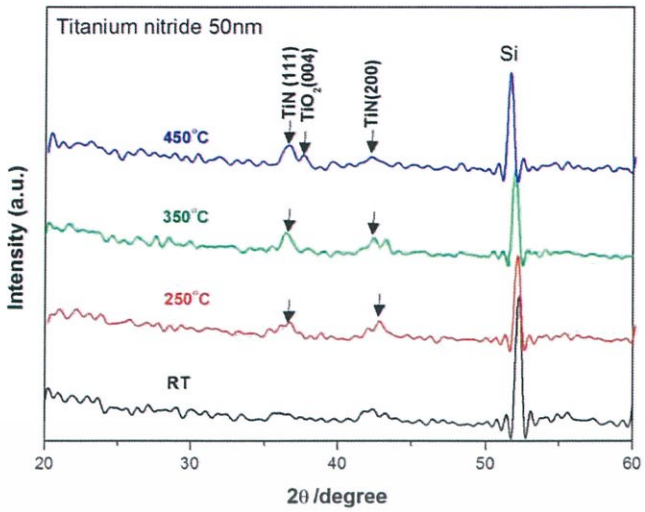

Figure 2. XRD pattern of the sputtered-TiN at difference substrate temperature of RT, 250, 350and 450°C

3.2 TiNThinFilmElectricalProperty

For electrical property of prepared-TiN thin film, the sheet resistance was measured by a four-point probe instrument. The sheet resistance values are 56.863, 51.338, 45.421 ohms per square for deposited-TiN thin films at substrate heating temperature of RT, 250, and 350°C, respectively. The sheet resistance of TiN thin film was decreased when the substrate heating temperature was increased. The higher sheet resistance of TiN thin film grown at 450°C than at 350°C may dues to the oxygen incorporation which formed TiO_2that agreedto XRD result as shown in Fig. 2. The insulating property of TiO_2 is affected to the increasing of sheet resistivity of thin film. So, the substrate heating temperature of 350°C was optimized for the growth of 50 nm-TiN thin film prepared by d.c magnetron sputtering method in this experiment.G.A. Battiston*et al.*[12] has been reportedon titanium (Ti) thin films grown in pure nitrogen gas at substrate temperaturebetween 393 and 523 Kand they found that the high substrate temperature yielded to the lower sheet resistivity of achieved thin films due to the formation of ions of unusual valence Ti(III) and Ti(II) that are known to influence the resistivity of TiO_2 films.

3.3 pH sensitivity of TiN-EGFET

The$V_{DS}$was set constantly at 300 mV in the pH sensitivity measurement while, the gate-source voltage (V_{GS}) was adjusted between from 0 to 1.5 V. The pH sensitivity was calculated by plotting of the I_{DS}-V_{GS}measurement of TiN-EGFET sensor devices. The pH sensitivity of MOSFET with TiN gate electrode devices was measured in standard pH buffer solution of 4, 7, and 10, respectively. The result, asshown in Fig. 3., revealed the shifting of V_{GS}at I_{DS} = 100 μA (dashed line)

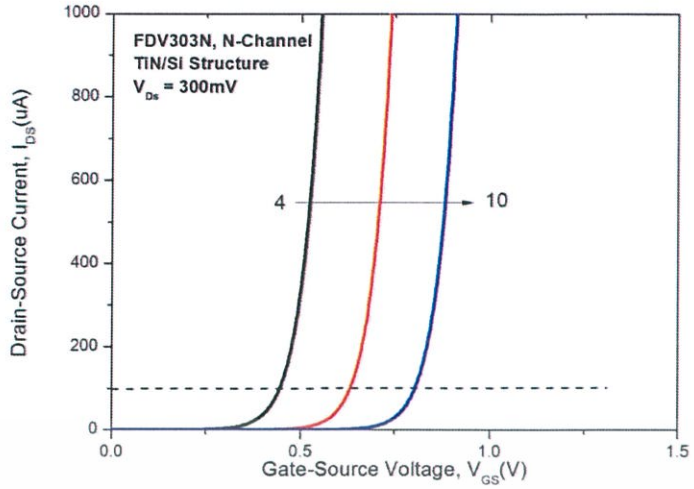

Figure. 3 Characteristics of MOSFET (FDV303N) with TiN gate-electrode, the I_{DS}-V_{GS} measured in pH 4, 7 and 10

The pH-sensitivity and the linearity of TiN-EGFET devices with different substrate heating temperature of RT, 250, 350 and 450°C is 46.46, 51.72, 59.82, 56.70 mV/pH and 0.9965, 0.9998,0.9999 and 0.9999, respectively were shown in Fig. 4. The experimental results show that the TiN-EGFET pH device fabricated from the nanocrystalTiN as gate electrodegrown with substrate heating temperature of 350°C determines the highest pH sensitivity. Moreover, the pH sensitivity of this device has consistent with the electrical property of TiN thin film. The sheet resistivity measurement has shown that the TiN thin film grown with the substrate heating temperature of 350°C by D.C. magnetron sputtering has the lowest sheet resistivity so this condition isoptimized for pH-EGFET structure [9].

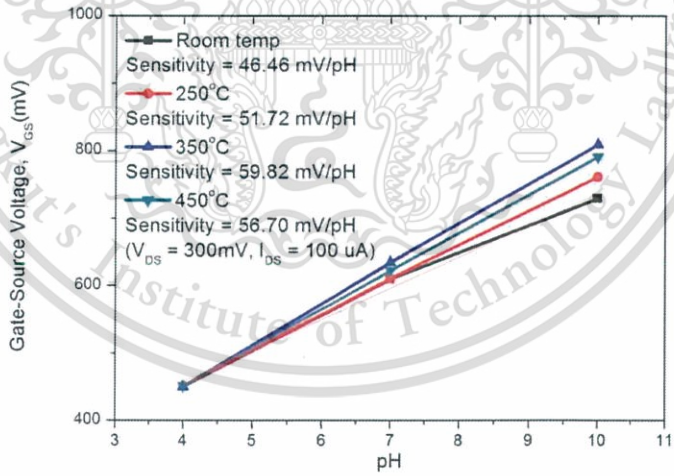

Figure. 4 The pH-Sensitivity of TiN-EGFET pH sensors at V_{DS} = 300 mV and I_{DS} = 100μA at substrate heating at RT, 250, 350 and 450°C

Chou *et al.*[9,10]has been reported to the sensitivities of a ruthenium-doped titanium dioxide (TiO_2:Ru) and a ruthenium nitride (RuN) for sensing membrane of extened-gate FET pH sensors that these deviceshadthe sensitivity of 55.20 mV/pH and 58.3 mV/pH, respectively. Guerra *et al.*[13] reported that the sensitivity of vanadium pentoxide (V_2O_5) sensing for pH-EGFET sensor was 58.1 mV/pH. Though, these deviceshad the high pH sensitivity but these sensing membrane were unstable then the fabricated devices had the poor linearity. Therefore, we can optimize the growth condition of TiN as stable sensing membrane of pH-EGFET which achieved high pH sensitivity.

Summary

We have successfully prepared the nanocryatal-TiN thin film as a sensing membrane of pH-EGFET devices by d.c. magnetron sputtering system used in the microfabrication line process. The property characteristics of sputtered thin films and the fabricateddevices have displayed that the TiN thin film grown at substrate temperature of 350°C has more efficiently forsensing membraneof pH-EGFET device with highest pH sensitivity of 59.82 mV/pH over than TiO_2:Ru, RuN, V_2O_5 and other thin films sensing membrane with EGFET structure device. The pH stability and the repeatability of fabricated devices is on our research work.

Acknowledgements

This work was financially supported by the KMITL Research Fund, Bangkok, Thailand, the thailand Excellent Physics Center (ThEPCenter), Bangkok, Thailand and the National Nanotechnology Center (NANOTEC), NSTDA, Ministryof Science and Technology, Thailand, through its program of Center of Excellence Network.

References

[1] P. Bergveld, Development of an ion-sensitive solid-state device for neurophysiological measurements, IEEE T. Bio-med. Eng. 17 (1970) 70–71.
[2] J.-L. Chiang, J.-C. Chou and Y.-C. Chen, Sensitivity and Hysteresis Properties of a-WO3, Ta2O5, and a-Si:H Gate Ion-sensitive Field-effect Transistors, Opt. Eng. 41(8) (2002) 2032–2038.
[3] J. C. Chou and Y. F. Wang, Study on the temperature dependence of the hysteresis for the a Si:H gate pH-ISFET, Mater. Chem. Phys. 70(1) (2001) 107–111.
[4] J.-C. Chou, C.-Y. Weng and H.-M. Tsai, Study on the temperature effects of Al2O3 gate pH-ISFET, Sensor Actuat. B-Chem. 81(2–3) (2002) 152–157.
[5] L.-T. Yin, J.-C. Chou, W.-Y. Chung, T.-P. Sun and S.-K. Hsiung, Characteristics of silicon nitride after O2 plasma surface treatment for pH-ISFET applications, IEEE T. Bio-med. Eng. 48(3) (2001) 340–344.
[6] J. C. Chou and Y. F. Wang, Preparation and study on the drift and hysteresis properties of the tin oxide gate ISFET by the sol-gel method, Sensor. Actuat. B-Chem. 86(1) (2002) 58–62.
[7] M. Lahav, A. B. Kharitonov and I. Willner, Imprinting of Chiral Molecular Recognition Sites in Thin TiO2 Films Associated with Field-Effect Transistors: Novel Functionalized Devices for Chiroselective and Chirospecific Analyses, Chem-Eur. J. 7(18) (2001) 3992–3997.
[8] J. van der spiegel, I. Lauks, P. Chan and D. Babic, The extended gate chemically sensitive field effect transistor as multi-species microprobe, Sensor Actuat. 4 (1983) 291–298.
[9] J.-C. Chou and C.-W. Chen, Fabrication and Application of Ruthenium-Doped Titanium Dioxide Films as Electrode Material for Ion-Sensitive Extended-Gate FETs, IEEE Sens. J. 9(3) (2009) 277–284.
[10] Y.-H. Liao and J.-C. Chou, Fabrication and Characterization of a Ruthenium Nitride Membrane for Electrochemical pH Sensors, Sensor 9(4) (2009) 2478–2490.
[11] Y.-Q. Hou, D.-M. Zhuang, G. Zhang, M. Zhao, and M.-S. Wu, Influence of annealing temperature on the properties of titanium oxide thin film, Appl. Surf. Sci. 218(2003) 98–106.
[12] G. A. Battiston, R. Gerbasi, A. Gregori, M. Porchia, S. Cattarin and G. A. Rizzi, PECVD of amorphous TiO2 thin films: effect of growth temperature and plasma gas composition
, Thin Solid Films. 371(1–2) (2000) 126–131.
[13] E. M. Guerra, G. R. Silva and M. Mulato, Extended gate field effect transistor using V2O5 xerogel sensing membrane by sol gel method, Solid State Sci. 11(2) (2009) 456–460.

Surface & Coatings Technology 306 (2016) 147–150

Contents lists available at ScienceDirect

Surface & Coatings Technology

journal homepage: www.elsevier.com/locate/surfcoat

Non-enzymatic urea sensor using molecularly imprinted polymers surface modified based-on ion-sensitive field effect transistor (ISFET)

Y. Rayanasukha [a,b,c], S. Pratontep [a,b,c], S. Porntheeraphat [b,d,*], W. Bunjongpru [e], J. Nukeaw [a,b,c]

[a] College of Nanotechnology, King Mongkut's Institute of Technology Ladkrabang, Bangkok 10520, Thailand
[b] Nanotec-KMITL Center of Excellence on Nanoelectronic Devices, Ladkrabang, Bangkok 10520, Thailand
[c] Thailand Center of Excellence in Physics, Commission on Higher Education, Ministry of Education, Bangkok 10400, Thailand
[d] National Electronics and Computer Technology Center, Klong Luang, Pathumthani 12120, Thailand
[e] Thai Microelectronics Center, 51/4 Moo 1, Wangtakien, Amphur Muang, Chachoengsao 24000, Thailand

ARTICLE INFO

Article history:
Received 24 December 2015
Revised 16 May 2016
Accepted in revised form 21 May 2016
Available online 21 May 2016

Keyword:
Molecularly imprinted technique
Electrochemical sensor
Urea detection
Non-enzymatic sensor
Ion-sensitive field effect transistor

ABSTRACT

A novel molecularly imprinted electrochemical sensor based on ISFET device has been developed for urea detection sensor. The molecularly imprinted polymers (MIPs) were prepared by photopolymerization on the surface of ISFET device using PMMA and urea as the functional polymer and molecular template, respectively. The fabricated sensors were characterized by potentiometry and UV-Vis spectroscopy. The preparation conditions were optimized for performance of the sensors, i.e. drop-cast volume and incubation time. The MIP modified ISFET sensors has linear range response from 1.0×10^{-4} to 1.0×10^{-1} M with the limit of detection of 1.0×10^{-4} M ($S/N = 3$). The MIP modified ISFET sensors also exhibit excellent reproducibility, repeatability and stability, as well as high selectivity to urea.

1. Introduction

Urea concentration is considerable indicator in agricultural chemistry, food science and environmental monitoring. Moreover, a urea has great significance in clinical diagnostics, i.e. Blood Urea Nitrogen or BUN. This is related to the concentration of nitrogen in the human serum in form of urea and indicator of the kidney function [1]. Typical urea concentration for urea nitrogen in serum is 15–40 mg/dl (2.5–7.5 mM) [2]. Urea determination has many methods such as gas chromatography, calorimetry and fluorimetric. These methods have disadvantages in complicated, expensive and time consuming. Nowadays, an electrochemical method for urea biosensor has been widely studied due to simplicity, low cost and high sensitivity [3]. Ion-sensitive field effect transistors (ISFET) is electrochemical biosensor has been interested in development to wide range application devices such as glucose [4], triglycerides [5], creatinine [6] galactose and polyphenol [7]. The advantages of ISFET based biosensor are small size, high sensitivity, high level of activity, low cost and rapid response time [8]. The ISFET was first introduced by Bergveld in 1970 [9]. And then, in 1980 ISFET based enzyme biosensor was described by Caras and Janata [10]. The analytical technique for urea biosensor based on ISFET is enzymatic hydrolysis of urea causes pH changes in the system [11]. However enzyme has limitations such as; enzyme activity, enzyme stability and the environment of using [12].

Recently, molecularly imprinting technique has been developed for non-enzymatic sensor in electrochemical sensing for organic compounds. The advantages over biological recognition including, stability, low cost, long lifetime, high sensitivity and widely applied in sensor development [13,14]. Preparation of molecularly imprinted polymers (MIPs), the molecular template and functional polymer are mixed in solutions to form a complex. The polymer-template solution is co-deposited on the surface of an electrode. After that, the molecular template was removed from the polymer matrix, leaving molecular cavities has complementary to the template in size, shape, and functional groups [15]. The response of MIP sensor to target molecules may be similarly enzymatic mechanisms into two strategies for molecular detection. One is response higher occurred the chemical reaction between polymeric membrane and template molecule, generated a charge or electron [16]. The other is the template molecules that are embedded into the molecular cavities which similar to the inhibition of enzymatic activities [17,18], obstruction for charge transfer to the surface of the electrode is the cause of the reduction of the response signal [19]. This approach has been presented for MIP sensor by incubating the sensor in a sample solution before measuring the response in an electrolyte [15].

* Corresponding author at: Photonics Technology Laboratory, National Electronics and Computer Technology Center, National Science and Technology Development Agency, 112 Thailand Science Park, Phahonyothin Rd., Klong 1, Klong Luang, Pathumthani, 12120 Thailand.
E-mail address: supanit.porntheeraphat@nectec.or.th (S. Porntheeraphat).

http://dx.doi.org/10.1016/j.surfcoat.2016.05.060
0257-8972/

In this paper, we reported a novel molecularly imprinted sensor based-on the ISFET device for urea detection. Urea was used as the molecule template and poly(methyl methacrylate) (PMMA) used as the functional polymer. The ISFET sensing area was coated by drop-casting of the PMMA-urea solution and exposed to UV irradiation for photopolymerization. Urea molecular templates were removed by immersion in DI water. The sensor was characterized by potentiometry and UV-Vis spectroscopy. The sensitivity, selectivity, repeatability and reproducibility of the fabricated sensor have been investigated.

2. Experimental

2.1. Chemicals and reagents

All chemicals and reagent were used analytical grade and de-ionized (DI) water (Resistivity > 18 MΩ/cm) was used in all experiments. Urea and sodium chloride (NaCl) from Sigma-Aldrich, poly(methyl methacrylate) (PMMA) from Acros organics, dimethylformamide (DMF) from Labscan Asia Co., Ltd., Na_2HPO_4, NaH_2PO_4 from Ajax Finechem Pty., Ltd. and pH buffer solution from CARLO ERBA Reagents.

2.2. ISFET device and measurement

The ISFET devices obtained from TMEC (Thai Microelectronic Center (TMEC), NECTEC, NSTDA, THAILAND). ISFET microdevice has gate area $100 \times 2000\ \mu m^2$ and has silicon nitride (Si_3N_4) as sensing membrane. For the electrochemical measurement, the ISFET and MIP modified ISFET were used as working electrode, while an Ag/AgCl (3 M of KCl) was used as reference electrode. The ISFET response characteristic was determined at gate-source voltage (V_{GS}) variations by using a constant drain-source current ($I_{DS} = 30\ \mu A$) and constant drain-source voltage ($V_{DS} = 300$ mV). The pH sensitivity and calibration curves of ISFET sensor have been measured with standard pH buffer solution. The MIPs modified electrode was incubated in urea solution for 5 min and immersed in phosphate buffer for electrochemical measurements [15].

2.3. ISFET surface modification

The ISFET surface was cleaned with Ethanol and DI water in ultrasonic bath for 5 min in each step. The polymer-urea solution was prepared by dissolve 2.5 wt% of PMMA and 0.4 wt% of urea in 10 ml of DMF [20] and sonication for 10 min. The ISFET surface area of 6 mm^2 was coated by 1 μl of mixture solution and curing with ultraviolet radiation (Stratagene UV Stratalinker 1800) for 15 min. After the polymer-urea layer on ISFET surface was immersed in DI water for 1 h to remove the urea template molecules form the polymer layer then the MIP membrane was produced. The template removal characteristic of the MIP membrane was investigated by UV-Vis spectroscopy [21] (T92 + UV-VIS spectrophotometer from PG Instruments Ltd.). For non-molecularly imprinted polymers (NIPs) sensor was fabricated by similar process but without the addition of urea template molecules.

3. Results and discussion

3.1. Characterization of MIP modified ISFET sensors

3.1.1. Electrochemical measurement

The pH sensitivity of ISFET sensors at different fabrication stages were tested in pH buffer solutions (4, 7, 10). The sensitivities of different fabricated ISFET devices were shown as the slope of characteristic curves displayed in Fig. 1. The PMMA-urea/ISFET sensor has lower sensitivity than Si_3N_4/ISFET sensor because of the polymer-urea layer obstructs the charges that pass through to the electrodes of device affected to high voltage. After the urea template molecule removal, the surface of sensor becomes to porous membrane so the MIP/ISFET sensor exhibits an increased sensitivity. However, the response voltage level of the MIP/ISFET sensor is higher than the Si_3N_4/ISFET sensor [15,19].

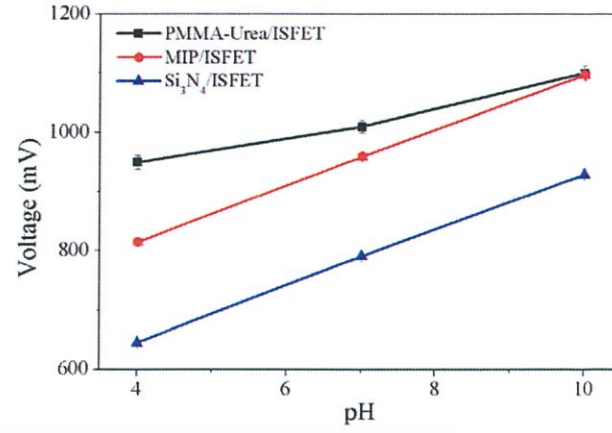

Fig. 1. The voltage and pH characteristic of fabricated sensors, PMMA-urea/ISFET (black line), MIP/ISFET (red line) and Si_3N_4/ISFET (blue line) in pH buffer solutions.

3.1.2. Characterization of removal template

The UV-Vis absorption spectroscopy was applied to confirm the template removal characteristic of DI water before and after washing PMMA-urea coating layer. Fig. 2 shows UV-Vis spectra of DI water and elution solution. The reference solution i.e. DI water has no absorption peak between 200 and 900 nm, while the elution after washing coating layer has the absorption peak of urea could fine at 230 nm. The reason is due to the urea template molecules have been removed from the polymer matrix.

3.2. Optimization of MIP modified ISFET sensor

3.2.1. Optimization of the volume of the polymer-urea composite solution

The performance of the MIP modified ISFET depends on the thickness of the polymer membrane. This is consistent with the drop-cast volume of the polymer-urea composite solution. Fig. 3a. shows the voltage response of MIP modified ISFET sensor to 1 mM urea. The volume of PMMA-urea composite solution at 1.0 μl obtains maximum response. When the volume of PMMA-urea composite solution < 1.0 μl, the response voltage was decreased because the polymer film maybe cracks when urea template molecule was removed. If the volume of composite

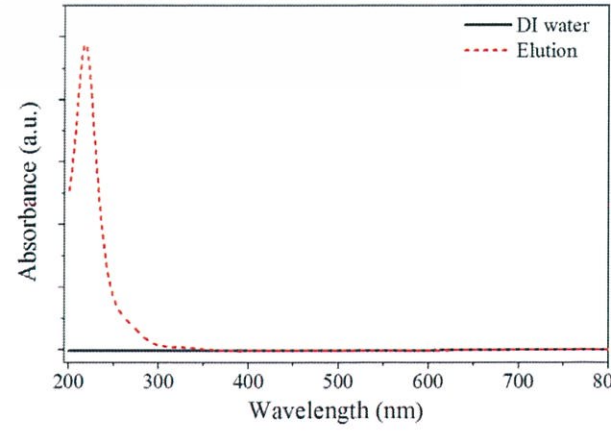

Fig. 2. UV-Vis absorption spectra of DI water and elution solution.

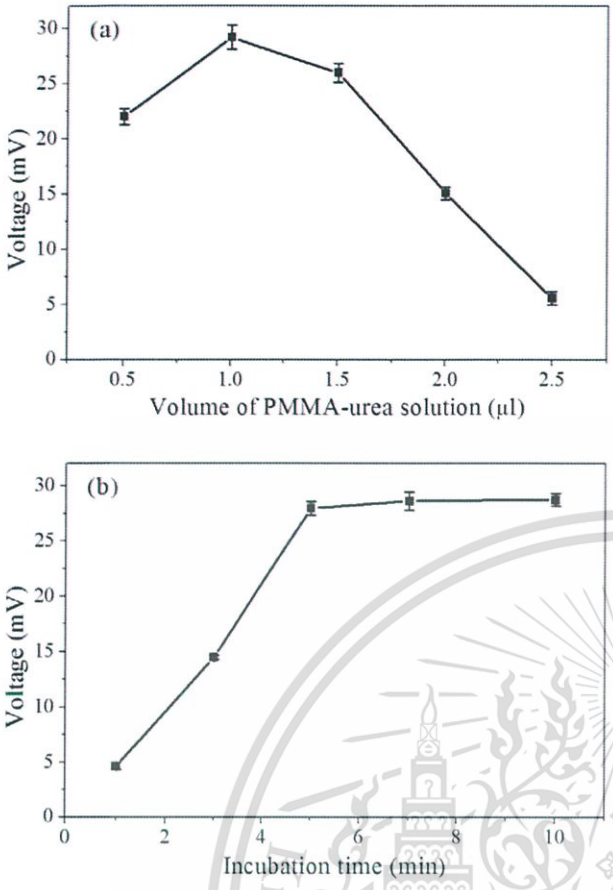

Fig. 3. Optimization of drop-cast volume (a), and incubation time (b) to voltage response of MIP modified ISFET in 1 mM urea.

solution >1.0 µl, the urea template molecule cannot completely remove from polymer matrix caused by the film thickness [15,21].

3.2.2. Effect of the incubation time

Investigation the effect of incubation time to the output response of the sensor, the MIP modified ISFET sensor was studied in 1 mM urea solution for 1, 3, 5, 10 and 15 min at room temperature. Fig. 3b shows the voltage response with the incubation time. When the incubation time is increased the voltage is increased and saturated after 5 min. Therefore, the optimal of incubation time is 5 min.

3.3. Determination of aqueous urea samples

The electrochemical responses of the MIP and NIP modified ISFET sensors have been investigated in urea solution at different concentrations (from 1.0×10^{-4} M to 1.0 M) as shown in Fig. 4. The results represent the obviously highest response of the MIP sensor, while the NIP sensor has no trend response for all urea concentration ranges. The response of the MIP sensor to urea was found to be linearity in the range of 1.0×10^{-4} M to 1.0×10^{-1} M, with the sensitivity of 18.4 mV per power of urea ($R^2 = 0.992$). The detection limit for urea is 1.0×10^{-4} M (S/N = 3).

3.4. Selectivity of the MIP modified ISFET sensor

Specific recognition to the urea target molecule has been important for develop the MIP modified ISFET sensor. In order to check the selectivity of molecularly imprinted sensor, carbamate, glutamic acid, potassium nitrate and sodium chloride were chosen for interference studies, which molecules of carbamate, glutamic acid and potassium nitrate have a similar structure to urea, while sodium chloride has interaction

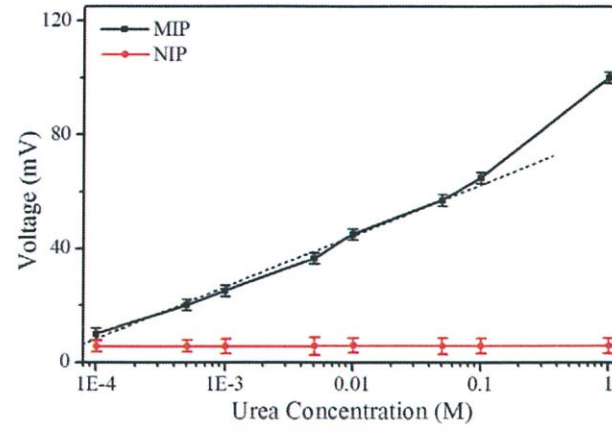

Fig. 4. Voltage response of MIP (black line) and NIP (red line) modified ISFET sensors in different urea concentrations (the dotted line is the trend line).

type to urea in the blood sample. Fig. 5 displays the voltage response of MIP modified ISFET sensor to urea and four substrates at concentration of 1 mM for all solutions. The result shows that the voltage response of urea has higher than four other interfering molecules. It can imply that the molecular cavities from removal template molecule on surface of fabricated MIP modified ISFET sensor has highly specific to urea molecules.

3.5. The reproducibility, the repeatability and the stability of the MIP modified ISFET sensor

The reproducibility of fabricated sensor was determined by using 1 mM urea with five MIP modified ISFET sensors which prepared as same conditions. The relative standard deviation (RSD) of voltage response was calculated to be 3.4%, represented that the MIP modified ISFET sensors are a good reproducibility [14].

The repeatability of the MIP modified ISFET sensor was defined by using five same fabricated sensors measured in 1 mM urea for 3 times. The RSD of 2.5% was observed for a good repeatability [14].

The stability of the MIP modified ISFET sensor has been investigated by comparing the voltage response of 1 mM urea for a period of two months at room temperature. The response of the sensors has retained 95% after two months. The result was indicated that our novel MIP modified ISFET sensor has excellent long-term storage stability.

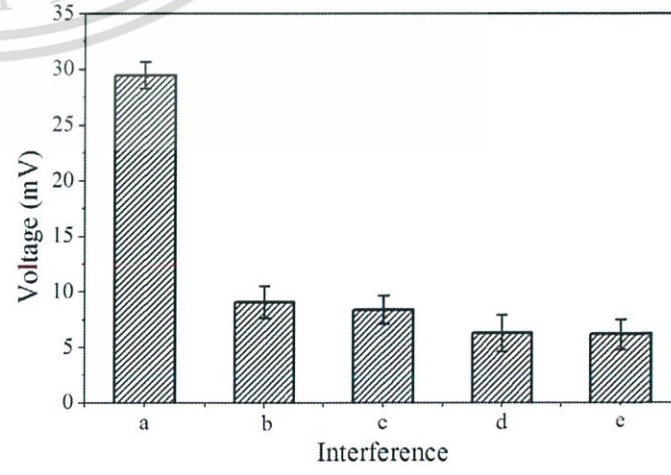

Fig. 5. Voltage response of MIP-Modified ISFET sensor to, urea (a), carbamate (b), glutamic acid (c), potassium nitrate (d), and sodium chloride (e).

4. Conclusions

We have demonstrated that the molecularly imprinted technique was successfully fabricated on the ISFET device. The PMMA was employed as the polymer matrix sensing membrane. Under optimization of the effective parameters, the fabricated sensor exhibited high reproducibility, repeatability, stability and specificity on recognition target molecule. The detection limit of fabricated sensor is found to be as low as the millimolar (mM) level. In addition, our novel MIP modified ISFET sensor has high linearity for urea detection and molecularly imprinted technique is very useful for specific molecule sensor.

Acknowledgments

This work has partially been supported by the National Nanotechnology Center (NANOTEC), NSTDA, Ministry of Science and Technology, Thailand, through its program of Center of Excellence Network, and National Research Council Thailand (NRCT), Bangkok, Thailand, under grant number RDG5750045.

References

[1] Rajesh, V. Bisht, W. Takashima, K. Kaneto, Surf. Coat. Technol. 198 (2005) 231.
[2] M. Singh, N. Verma, A.K. Garg, N. Redhu, Sensors Actuators B Chem. 134 (2008) 345.
[3] A. Kaushik, P.R. Solanki, A.A. Ansari, G. Sumana, S. Ahmad, B.D. Malhotra, Sensors Actuators B Chem. 138 (2009) 572.
[4] K.-Y. Park, S.-B. Choi, M. Lee, B.-K. Sohn, S.-Y. Choi, Sensors Actuators B Chem. 83 (2002) 90.
[5] A. Vijayalakshmi, Y. Tarunashree, B. Baruwati, S.V. Manorama, B.L. Narayana, R.E.C. Johnson, N.M. Rao, Biosens. Bioelectron. 23 (2008) 1708.
[6] B. Premanode, C. Toumazou, Sensors Actuators B Chem. 120 (2007) 732.
[7] Y. Sasaki, J. Ogawa, T. Tani, Biocatal. Agric. Biotechnol. 1 (2012) 259.
[8] G. Dhawan, G. Sumana, B.D. Malhotra, Biochem. Eng. J. 44 (2009) 42.
[9] P. Bergveld, IEEE Trans. Biomed. Eng. 17 (1970) 70.
[10] S. Caras, J. Janata, Anal. Chem. 52 (1980) 1935.
[11] A.P. Soldatkin, J. Montoriol, W. Sant, C. Martelet, N. Jaffrezic-Renault, Biosens. Bioelectron. 19 (2003) 131.
[12] H.-T. Lian, B. Liu, Y.-P. Chen, X.-Y. Sun, Anal. Biochem. 426 (2012) 40.
[13] Z. Wang, H. Li, J. Chen, Z. Xue, B. Wu, X. Lu, Talanta 85 (2011) 1672.
[14] X. Xing, S. Liu, J. Yu, W. Lian, J. Huang, Biosens. Bioelectron. 31 (2012) 277.
[15] W. Lian, S. Liu, J. Yu, J. Li, M. Cui, W. Xu, J. Huang, Biosens. Bioelectron. 44 (2013) 70.
[16] S. Sadeghi, A. Motaharian, V Mater. Sci. Eng. C. 33 (2013) 4884.
[17] S. Viswanathan, H. Radecka, J. Radecki, Biosens. Bioelectron. 24 (2009) 2772.
[18] D. Du, X. Huang, J. Cai, A. Zhang, Biosens. Bioelectron. 23 (2007) 285.
[19] J.-L. Gong, F.-C. Gong, G.-M. Zeng, G.-L. Shen, R.-Q. Yu, Talanta 61 (2003) 447.
[20] C.-Y. Huang, T.-C. Tsai, J.L. Thomas, M.-H. Lee, B.-D. Liu, H.-Y. Lin, Biosens. Bioelectron. 24 (2009) 2611.
[21] W. Lian, S. Liu, J. Yu, X. Xing, J. Li, M. Cui, J. Huang, Biosens. Bioelectron. 38 (2012) 163.

คำขอรับสิทธิบัตร/อนุสิทธิบัตร

☑ การประดิษฐ์
☐ การออกแบบผลิตภัณฑ์
☐ อนุสิทธิบัตร

ข้าพเจ้าผู้ลงลายมือชื่อในคำขอรับสิทธิบัตร/~~อนุสิทธิบัตร~~นี้ ขอรับสิทธิบัตร/~~อนุสิทธิบัตร~~ ตามพระราชบัญญัติสิทธิบัตร พ.ศ.2522 แก้ไขเพิ่มเติมโดยพระราชบัญญัติสิทธิบัตร (ฉบับที่2) พ.ศ.2535 และพระราชบัญญัติสิทธิบัตร (ฉบับที่3) พ.ศ.2542

สำหรับเจ้าหน้าที่	
วันรับคำขอ 6 ก.พ. 2558	เลขที่คำขอ 1501000653
วันยื่นคำขอ 6 ก.พ. 2558	
สัญลักษณ์จำแนกการประดิษฐ์ระหว่างประเทศ	
ใช้กับแบบผลิตภัณฑ์ ประเภทผลิตภัณฑ์	
วันประกาศโฆษณา	เลขที่ประกาศโฆษณา
วันออกสิทธิบัตร/อนุสิทธิบัตร	เลขที่สิทธิบัตร/อนุสิทธิบัตร
ลายมือชื่อเจ้าหน้าที่	

1. ชื่อที่แสดงถึงการประดิษฐ์/~~การออกแบบผลิตภัณฑ์~~
กรรมวิธีการสร้างพอลิเมอร์เยื่อเลือกผ่านโมเลกุลสำหรับอุปกรณ์ตรวจวัดสารยูเรียและสารประกอบอินทรีย์ในน้ำแบบไม่ใช้เอนไซม์ (Polymeric Selective Membranes for non-enzymatic detection of urea and organic compounds)

2. คำขอรับสิทธิบัตรการออกแบบผลิตภัณฑ์นี้เป็นคำขอสำหรับแบบผลิตภัณฑ์ย่อยเดียวกันและเป็นคำขอลำดับที่ ในจำนวน

3. ผู้ขอรับสิทธิบัตร/~~อนุสิทธิบัตร~~ และที่อยู่ (เลขที่ ถนน ประเทศ)
สถาบันเทคโนโลยีพระจอมเกล้าเจ้าคุณทหารลาดกระบัง
เลขที่ 1 ซอยฉลองกรุง 1 แขวงลาดกระบัง เขตลาดกระบัง
กรุงเทพฯ 10520

3.1 สัญชาติ	ไทย
3.2 โทรศัพท์	02-329-8212 ถึง 3 กด 17, 18
3.3 โทรสาร	02-329-8212 ถึง 3 กด 1
3.4 อีเมล์	ip_kmitl@hotmail.com

4. สิทธิในการขอรับสิทธิบัตร/~~อนุสิทธิบัตร~~
☐ ผู้ประดิษฐ์/ผู้ออกแบบ ☑ ผู้รับโอน ☐ ผู้ขอรับสิทธิโดยเหตุอื่น

5. ตัวแทน (ถ้ามี)/ที่อยู่ (เลขที่ ถนน จังหวัด รหัสไปรษณีย์)
นางสาวณิชยา สืบสุข
อยู่ที่ สถาบันเทคโนโลยีพระจอมเกล้าเจ้าคุณทหารลาดกระบัง
สำนักส่งเสริมและบริการวิชาการพระจอมเกล้าลาดกระบัง
เลขที่ 1 ซอยฉลองกรุง 1 แขวงลาดกระบัง เขตลาดกระบัง
กรุงเทพฯ 10520

5.1 ตัวแทนเลขที่	2218
5.2 โทรศัพท์	0-2329-8212 ถึง 3 กด 17, 18
5.3 โทรสาร	02-329-8212 ถึง 3 กด 1
5.4 อีเมล์	ip_kmitl@hotmail.com

6. ผู้ประดิษฐ์/~~ผู้ออกแบบผลิตภัณฑ์~~ และที่อยู่ (เลขที่ ถนน ประเทศ)
1. นายสิรพัฒน์ ประโทนเทพ 2. นายจิติ หนูแก้ว และ 3. นางสาวนงลักษณ์ หวงกำแหง อยู่ที่ สถาบันเทคโนโลยีพระจอมเกล้าเจ้าคุณทหารลาดกระบัง เลขที่ 1 ซอยฉลองกรุง 1 แขวงลาดกระบัง เขตลาดกระบัง กรุงเทพมหานคร 10520 (ต่อหน้า 3)

7. คำขอรับสิทธิบัตร/อนุสิทธิบัตรนี้แยกจากหรือเกี่ยวข้องกับคำขอเดิม
ผู้ขอรับสิทธิบัตร/อนุสิทธิบัตร ขอให้ถือว่าได้ยื่นคำขอรับสิทธิบัตร/อนุสิทธิบัตรนี้ ในวันเดียวกับคำขอรับสิทธิบัตร เลขที่ วันยื่น เพราะคำขอรับสิทธิบัตร/อนุสิทธิบัตรนี้แยกจากหรือเกี่ยวข้องกับคำขอเดิมเพราะ
☐ คำขอเดิมมีการประดิษฐ์หลายอย่าง ☐ ถูกคัดค้านเนื่องจากผู้ขอไม่มีสิทธิ ☐ ขอเปลี่ยนแปลงประเภทของสิทธิ

หมายเหตุ ในกรณีที่ไม่อาจระบุรายละเอียดได้ครบถ้วน ให้จัดทำเป็นเอกสารแนบท้ายแบบพิมพ์นี้โดยระบุหมายเลข กำกับข้อและหัวข้อที่แสดงรายละเอียดเพิ่มเติมดังกล่าวด้วย

8. การยื่นคำขอนอกราชอาณาจักร

วันยื่นคำขอ	เลขที่คำขอ	ประเทศ	สัญลักษณ์จำแนกการประดิษฐ์ระหว่างประเทศ	สถานะคำขอ
8.1				
8.2				
8.3				

8.4 ☐ ผู้ขอรับสิทธิบัตร/อนุสิทธิบัตรให้ถือว่าได้ยื่นคำขอนี้ในวันที่ได้ยื่นคำขอรับสิทธิบัตร/อนุสิทธิบัตรในต่างประเทศเป็นครั้งแรกโดย
☐ ได้ยื่นเอกสารหลักฐานพร้อมคำขอนี้ ☐ ขอยื่นเอกสารหลักฐานหลังจากวันยื่นคำขอนี้

9. การแสดงการประดิษฐ์หรือการออกแบบผลิตภัณฑ์ ผู้ขอรับสิทธิบัตร/อนุสิทธิบัตรได้แสดงการประดิษฐ์ที่หน่วยงานของรัฐเป็นผู้จัด
วันแสดง วันเปิดงานแสดง ผู้จัด

10. การประดิษฐ์เกี่ยวกับจุลชีพ

10.1 เลขทะเบียนฝากเก็บ	10.2 วันที่ฝากเก็บ	10.3 สถาบันฝากเก็บ/ประเทศ

11. ผู้ขอรับสิทธิบัตร/อนุสิทธิบัตร ขอยื่นเอกสารภาษาต่างประเทศก่อนในวันที่ยื่นคำขอนี้ และจะจัดยื่นคำขอรับสิทธิบัตร/อนุสิทธิบัตรนี้ที่จัดทำ เป็นภาษาไทยภายใน 90 วัน นับจากวันยื่นคำขอนี้ โดยขอยื่นเป็นภาษา
☐ อังกฤษ ☐ ฝรั่งเศส ☐ เยอรมัน ☐ ญี่ปุ่น ☐ อื่น ๆ

12. ผู้ขอรับสิทธิบัตร/อนุสิทธิบัตร ขอให้อธิบดีประกาศโฆษณาคำขอรับสิทธิบัตร หรือรับจดทะเบียน และประกาศโฆษณาอนุสิทธิบัตรนี้ หลังจากวันที่ เดือน พ.ศ.
☐ ผู้ขอรับสิทธิบัตร/อนุสิทธิบัตรขอให้ใช้รูปเขียนหมายเลข ในการประกาศโฆษณา

13. คำขอรับสิทธิบัตร/~~อนุสิทธิบัตร~~นี้ประกอบด้วย

ก. แบบพิมพ์คำขอ		3	หน้า
ข. รายละเอียดการประดิษฐ์ หรือ~~คำพรรณนาแบบผลิตภัณฑ์~~		8	หน้า
ค. ข้อถือสิทธิ		1	หน้า
ง. รูปเขียน	4 รูป	2	หน้า
จ. ภาพแสดงแบบผลิตภัณฑ์			
☐ รูปเขียน	- รูป	-	หน้า
☐ ภาพถ่าย	- รูป	-	หน้า
ฉ. บทสรุปการประดิษฐ์		1	หน้า

14.เอกสารประกอบด้วย
☐ เอกสารแสดงสิทธิในการขอรับสิทธิบัตร/อนุสิทธิบัตร
☐ หนังสือรับรองการแสดงการประดิษฐ์/การออกแบบผลิตภัณฑ์
☑ หนังสือมอบอำนาจ
☐ เอกสารรายละเอียดเกี่ยวกับจุลชีพ
☐ เอกสารการขอนับวันยื่นคำขอในต่างประเทศเป็นวันยื่นคำขอในประเทศไทย
☐ เอกสารขอเปลี่ยนแปลงประเภทของสิทธิ
☑ เอกสารอื่นๆ สัญญาโอนสิทธิ สำเนาประกาศฯ แต่งตั้งอธิการบ

15. ข้าพเจ้าขอรับรองว่า
☑ การประดิษฐ์นี้ไม่เคยยื่นขอรับสิทธิบัตร/~~อนุสิทธิบัตร~~มาก่อน
☐ การประดิษฐ์นี้ได้พัฒนาปรับปรุงมาจาก.....

16. ลายมือชื่อ (☐ ผู้ขอรับสิทธิบัตร/อนุสิทธิบัตร; ☑ ตัวแทน)

(นางสาวณิชยา สืบสุข)
ตัวแทนผู้รับมอบอำนาจ

<u>หมายเหตุ</u> บุคคลใดยื่นขอรับสิทธิบัตรการประดิษฐ์หรือการออกแบบผลิตภัณฑ์ หรืออนุสิทธิบัตร โดยการแสดงข้อความอันเป็นเท็จแก่พนักงานเจ้าหน้าที่เพื่อให้ได้ไปซึ่งสิทธิบัตรหรืออนุสิทธิบัตร ต้องระวางโทษจำคุกไม่เกินหกเดือน หรือปรับไม่เกินห้าพันบาท หรือทั้งจำทั้งปรับ

6. ผู้ประดิษฐ์ และที่อยู่ (เลขที่ ถนน ประเทศ)

4. นางสาวศุภนิจ พรธีระภัทร
ศูนย์เทคโนโลยีอิเล็กทรอนิกส์และคอมพิวเตอร์แห่งชาติ สำนักงานพัฒนาวิทยาศาสตร์และเทคโนโลยีแห่งชาติ
112 อุทยาวิทยาศาสตร์ ถนนพหลโยธิน อำเภอคลองหลวง จังหวัดปทุมธานี 12120

5. นายยศวัต รายณะสุข
244 หมู่ 7 ตำบลหัวทะเล อำเภอเมือง จังหวัดนครราชสีมา 30000

6. นายศุภณัฐ ศศิพงศ์พนา
384/21 หมู่ 8 ตำบลสันทรายน้อย อำเภอสันทราย จังหวัดเชียงใหม่ 50210

7. นางวันทนา เกิดนิยม
139/35 หมู่ 1 ตำบลวัดชลอ อำเภอบางกรวย จังหวัดนนทบุรี 11130

8. นายคุณานนต์ ฉัตรไตรรัตน์
69/12 หมู่ 2 ตำบลโพไร่หวาน อำเภอเมืองเพชรบุรี จังหวัดเพชรบุรี 76000

9. นายประภากร รัตนวารินทร์ชัย
7 หมู่ 1 ตำบลวิหารแดง อำเภอวิหารแดง จังหวัดสระบุรี 18150

รายละเอียดการประดิษฐ์

ชื่อที่แสดงถึงการประดิษฐ์

กรรมวิธีการสร้างพอลิเมอร์เยื่อเลือกผ่านโมเลกุลสำหรับอุปกรณ์ตรวจวัดสารยูเรียและสารประกอบอินทรีย์ในน้ำแบบไม่ใช้เอนไซม์ (Polymeric Selective Membranes for non-enzymatic detection of urea and organic compounds)

ลักษณะและความมุ่งหมายของการประดิษฐ์

การประดิษฐ์นี้เกี่ยวกับการสร้างชั้นฟิล์มพอลิเมอร์สำหรับอุปกรณ์ตรวจวัดสารยูเรียและสารประกอบอินทรีย์ในน้ำ ชั้นฟิล์มพอลิเมอร์ดังกล่าวสามารถเตรียมได้โดยอาศัยหลักการของเทคนิคโมเลกุลาร์อิมพรินท์ (molecular imprinting) ด้วยการผสมพอลิเมอร์เทอร์โมพลาสติกและโมเลกุลของสารประกอบอินทรีย์ต้นแบบในตัวทำละลายสารอินทรีย์และเคลือบเป็นชั้นฟิล์มซึ่งทำหน้าที่เป็นชั้นเยื่อเลือกผ่านลงบนพื้นผิวของวัสดุสารกึ่งตัวนำหรือวัสดุตัวนำที่ทำหน้าที่เป็นพื้นที่ตรวจวัด (sensing area) สำหรับอุปกรณ์ตรวจวัดสารยูเรียและสารประกอบอินทรีย์ในน้ำ จากนั้นนำไปอบด้วยความร้อนหรือฉายรังสีอัลตราไวโอเลต (ultraviolet) เพื่อระเหยตัวทำละลายออกและเป็นการทำให้พอลิเมอร์สร้างตัว และการล้างโมเลกุลเป้าหมายนั้นออกจากชั้นพอลิเมอร์ด้วยตัวทำละลายที่ไม่ละลายพอลิเมอร์เทอร์โมพลาสติก เพื่อให้เกิดเป็นช่องว่างลักษณะคล้ายรูปร่างโมเลกุลเป้าหมาย กระบวนการนำอุปกรณ์ตรวจวัดสารยูเรียและสารประกอบอินทรีย์ในน้ำไปใช้งานจะใช้ร่วมกับขั้วไฟฟ้าอ้างอิง (เงิน-เงินคลอไรด์) และวัดค่าความต่างศักย์ของอุปกรณ์ตรวจวัดสารเคมีในน้ำเทียบกับขั้วไฟฟ้าอ้างอิง

จุดมุ่งหมายของการประดิษฐ์นี้ คือ วิธีการสร้างอุปกรณ์ตรวจวัดสารยูเรียหรือสารประกอบอินทรีย์ในน้ำโดยไม่ใช้เอนไซม์ โดยการสร้างชั้นฟิล์มพอลิเมอร์ให้มีลักษณะคล้ายเยื่อเลือกผ่านด้วยเทคนิคโมเลกุลลาร์อิมพรินท์ ซึ่งมีกระบวนการเตรียมง่าย รวดเร็ว และต้นทุนการผลิตต่ำ อุปกรณ์ตรวจวัดสารประกอบอินทรีย์ที่สร้างขึ้นสามารถใช้ตรวจวัดสารประกอบอินทรีย์ได้อย่างรวดเร็ว สามารถตรวจวัดปริมาณของโมเลกุลเป้าหมายได้ในช่วงความเข้มข้นต่ำๆ และมีความจำเพาะเจาะจงต่อโมเลกุลเป้าหมาย

สาขาวิทยาการที่เกี่ยวข้องกับการประดิษฐ์

วิทยาการทางสาขาเคมี ฟิสิกส์ และวิศวกรรมอิเล็กทรอนิกส์ในส่วนที่เกี่ยวข้องกับกรรมวิธีการสร้างพอลิเมอร์เยื่อเลือกผ่านโมเลกุลสำหรับอุปกรณ์ตรวจวัดสารยูเรียและสารประกอบอินทรีย์ในน้ำแบบไม่ใช้เอนไซม์ (Polymeric Selective Membranes for non-enzymatic detection of urea and organic compounds)

ภูมิหลังของศิลปะหรือวิทยาการที่เกี่ยวข้อง

ปัญหาการปนเปื้อนของสารเคมีในสิ่งแวดล้อมที่สำคัญ ซึ่งวิทยาศาสตร์และเทคโนโลยีนำไปประยุกต์ช่วยแก้ปัญหา เช่น ปัญหาน้ำเสียจากโรงงานอุตสาหกรรม สารพิษจากปุ๋ยและยาฆ่าแมลงในภาคเกษตรกรรม รวมถึงปัญหามลพิษทางน้ำจากการปนปื้อนของสารเคมี เป็นต้น จากปัญหาต่างๆ ที่เกิดขึ้นพบว่า ปัญหาสำคัญของอุปกรณ์ตรวจวัดสารเคมีในน้ำในปัจจุบันคือ การใช้เอนไซม์ที่มีความจำเพาะสำหรับเป็นสารตรวจจับสารยูเรียหรือสารประกอบอินทรีย์ชนิดนั้น ซึ่งเอนไซม์จะมีราคาแพงและเก็บรักษาได้ยาก ดังสิทธิบัตรสหรัฐอเมริกาเลขที่ US5698083 (R. S. Glass et al. Chemiresistor urea sensor) ได้เปิดเผยรายละเอียดเกี่ยวกับอุปกรณ์สำหรับตรวจวัดยูเรียโดยใช้เอมไซม์ยูเรียส (urease) บนขั้วอินเตอร์ดิจิเตจ (interdigitates) และวัดค่าความต้านทานเชิงซ้อน (impedance) ที่เปลี่ยนไปของอุปกรณ์เมื่อสัมผัสกับสารตัวอย่าง แต่การวัดต้านทานเชิงซ้อนนั้นจำเป็นต้องใช้แหล่งกำเนิดสัญญาณไฟกระแสสลับ อีกทั้งการวัดความต้านทานนั้นจะเปลี่ยนแปลงเมื่อสารตัวอย่างมีความนำไฟฟ้าที่ไม่เท่ากัน จึงมีการใช้เยื่อเลือกผ่านไอออน (ion-selective membrane) เพื่อให้มีความจำเพาะต่อสารที่ต้องการจะตรวจวัด ดังสิทธิบัตรสหรัฐอเมริกาเลขที่ US 2009/0266719 (S.K. Hsiung et al. Potentiometric urea sensor based on ion-selective electrode) ได้เปิดเผยรายละเอียดเกี่ยวกับการสร้างเยื่อเลือกผ่านไอออนสำหรับไอออนแอมโมเนียมก่อนที่จะตรึงเอนไซม์ยูเรียส เมื่อเอนไซม์ทำปฏิกิริยากับยูเรียจะทำให้เกิดแอมโมเนียมไอออนแล้วทำการตรวจวัดผลิตภัณฑ์ที่เกิดขึ้นจากกระบวนการนี้

เทคโนโลยีที่สามารถสร้างอุปกรณ์ตรวจวัดสารเคมีหรือไอออนในสารละลายแบบไม่ใช้เอนไซม์เป็นที่ต้องการและมีการพัฒนาเป็นอย่างมาก กระบวนการสร้างอุปกรณ์ตรวจวัดสารเคมีหรือไอออนในสารละลายแบบไม่ใช้เอนไซม์มีอยู่หลายแนวทาง ตัวอย่างเช่น การสร้างช่องว่างพอลิเมอร์ (Ionophore) สำหรับใช้เป็นเยื่อเลือกผ่านไอออน ซึ่งโดยมากเป็นไอออนสารอนินทรีย์ ดังสิทธิบัตรสหภาพยุโรปเลขที่ EP1565736 (J. Slater and L. Murphy, Multi-Ionophore Membrane Electerode) ได้เปิดเผยรายละเอียดเกี่ยวกับการหยดสารผสมหลายชนิดและพอลิเมอร์ลงบนขั้วไฟฟ้า ข้อเสียของอุปกรณ์ชนิดนี้คือ กระบวนการเตรียมสารผสมพอลิเมอร์ที่มีซับซ้อนโดยอาศัยสารเติมแต่งหลายชนิดเพื่อปรับโครงสร้างพอลิเมอร์ให้เฉพาะเจาะจงในการเลือกผ่านไอออนบางชนิด

อีกกระบวนการหนึ่งสำหรับสร้างอุปกรณ์ตรวจวัดสารยูเรียและสารประกอบอินทรีย์ในน้ำที่ได้รับความนิยมไม่น้อยกว่าการใช้เอนไซม์คือ การจำลองรูปร่างโมเลกุล (Molecular Imprinted) โดยการใช้สารเคมีและโมเลกุลแม่แบบ (template) สำหรับสร้างช่องว่างที่เหมือนกับสารที่ต้องการจะตรวจวัด ดังสิทธิบัตรสหรัฐอเมริกาเลขที่ US 2010/0203623 (Y. Zhou, Substrate Imprinted Universal Sensor and Sensors

having Nano-Tunneling Effect) โดยการสร้างชั้นฟิล์มบนฐานรองรับนำไฟฟ้า นอกจากนั้นการสร้างชั้นฟิล์มโดยการจำลองรูปร่างโมเลกุลยังสามารถทำได้บนฐานรองรับที่มีโครงสร้างเป็นทรานซิสเตอร์ (transistor) ดังสิทธิบัตรสหรัฐอเมริกาเลขที่ US 2013/0106443 (W. Jackson et al., Sensor having a Transistor and Imprint sides) การใช้ทรานซิสเตอร์เป็นฐานรองรับนั้นจะช่วยในด้านการขยายสัญญาณของการตรวจวัดและเพิ่มความเร็วในการตอบสนองของอุปกรณ์ แต่การใช้โมโนเมอร์ (monomer) มาสร้างให้เป็นชั้นฟิล์มพอลิเมอร์ที่มีการจำลองรูปแบบโมเลกุลที่ต้องการตรวจวัด ต้องอาศัยกระบวนการพอลิเมอไรเซชัน (polymerization) ที่มีขั้นตอนค่อนข้างซับซ้อนและใช้เวลาในการสร้างอุปกรณ์นาน

<u>การเปิดเผยการประดิษฐ์โดยสมบูรณ์</u>

การประดิษฐ์นี้เกี่ยวกับการเตรียมชั้นพอลิเมอร์ให้มีลักษณะคล้ายเยื่อเลือกผ่านสำหรับอุปกรณ์ตรวจวัดสารยูเรียและสารประกอบอินทรีย์ในน้ำ โดยอาศัยการผสมเพียงขั้นตอนเดียวของพอลิเมอร์และโมเลกุลเป้าหมาย (target molecule) ในตัวทำละลายชนิดที่หนึ่ง แล้วนำไปเคลือบบนขั้วไฟฟ้าและล้างโมเลกุลต้นแบบด้วยตัวทำละลายชนิดที่สอง เพื่อให้ได้โครงสร้างชั้นพอลิเมอร์ที่มีช่องว่างซึ่งจำลองรูปร่างโมเลกุลเป้าหมาย พอลิเมอร์ดังกล่าวเป็นกลุ่มพอลิเมอร์เทอร์โมพลาสติก (thermoplastic polymer) เช่น พอลิเมทิลเมทาคริเลต (Poly methyl methacrylate); PMMA) และพอลิเมอร์เทอร์โมพลาสติกชนิดอื่นๆ ส่วนโมเลกุลเป้าหมายนั้นสามารถใช้กับสารประกอบอินทรีย์ได้หลายชนิด เช่น ยูเรียและสารประกอบอินทรีย์อื่นๆ วิธีการเตรียมฟิล์มเป็นกรรมวิธีที่ง่าย ไม่ยุ่งยาก อาศัยหลักการของเทคนิคโมเลกุลาร์อิมพรินท์ (molecular imprinting) โดยที่การใช้งานในการตรวจวัดสารแบบไฟฟ้าเคมีจะอาศัยช่องว่างลักษณะคล้ายรูปร่างโมเลกุลเป้าหมายจะเป็นเยื่อเลือกผ่านให้โมเลกุลเป้าหมายเข้าไปแทรกฝังตัวในช่องว่างของชั้นพอลิเมอร์ได้ ซึ่งทำให้สารละลายหรือไอออนในสารละลายที่ใช้ในการตรวจวัดแบบไฟฟ้าเคมีไม่สามารถเข้าไปถึงขั้วไฟฟ้าได้จึงทำให้สัญญาณการตอบสนองของเซ็นเซอร์นั้นมีการเปลี่ยนแปลง กระบวนการนี้จะเกิดได้น้อยกว่าในกรณีที่ไม่ใช้โมเลกุลเป้าหมายสำหรับเตรียมเป็นเยื่อเลือกผ่าน นอกจากนี้การเข้าไปของโมเลกุลเป้าหมายนั้นจะไม่ได้เกิดปฏิกิริยาการจับถาวรกับชั้นพอลิเมอร์ ทำให้สามารถนำชั้นพอลิเมอร์ไปล้างเพื่อนำกลับมาใช้ในการตรวจวัดซ้ำ

การเตรียมสารผสมระหว่างพอลิเมอร์เทอร์โมพลาสติกและโมเลกุลเป้าหมายสารประกอบอินทรีย์นั้นสามารถเตรียมได้โดยผสมพอลิเมอร์เทอร์โมพลาสติกและโมเลกุลเป้าหมายอยู่ในช่วง 0.1 ถึง 10 เปอร์เซ็นต์โดยน้ำหนักต่อปริมาตร และผสมในตัวทำละลายสารอินทรีย์ (organic solvent) ความเข้มข้นรวมอยู่ในช่วง 0.1 ถึง 10 เปอร์เซ็นต์โดยน้ำหนักต่อปริมาตร เพื่อให้สารผสมนั้นละลายและเป็นเนื้อเดียวกัน ต้องมีการผสมด้วยกระบวนการปั่นกวน (stirring) หรือการสั่นด้วยความถี่สูง (ultrasonocation)

จากรูปที่ 1(a) แสดงการเตรียมชั้นฟิล์มพอลิเมอร์ให้มีลักษณะคล้ายเยื่อเลือกผ่านสำหรับอุปกรณ์ตรวจวัดสารเคมีในน้ำ โดยการใช้ไมโครปิเปตต์ (micropipette) 5 หยดสารผสมพอลิเมอร์ 4 ในปริมาณ 0.5 ถึง 3 ไมโครลิตร ลงบนพื้นผิววัสดุนำไฟฟ้าหรือวัสดุสารกึ่งตัวนำของเซ็นเซอร์ 6 จากนั้นนำไประเหยเอาตัวทำละลายสารอินทรีย์ 3 ออก ซึ่งสามารถทำได้หลายวิธี โดยรูปที่ 1(b) แสดงถึงเซ็นเซอร์ 6 ที่มีชั้นฟิล์มพอลิเมอร์ 2 และโมเลกุลเป้าหมาย 1 เคลือบอยู่บนพื้นผิว 7a หลังจากนั้นนำเซ็นเซอร์ 6 ไปจุ่มในน้ำที่ทำหน้าที่เป็นตัวทำละลายชนิดที่สองเพื่อทำให้โมเลกุลเป้าหมาย 1 ละลายหลุดออกมากับน้ำ ดังแสดงในรูปที่ 1(c) จึงเกิดเป็นช่องว่างลักษณะคล้ายรูปร่างจำลองของโมเลกุลเป้าหมาย 1 ขึ้นในชั้นฟิล์มพอลิเมอร์ 2 และสามารถนำเซ็นเซอร์ 6 ที่มีชั้นฟิล์มพอลิเมอร์ 2 บนพื้นผิว 7b ไปใช้ในการตรวจวัดโมเลกุลเป้าหมาย 1 ต่อไป รูปที่ 1(d) แสดงภาพขยายการเปรียบเทียบพื้นผิว 7a ที่มีชั้นฟิล์มพอลิเมอร์ 2 และโมเลกุลเป้าหมาย 1 กับพื้นผิว 7b ที่มีชั้นฟิล์มพอลิเมอร์ 2 แต่ไม่มีโมเลกุลเป้าหมาย 1 อย่างไรก็ตามการจำลองรูปร่างโมเลกุลเป้าหมาย 1 สามารถทำโดยวิธีอื่น เช่น พอลิเมอไรเซชัน (polymerization) เป็นต้น

วิธีการเตรียมชั้นฟิล์มจำลองรูปร่างโมเลกุลจากสิ่งประดิษฐ์นี้มีข้อดีคือ เป็นวิธีที่เตรียมง่ายและไม่ซับซ้อน เนื่องจากไม่ต้องผ่านการทำพอลิเมอไรเซชันของพอลิเมอร์และโมเลกุลเป้าหมาย นอกจากนี้ในบางการทดลองยังไม่ต้องอาศัยการตรึงเอนไซม์ลงบนพื้นผิวเซ็นเซอร์เพื่อใช้ในการตรวจวัดสารต่างๆ โดยปริมาณของพอลิเมอร์ต่อโมเลกุลเป้าหมายต้องมีสัดส่วนที่เหมาะสม เพราะจะมีผลต่อการสร้างชั้นฟิล์มจำลองรูปร่างโมเลกุล พอลิเมอร์ต้องมีความเข้มข้นไม่น้อยเกินไป ซึ่งอาจจะทำให้ชั้นฟิล์มไม่เกิดการฟอร์มตัวหรือต้องไม่เข้มข้นมากเกินไป ซึ่งอาจจะทำให้ชั้นฟิล์มมีความหนามาก

ต่อไปนี้เป็นตัวอย่างการเตรียมชั้นฟิล์มจำลองรูปร่างโมเลกุลเพื่อใช้สำหรับตรวจวัดยูเรียโดยอาศัยเซ็นเซอร์อิสเฟต (ion-sensitive field effect transisitor; ISFET) และขอบเขตของการประดิษฐ์จะเป็นไปตามข้อถือสิทธิที่แนบท้าย

การประดิษฐ์นี้แสดงโดยตัวอย่างที่ไม่จำกัดดังต่อไปนี้

ตัวอย่างที่ 1

ละลายพอลิเมอร์พอลิเมทิลเมทาคริเลต (Poly(methyl methacrylate); PMMA) ในตัวทำละลายสารอินทรีย์ไดเมทิลฟอร์มาไมด์ (dimethylformamide; DMF) เข้าเป็นเนื้อเดียวกันในภาชนะปิดด้วยการสั่นด้วยความถี่สูง (ultrasonication) เป็นเวลา 10 ถึง 20 นาที โดยในสารละลายผสมมีปริมาณพอลิเมทิลเมทาคริเลต 2.5 เปอร์เซ็นต์โดยน้ำหนักต่อปริมาตร ซึ่งเป็นอัตราส่วนหนึ่งในหลายอัตราส่วนที่ได้ทำการทดสอบในช่วง 0.1 ถึง 10 เปอร์เซ็นต์โดยน้ำหนักต่อปริมาตร จากนั้นนำสารละลายผสมนี้ปริมาตร 1 ไมโครลิตรไปหยดลงบน

พื้นผิวเซ็นเซอร์อิสเฟตที่มีพื้นที่ไม่มากกว่า 6 ตารางมิลลิเมตร ซึ่งพื้นผิวผ่านการทำความสะอาดแล้ว โดยการสั่นด้วยความถี่สูง (ultrasonication) ในเอทานอล (ethanol) เป็นเวลา 5 นาที และน้ำปราศจากไอออน (Deionized water) เป็นเวลา 5 นาที จากนั้นนำพื้นผิวอิสเฟตที่ถูกหยดด้วยสารละลายผสมไประเหยเอาตัวทำละลายสารอินทรีย์ออก ด้วยการอบด้วยความร้อนที่อุณหภูมิอยู่ในช่วง 40 ถึง 70 องศาเซลเซียส เป็นเวลา 5 นาที ถึง 12 ชั่วโมง ผสมพอลิเมอร์พอลิเมทิลเมทาคริเลต (Poly(methyl methacrylate); PMMA) และยูเรีย (Urea) ในตัวทำละลายสารอินทรีย์ไดเมทิลฟอร์มาไมด์ (dimethylformamide; DMF) เข้าเป็นเนื้อเดียวกันในภาชนะปิดด้วยการสั่นด้วยความถี่สูง (ultrasonication) เป็นเวลา 10 ถึง 20 นาที โดยในสารละลายผสมมีปริมาณพอลิเมทิลเมทาคริเลต 2.5 เปอร์เซ็นต์โดยน้ำหนักต่อปริมาตรและยูเรีย 0.3 เปอร์เซ็นต์โดยน้ำหนักต่อปริมาตร โดยที่อัตราส่วนนี้เป็นหนึ่งในเงื่อนไขที่ทำการทดลองในช่วงอัตราส่วนผสมของพอลิเมอร์และโมเลกุลเป้าหมายที่ต้องการตรวจวัดในช่วง 0.1 ถึง 10 เปอร์เซ็นต์โดยน้ำหนักต่อปริมาตร จากนั้นนำสารละลายผสมนี้ปริมาตร 1 ไมโครลิตร ไปหยดลงบนพื้นผิวเซ็นเซอร์อิสเฟตที่มีพื้นที่ไม่มากกว่า 6 ตารางมิลลิเมตร ซึ่งพื้นผิวผ่านการทำความสะอาดแล้วโดยการสั่นด้วยความถี่สูง (ultrasonication) ในเอทานอล (ethanol) เป็นเวลา 5 นาที และน้ำปราศจากไอออน (Deionized water) เป็นเวลา 5 นาที หลังจากนั้นนำพื้นผิวอิสเฟตที่ถูกหยดด้วยสารละลายผสมไประเหยเอาตัวทำละลายสารอินทรีย์ออก ด้วยการอบด้วยความร้อนที่อุณหภูมิอยู่ในช่วง 40 ถึง 70 องศาเซลเซียส เป็นเวลา 5 นาที ถึง 12 ชั่วโมง

วิธีการล้างโมเลกุลยูเรียออกจากชั้นฟิล์มบนพื้นผิวอิสเฟต เพื่อทำให้เกิดเป็นแบบจำลองของรูปร่างโมเลกุลยูเรียนั้น ทำได้โดยการจุ่มพื้นผิวอิสเฟตลงในน้ำเป็นเวลา 5 ถึง 60 นาที ซึ่งจะทำให้โมเลกุลยูเรียละลายหลุดออกมากับน้ำ ในขณะที่ชั้นฟิล์มซึ่งเป็นพอลิเมทิลเมทาคริเลตจะไม่ละลายน้ำ จึงทำให้เกิดเป็นช่องว่างลักษณะคล้ายรูปร่างโมเลกุลยูเรียขึ้นที่ชั้นฟิล์มพอลิเมอร์ โดยชั้นฟิล์มพอลิเมอร์นี้จะทำหน้าที่เป็นเยื่อเลือกผ่านสำหรับอุปกรณ์ตรวจวัดสารละลายยูเรียในน้ำ

การวัดสัญญาณการตอบสนองของอุปกรณ์จากตัวอย่างที่ 1 ต่อสารยูเรียในรูปแบบของสารละลายทำได้โดยการวัดความต่างศักย์ของอุปกรณ์ที่ประดิษฐ์นี้เทียบกับขั้วโลหะเงิน เงินคลอไรด์ (Ag/AgCl) ซึ่งมีสารละลายโปแตสเซียมคลอไรด์อิ่มตัว (saturated KCL) บรรจุอยู่ภายใน ซึ่งทำหน้าที่เป็นขั้วไฟฟ้าอ้างอิง ตามรูปที่ 2 แสดงการตอบสนองของอุปกรณ์เทียบกับความเข้มข้นของยูเรียในช่วง 10^{-6} ถึง 1 โมลต่อลิตรในตัวทำละลายน้ำเกลือโซเดียมคลอไรด์ความเข้มข้น 0.1 โมลต่อลิตร โดยเปรียบเทียบระหว่างเซ็นเซอร์อิสเฟตเปล่า, เซ็นเซอร์อิสเฟตที่เคลือบด้วยพอลิเมทิลเมทาคริเลตความเข้มข้น 2.5 เปอร์เซ็นต์โดยน้ำหนักต่อปริมาตร และเซ็นเซอร์อิสเฟตที่เคลือบด้วยชั้นฟิล์มจากสิ่งประดิษฐ์นี้ โดยค่าสัญญาณที่แสดงเป็นค่าผลต่างของสัญญาณก่อนและ

หลังจากการวัดยูเรียที่ความเข้มข้นต่างๆ จากผลพบว่าเซ็นเซอร์อิสเฟตที่เคลือบด้วยชั้นฟิล์มจากสิ่งประดิษฐ์นี้มีความไวต่อการวัดยูเรีย โดยมีความสัมพันธ์แบบเชิงเส้นในช่วงความเข้มข้น 10^{-4} ถึง 0.1 โมลต่อลิตร

ตัวอย่างที่ 2

ละลายพอลิเมอร์พอลิเมทิลเมทาคริเลต (Poly(methyl methacrylate); PMMA) ในตัวทำละลายสารอินทรีย์ไดเมทิลฟอร์มาไมด์ (dimethylformamide; DMF) เข้าเป็นเนื้อเดียวกันในภาชนะปิดด้วยการสั่นด้วยความถี่สูง (ultrasonication) เป็นเวลา 10 ถึง 20 นาที โดยในสารละลายผสมมีปริมาณพอลิเมทิลเมทาคริเลต 2.5 เปอร์เซ็นต์โดยน้ำหนักต่อปริมาตร จากนั้นนำสารละลายผสมนี้ปริมาตร 1 ไมโครลิตรไปหยดลงบนพื้นผิวเซ็นเซอร์อิสเฟตที่มีพื้นที่ไม่มากกว่า 6 ตารางมิลลิเมตร ซึ่งพื้นผิวผ่านการทำความสะอาดแล้วโดยการสั่นด้วยความถี่สูง (ultrasonication) ในเอทานอล (ethanol) เป็นเวลา 5 นาที และน้ำปราศจากไอออน (Deionized water) เป็นเวลา 5 นาที หลังจากนั้นนำพื้นผิวอิสเฟตที่ถูกหยดด้วยสารละลายผสมไประเหยเอาตัวทำละลายสารอินทรีย์ออก ด้วยการฉายรังสีอัลตราไวโอเลตที่มีความยาวคลื่นในช่วง 200 ถึง 400 นาโนเมตร เป็นเวลา 1 ถึง 60 นาที ผสมพอลิเมอร์พอลิเมทิลเมทาคริเลต (Poly methyl methacrylate); PMMA) และยูเรีย (Urea) ในตัวทำละลายสารอินทรีย์ไดเมทิลฟอร์มาไมด์ (dimethylformamide; DMF) เข้าเป็นเนื้อเดียวกันในภาชนะปิดด้วยการสั่นด้วยความถี่สูง (ultrasonication) เป็นเวลา 10 ถึง 20 นาที โดยในสารละลายผสมมีปริมาณพอลิเมทิลเมทาคริเลต 2.5 เปอร์เซ็นต์โดยน้ำหนักต่อปริมาตร และยูเรีย 0.3 เปอร์เซ็นต์โดยน้ำหนักต่อปริมาตร จากนั้นนำสารละลายผสมดังกล่าวในปริมาตร 1 ไมโครลิตรหยดลงบนพื้นผิวเซ็นเซอร์อิสเฟตที่มีพื้นที่ไม่มากกว่า 6 ตารางมิลลิเมตร ซึ่งพื้นผิวผ่านการทำความสะอาดแล้วโดยการสั่นด้วยความถี่สูง (ultrasonication) ในเอทานอล (ethanol) เป็นเวลา 5 นาที และน้ำปราศจากไอออน (Deionized water) เป็นเวลา 5 นาที หลังจากนั้นนำพื้นผิวอิสเฟตที่ถูกหยดด้วยสารละลายผสมไประเหยเอาตัวทำละลายสารอินทรีย์ออก ด้วยการฉายรังสีอัลตราไวโอเลตที่มีความยาวคลื่นในช่วง 200 ถึง 400 นาโนเมตร เป็นเวลา 1 ถึง 60 นาที

วิธีการล้างโมเลกุลยูเรียออกจากชั้นฟิล์มบนพื้นผิวอิสเฟต เพื่อทำให้เกิดเป็นแบบจำลองของรูปร่างโมเลกุลยูเรียนั้น ทำได้โดยการจุ่มพื้นผิวอิสเฟตลงในน้ำเป็นเวลา 5 ถึง 60 นาที ซึ่งจะทำให้โมเลกุลยูเรียละลายหลุดออกมากับน้ำ ในขณะที่ชั้นฟิล์มซึ่งเป็นพอลิเมทิลเมทาคริเลตจะไม่ละลายน้ำ จึงทำให้เกิดเป็นช่องว่างลักษณะคล้ายรูปร่างโมเลกุลยูเรียขึ้นที่ชั้นฟิล์มพอลิเมอร์ โดยชั้นฟิล์มพอลิเมอร์นี้จะทำหน้าที่เป็นเยื่อเลือกผ่านสำหรับอุปกรณ์ตรวจวัดสารละลายยูเรียในน้ำ

การวัดสัญญาณการตอบสนองของอุปกรณ์จากตัวอย่างที่ 2 ต่อสารยูเรียในรูปแบบของสารละลายทำได้โดยการวัดความต่างศักย์ของอุปกรณ์ที่ประดิษฐ์นี้เทียบกับขั้วโลหะเงิน เงินคลอไรด์ (Ag/AgCl) ซึ่งมี

สารละลายโปแตสเซียมคลอไรด์อิ่มตัว (saturated KCL) บรรจุอยู่ภายใน ทำหน้าที่เป็นขั้วไฟฟ้าอ้างอิง ตามรูปที่ 3 แสดงการตอบสนองของอุปกรณ์เทียบกับความเข้มข้นของยูเรียในช่วง 10^{-6} ถึง 1 โมลต่อลิตรในตัวทำละลายน้ำเกลือโซเดียมคลอไรด์ความเข้มข้น 0.1 โมลต่อลิตร โดยเปรียบเทียบระหว่างเซ็นเซอร์อิสเฟตเปล่า, เซ็นเซอร์อิสเฟตที่เคลือบด้วยพอลิเมทิลเมทาคริเลตความเข้มข้น 2.5 เปอร์เซ็นต์โดยน้ำหนักต่อปริมาตร และเซ็นเซอร์อิสเฟตที่เคลือบด้วยชั้นฟิล์มจากสิ่งประดิษฐ์นี้ โดยค่าสัญญาณที่แสดงเป็นค่าผลต่างของสัญญาณก่อนและหลังจากการวัดยูเรียที่ความเข้มข้นต่างๆ จากผลพบว่าเซ็นเซอร์อิสเฟตที่เคลือบด้วยชั้นฟิล์มจากสิ่งประดิษฐ์นี้มีความไวต่อการวัดยูเรีย โดยมีความสัมพันธ์แบบเชิงเส้นในช่วงความเข้มข้น 10^{-5} ถึง 0.1 โมลต่อลิตร

ตัวอย่างที่ 3

การนำอุปกรณ์ตรวจวัดสารยูเรียด้วยเทคนิคโมเลกุลาร์อิมพรินท์จากตัวอย่างที่ 2 ทดสอบความจำเพาะเจาะจงโดยการทดสอบวัดปริมาณวัดยูเรียและโพแทสเซียมไนเตรตที่ความเข้มข้นในช่วง 10^{-6} ถึง 1 โมลต่อลิตรในตัวทำละลายน้ำเกลือโซเดียมคลอไรด์ความเข้มข้น 0.1 โมลต่อลิตร ซึ่งแสดงตามรูปที่ 4 ที่เปรียบเทียบสัญญาณการตอบสนองระหว่างอุปกรณ์ตรวจวัดยูเรียด้วยเทคนิคโมเลกุลาร์อิมพรินท์ในสารละลายยูเรียและอุปกรณ์ตรวจวัดยูเรียด้วยเทคนิคโมเลกุลาร์อิมพรินท์ในสารละลายโพแทสเซียมไนเตรต

นอกจากนี้วิธีการของตัวอย่างที่ 1 ถึง 3 ยังสามารถนำไปใช้กับโมเลกุลเป้าหมายซึ่งเป็นสารกลุ่มที่ใกล้เคียงกับยูเรีย เช่น คาร์บาร์เมต และสารกลุ่มอื่น เช่น ยาฆ่าแมลงกลุ่มออร์กาโนฟอสเฟตซึ่งมีความสามารถในการละลายน้ำได้

<u>คำอธิบายรูปเขียนโดยย่อ</u>

รูปที่ 1 แผนภาพแสดงวิธีการเตรียมชั้นฟิล์มจำลองรูปร่างโมเลกุลจากสิ่งประดิษฐ์นี้

รูปที่ 2 กราฟสัญญาณการตอบสนองของอุปกรณ์อิสเฟต อุปกรณ์อิสเฟตที่ถูกเคลือบด้วยพอลิเมอร์พอลิเมทิลเมทาคริเลต อุปกรณ์อิสเฟตที่ผ่านกระบวนการโมเลกุลาร์อิมพรินท์ด้วยพอลิเมอร์พอลิเมทิลเมทาคริเลตโดยมียูเรียเป็นโมเลกุลเป้าหมายและอบด้วยอุณหภูมิ 60 องศาเซลเซียสต่อสารละลายยูเรียที่ความเข้มข้น 10^{-6} ถึง 1 โมลต่อลิตร

รูปที่ 3 กราฟสัญญาณการตอบสนองของอุปกรณ์อิสเฟต อุปกรณ์อิสเฟตที่ถูกเคลือบด้วยพอลิเมอร์พอลิเมทิลเมทาคริเลต อุปกรณ์อิสเฟตที่ผ่านกระบวนการโมเลกุลาร์อิมพรินท์ด้วยพอลิเมอร์พอลิเมทิลเมทาคริเลตโดยมียูเรียเป็นโมเลกุลเป้าหมายและฉายตัวแสงยูวีความยาวคลื่น 254 นาโนเมตรต่อสารละลายยูเรียที่ความเข้มข้น 10^{-6} ถึง 1 โมลต่อลิตร

รูปที่ 4 กราฟสัญญาณการตอบสนองของอุปกรณ์อิสเฟตที่ผ่านกระบวนการโมเลกุลาร์อิมพรินท์ด้วยพอลิเมอร์พอลิเมทิลเมทาคริเลตโดยมียูเรียเป็นโมเลกุลเป้าหมายและฉายตัวแสงยูวีความยาวคลื่น 254 นาโนเมตร ต่อสารละลายยูเรียเปรียบเทียบกับสารละลายโพแทสเซียมไนเตรตที่ความเข้มข้น 10^{-6} ถึง 1 โมลต่อลิตร

<u>วิธีการในการประดิษฐ์ที่ดีที่สุด</u>

ดังที่ได้กล่าวมาแล้วในหัวข้อการเปิดเผยการประดิษฐ์โดยสมบูรณ์

ข้อถือสิทธิ

1. กรรมวิธีการสร้างชั้นพอลิเมอร์เยื่อเลือกผ่านโมเลกุลสำหรับอุปกรณ์ตรวจวัดสารยูเรียและสารประกอบอินทรีย์ในน้ำแบบไม่ใช้เอนไซม์ ซึ่งประกอบด้วยขั้นตอนดังนี้

ก. การผสมพอลิเมอร์และโมเลกุลเป้าหมายในตัวทำละลายชนิดที่หนึ่ง

ข. การนำสารผสมพอลิเมอร์และโมเลกุลเป้าหมายไปเคลือบบนขั้วไฟฟ้า

ค. การล้างโมเลกุลเป้าหมายออกจากชั้นพอลิเมอร์ที่อยู่บนขั้วไฟฟ้าด้วยตัวทำละลายชนิดที่สอง

2. กรรมวิธีการสร้างชั้นพอลิเมอร์เยื่อเลือกผ่านโมเลกุลตามข้อถือสิทธิ 1 ที่ซึ่งตัวทำละลายชนิดที่หนึ่งเลือกได้จากหรือทั้งหมดของกลุ่มตัวทำละลาย ได้แก่ ไดเมทิลฟอร์มาไมด์ คลอโรเบนซีน ไดคลอโรเบนซีน ไตรคลอโรเบนซีน และเอทานอลผสมน้ำ

3. กรรมวิธีการสร้างชั้นพอลิเมอร์เยื่อเลือกผ่านโมเลกุลตามข้อถือสิทธิ 1 ที่ซึ่งตัวทำละลายชนิดที่สองคือ น้ำหรือสารละลายในน้ำ

4. กรรมวิธีการสร้างชั้นพอลิเมอร์เยื่อเลือกผ่านโมเลกุลตามข้อถือสิทธิ 1 ที่ซึ่งวัสดุพอลิเมอร์เลือกได้จากหรือทั้งหมดของกลุ่มพอลิเมทิลเมทาคริเลต (Poly(methyl methacrylate); PMMA) และอนุพันธ์

5. กรรมวิธีการสร้างชั้นพอลิเมอร์เยื่อเลือกผ่านโมเลกุลตามข้อถือสิทธิ 1 ที่ซึ่งโมเลกุลเป้าหมายเลือกได้จากหรือทั้งหมดของกลุ่มสารประกอบอินทรีย์ ได้แก่ ยูเรีย คาร์บาร์เมต และออร์กาโนฟอสเฟต

6. กรรมวิธีการสร้างชั้นพอลิเมอร์เยื่อเลือกผ่านโมเลกุลตามข้อถือสิทธิ 1 ถึง 5 ข้อใดข้อหนึ่ง ที่ซึ่งอัตราส่วนในการผสมพอลิเมอร์และโมเลกุลเป้าหมายอยู่ในช่วง 0.1 ถึง 10 เปอร์เซ็นต์โดยน้ำหนักต่อปริมาตร และผสมในตัวทำละลายสารอินทรีย์ ความเข้มข้นรวมในช่วง 0.1 ถึง 10 เปอร์เซ็นต์โดยน้ำหนักต่อปริมาตร

7. กรรมวิธีการสร้างชั้นพอลิเมอร์เยื่อเลือกผ่านโมเลกุลตามข้อถือสิทธิ 1 ถึง 6 ข้อใดข้อหนึ่ง ที่ซึ่งนำสารผสมพอลิเมอร์และโมเลกุลเป้าหมายเคลือบบนขั้วไฟฟ้าด้วยความร้อนหรือฉายรังสีอัลตราไวโอเลตที่มีความยาวคลื่นในช่วง 200 ถึง 400 นาโนเมตร เป็นเวลา 1 ถึง 60 นาที

8. กรรมวิธีการสร้างชั้นพอลิเมอร์เยื่อเลือกผ่านโมเลกุลตามข้อถือสิทธิ 7 ที่ซึ่งขั้วไฟฟ้าเลือกได้จากหรือทั้งหมดของกลุ่มวัสดุ ได้แก่ ทอง เงิน ทองแดง ซิลิคอน ซิลิคอนไนไตรด์ ซิงค์ออกไซด์ ทินออกไซด์ ทินออกไซด์เจืออิเดียม คาร์บอน และพอลิเมอร์นำไฟฟ้า

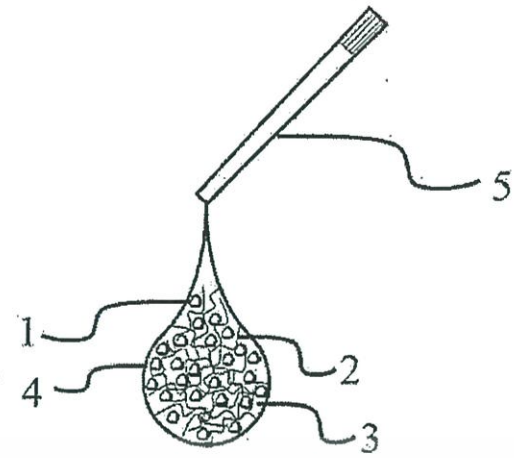

(a)

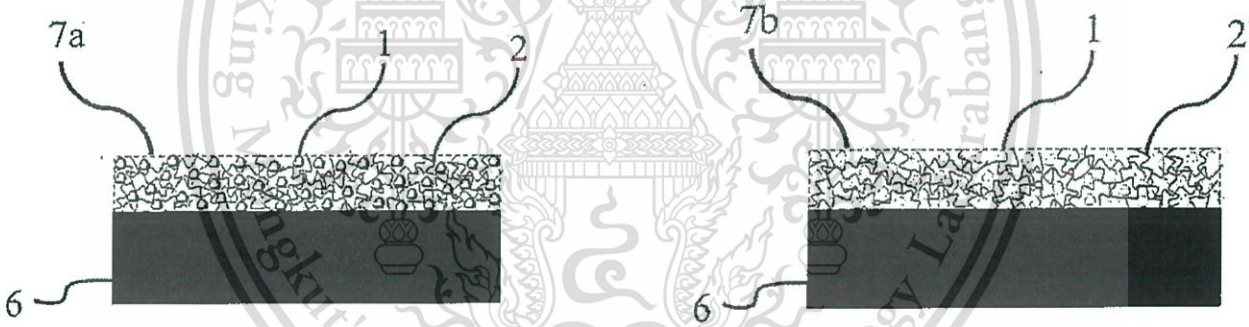

(b) (c)

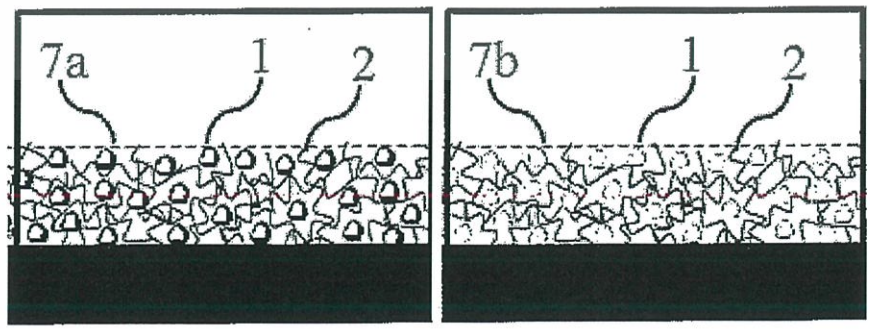

(d)

รูปที่ 1

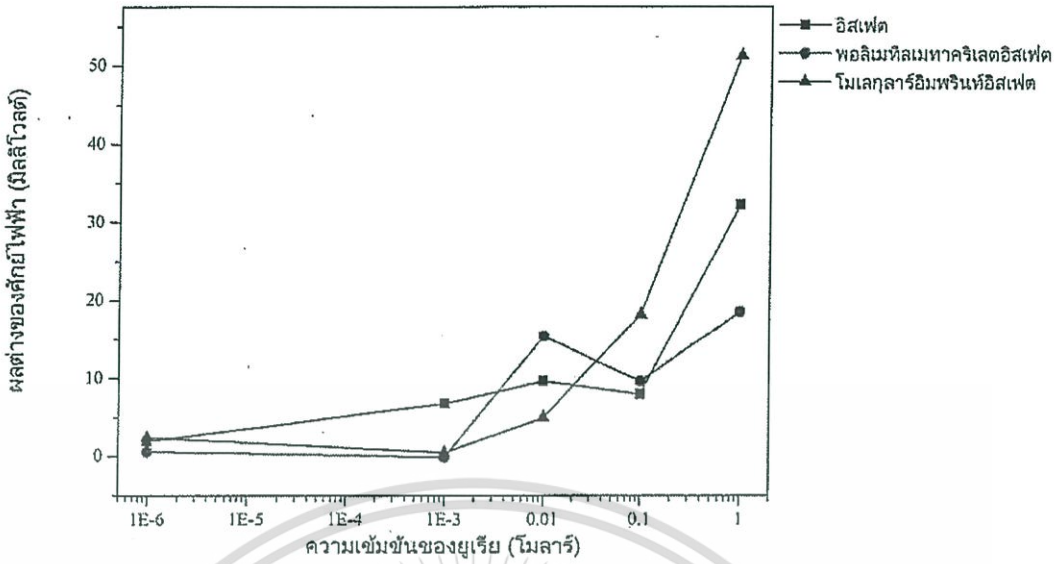

รูปที่ 2

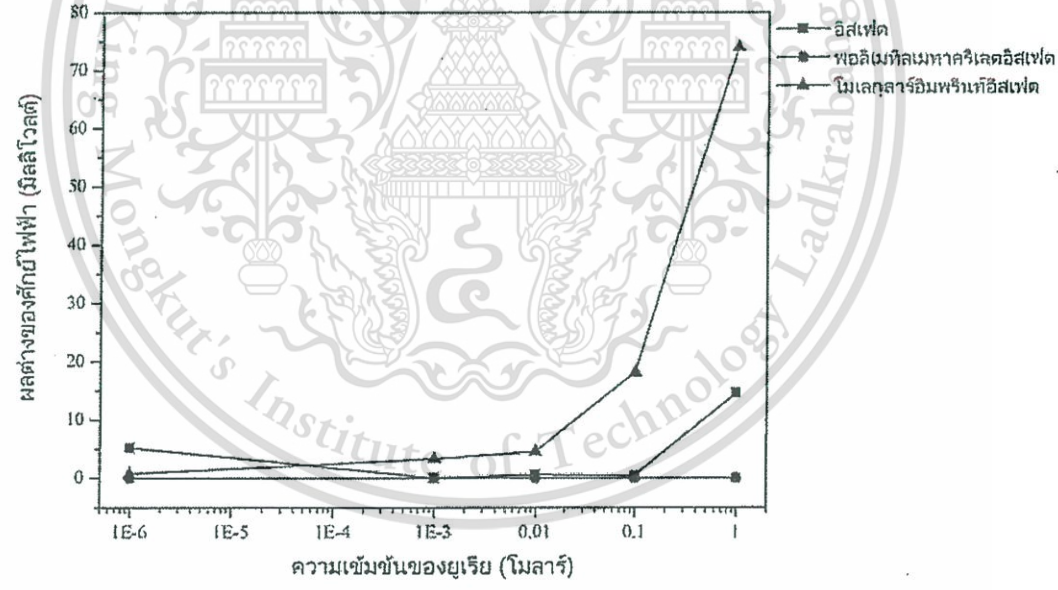

รูปที่ 3

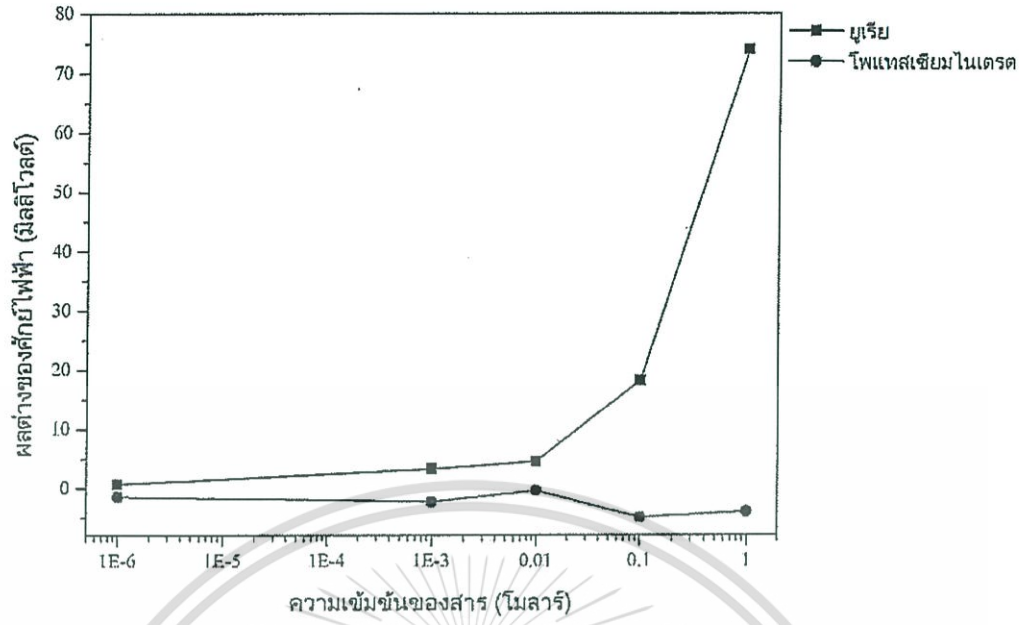

รูปที่ 4

บทสรุปการประดิษฐ์

การประดิษฐ์นี้แสดงวิธีการเตรียมชั้นฟิล์มพอลิเมอร์ที่มีการจำลองรูปร่างโมเลกุลเพื่อเคลือบบนพื้นผิวและใช้ในการตรวจวัดโมเลกุลดังกล่าวในสารละลาย โดยอาศัยหลักการพื้นฐานของเทคนิคโมเลกุลาร์อิมพรินท์ในการจำลองรูปร่างโมเลกุลเป้าหมายด้วยการผสมกับพอลิเมอร์ในอัตราส่วนที่เหมาะสมเพื่อขึ้นรูปเป็นฟิล์ม แล้วล้างโมเลกุลเป้าหมายออก เพื่อนำฟิล์มที่ได้ไปใช้เป็นเยื่อเลือกผ่านที่มีความจำเพาะเจาะจงต่อโมเลกุลเป้าหมาย วิธีการนี้เป็นวิธีการที่สะดวกและไม่ต้องอาศัยปฏิกิริยาพอลิเมอไรเซชัน (polymerization) ในการเตรียมชั้นฟิล์ม ซึ่งต่างจากเทคนิคโมเลกุลาร์อิมพรินท์โดยทั่วไป จากตัวอย่างการเตรียมชั้นฟิล์มสำหรับการตรวจวัดยูเรียลงบนเซ็นเซอร์อิสเฟต สามารถใช้ตรวจวัดยูเรียได้ในระดับความเข้มข้นต่ำ โดยไม่ต้องอาศัยการตรึงเอนไซม์บนเซ็นเซอร์อิสเฟตตามวิธีปกติ อีกทั้งยังสามารถล้างแล้วใช้ซ้ำได้ การประดิษฐ์นี้จึงเป็นวิธีการที่สะดวกและต้นทุนต่ำในการเตรียมเซ็นเซอร์ตรวจจับโมเลกุลเคมีได้หลากหลายชนิด